DOE/NE/44139-14
(DE87005887)
Distribution Category UC-70

HIGH-LEVEL WASTE CHARACTERIZATION AT WEST VALLEY

REPORT OF WORK PERFORMED
1982 - 1985

By
Larry E. Rykken

June 2, 1986

Work Performed Under Contract No. DE-AC07-81NE 44139

Prepared for
U.S. Department of Energy
Assistant Secretary for Nuclear Energy

Prepared by
West Valley, New York 14171

TOPICAL REPORT

HIGH-LEVEL WASTE CHARACTERIZATION
AT WEST VALLEY

TABLE OF CONTENTS

TOPICAL REPORT

HIGH-LEVEL WASTE CHARACTERIZATION
AT WEST VALLEY

TABLE OF CONTENTS (CONTINUED)

FIGURES

FIGURES (CONTINUED)

TABLES

ABSTRACT

This is a report on the work that was carried out at West Valley under the Waste Characterization Program. This Program covered a number of tasks in support of the design of facilities for the pretreatment and final encapsulation of the high level waste stored at West Valley. In particular, necessary physical, chemical, and radiological characterization of high-level reprocessing waste stored in two vaulted underground tanks was carried out over the period 1982-1985.

ACKNOWLEDGMENTS

The successful completion of the tasks reported here required the support of a number of on-site and off-site organizations - the site Facility Engineering, Operations, Maintenance and Analytical Departments, Dames and Moore, Battelle Pacific Northwest Laboratories, Westinghouse Atomic Energy Systems Division (AESD) Laboratories, and Babcock and Wilcox Analytical Laboratories, to name a few. Of the many people involved in this support, I would like to single out two:

1. Larry Wiedemann, site Facilities Engineer, was instrumental in overall operational coordination of several of the in-tank sampling and testing projects. He was also responsible for mechanical design of much of the equipment.

2. James Strom, Dames and Moore, Senior Design Engineer, was responsible for the design of the in situ sludge characterization and sampling equipment. His skill and dedication at turning vague ideas into workable pieces of equipment was essential to the program and is much appreciated.

EXECUTIVE SUMMARY

The Department of Energy (DOE) facility at West Valley, New York, has been mandated by Congress to carry out a high-level waste (HLW) management demonstration project at the West Valley site in Western New York. The West Valley site was a commercial nuclear fuel processing center that operated from 1966 to 1972. The Project involves the cleanup of approximately 2.1 million litres of fuel reprocessing wastes. The HLW terminal form will be borosilicate glass.

The DOE, together with its prime contractor, Westinghouse Electric Corp., officially took over site operation in February of 1982. A Waste Characterization Program was immediately set in place to provide necessary input into several process design activities. Major accomplishments of this program include:

1. Very extensive chemical and radiological characterization of the liquid portions of the HLW.

2. In situ physical characterization of the sludge layer at the bottom of the main waste tank with specially designed mechanical devices (buoyancy probe and shear vane).

3. Core sampling of the sludge layer with a specially designed sampler together with chemical/radiological analysis and in-cell physical characterization.

4. In-cell screening and verification of the reference process to decontaminate the supernatant (liquid portion of the main HLW tank).

5. Leach test qualification of cement cylinders fabricated from actual decontaminated supernatant. Encapsulation in concrete to produce a low-level waste (LLW) is the reference process for treatment of the decontaminated supernatant.

The major process operations in which the Waste Characterization Program has provided input are:

1. The Supernatant Treatment System will process the supernatant and sludge wash solutions through ion exchange columns to remove the major radionuclide, Cs-137.

2. The Low-Level Waste System will receive the decontaminated supernatant and wash solutions, and evaporate them. The evaporator bottoms will be encapsulated in cement while the evaporated overheads will be treated to produce reusable process water or water that will meet discharge standards.

3. The Waste Mobilization Facility will consist primarily of several long-shafted sluicing pumps that will mobilize (loosen) the sludge solids from the tank bottom and provide extensive slurry blending for the purpose of washing impurities from the sludge layer and suspending the solids for removal to the Vitrification Facility.

4. The Vitrification Facility will combine the washed sludge solids, the ion exchange material (zeolite) containing the radioactive cesium, and a small amount of acidic (THOREX process) waste with glass former chemicals; process this mixture through a slurry-fed ceramic melter; and produce approximately 300 0.6 m x 3 m glass logs which will be the ultimate waste form.

This report provides details on the equipment and methods used, the information gained, and the utility of this information.

1. INTRODUCTION

The West Valley Demonstration Project Act of October 1, 1980, (Public Law 96-368) directs the Department of Energy (DOE) to carry out a high-level radioactive waste (HLW) management demonstration project at the West Valley site. Under the Act, the Department is responsible for removing the HLW from the tanks and solidifying it in a form suitable for ultimate transportation to a federal repository for final disposal. The DOE facility at West Valley, New York, was formerly operated by Nuclear Fuel Services, Inc., (NFS) as a commercial nuclear fuel reprocessing plant. West Valley Nuclear Services Co., Inc. (WVNS), a subsidiary of Westinghouse Electric Corporation, was selected to be the prime contractor for site operations, and officially took over site operations in February of 1982.

The West Valley site was the location of the first (and only) operating commercial nuclear fuel reprocessing center in the United States. NFS operated this facility from 1966 to 1972, processing 640 metric tons of commercial and defense fuels using the PUREX process. Approximately 2.1 million litres of fuel reprocessing wastes resulted from this reprocessing operation. The major portion (~98 percent by volume) of these wastes are stored in a single vaulted underground storage tank, designated 8D-2. The bulk of its contents was formed by adding excess caustic (NaOH) to a nitric acid-based stream originating from the operation of the NFS reprocessing plant to reprocess uranium fuel using the PUREX process, although other additions of decontamination and cleanup waste have been made. Concentration of the neutralized solution has resulted in the formation of a sludge layer at the bottom of the waste tank. A small amount of acidic (THOREX) waste is stored separately (in a tank designated 8D-4) as a result of a special campaign to process a mixed uranium-thorium fuel.

Early in the project, two decisions were made which determined the major thrust of the effort:

1. The HLW alkaline supernatant would be separated from the sludge, and the radioactive components in the supernatant would be chemically separated and combined with the sludge into a HLW terminal form. The treated supernatant would be processed into a suitable low-level waste (LLW) form (the separated salt/sludge option of the Final Environmental Impact Statement).[1]

2. The HLW terminal form would be borosilicate glass.

It then became important that various characteristics of the waste become defined to support the effort leading to final design of the overall process. Some of the broad categories of this effort were:

1. Defining the chemical composition of the 8D-2 tank liquid* to allow preparation of suitable simulants.

* Henceforth, the 8D-2 tank alkaline liquid will be referred to as the supernatant.

2. Defining the radiological composition of the supernatant to determine decontamination necessary to produce a LLW form and the parameters necessary for its long-term storage (environmental assessment).

3. Defining the chemical/radiological composition of the 8D-2 sludge solids and the THOREX waste in order to develop vitrification processing parameters and a reference glass formulation that would meet both durability and processibility specifications.

4. Developing tank topography and physical (in situ) characteristics of the 8D-2 sludge in support of the design of the sludge mobilization process.

5. Use of actual supernatant in-cell to verify decontamination parameters and the workability of the reference series operation (with Shanks process rotation) of the ion exchange (IX) columns.

6. Use of actual decontaminated supernatant to determine physical characteristics for detailed Supernatant Treatment System (STS) design and to make concrete cylinders to verify leaching parameters of the LLW form.

7. Use of actual 8D-2 sludge in-cell to determine physical characteristics and processing parameters such as washability and settling rates.

In addition to the general task of "obtaining as much information as possible regarding the high-level waste," several "miscellaneous" projects were conducted under the auspices of the Waste Characterization Program. These included:

1. Video camera inspection of the 8D-4 and 8D-3 (spare to 8D-4) tanks.

2. Temperature profiling of 8D-2 tank/vault system and its contents.

3. Sampling of the solids at the bottom of the 8D-1 tank (spare to 8D-2).

2. SUMMARY

Table 1 summarizes the major accomplishments of the Waste Characterization Program. In the discussion that follows, the activities are reported from a "systems" standpoint rather than in chronological order.

3. 8D-2 SUPERNATANT CHEMICAL CHARACTERIZATION

The initial project under the Waste Characterization Program was sampling and analysis of the 8D-2 supernatant. At this time, there was minimal analytical capability on site, so we worked closely with Westinghouse Advanced Reactors Division (now Advanced Energy System Division) Laboratory in Madison, Pennsylvania, who were contracted to receive the samples and perform the analyses. Since this was the Project's first direct contact with the HLW and breach of the containment system, a considerable amount of planning and mockup testing went into the sampling methods and procedures.

TABLE 1: WASTE CHARACTERIZATION ACCOMPLISHMENTS

Item	Results
1. Sampled and analyzed 8D-2 supernatant.	1. Determined complete chemical/ radiological makeup of HLW alkaline liquid. Refined estimate of solids content. Homogeneity inferred from multiple samples.
2. Sampled and analyzed 8D-4 waste.	2. Determined complete chemical/ radiological makeup of acidic HLW. Inferred presence of precipitated solids through a thorium balance where production records indicated more Th transferrred to 8D-4 than accounted for by this analysis.
3. Performed Buoyancy probe testing in 8D-2 tank.	3. Measured supernatant density at tank temperature. Verified supernatant homogeneity by constancy of density. Determined location of "hard" and "soft" layers at one location.
4. Performed shear vane testing in 8D-2 tank.	4. Determined shear strength properties (by resistance to rotation of a devise of known geometry) in the hard and soft sludge layers (two locations in each).
5. Performed extended buoyancy probe testing in 8D-2 tank.	5. Modified buoyancy probe (Item 3) with use of articulated arm. Mapped hard and soft layers within a 3 m diameter circle.
6. Obtained "undisturbed" 8D-2 sludge core sample. Obtained horizon samples representing ~80 percent of hard layer.	6. Discovered high sulfate layer in bottom 75 mm. Updated chemical/ radiological sludge solids composition based on analytical work. Used sludge sample with other components to make radioactive glass.
7. Performed in-cell batch equilibrium tests with real supernatant and several candidate decontamination reagents (Na-TPB, Na-TiA, CS-100,^{R} IRC-718^{R}, IE-95^{R}, PTA, Ni/Cu FeCN).	7. Verification/extension of PNL tests with simulant.
8. Performed single-column test with IE-95^{R} and Durasil^{R}.	8. Verification/extension of PNL tests with simulant.

TABLE 1: WASTE CHARACTERIZATION ACCOMPLISHMENTS (CONTINUED)

Item	Results
9. Performed in-cell 3-column test with IE-96® simulating design series operation.	9. Average cesium decontamination factor (DF) of >2 x 10^5 was demonstrated with >95 percent zeolite utilization.
10. Column effluent was used to make cement cylinders; performed leach tests for Cs, Sr, and Pu.	10. Obtained significantly lower leachability than maximum allowed by NRC for class "C" wastes.
11. Column effluent used to measure physical properties as a function of dilution and temperature: density, viscosity, boiling point rise (BPR), crystalization and freezing points, total dissolved solids (TDS), pH.	11. Correlated and summarized properties for use as STS design data.
12. Obtained second sample of hard and soft layer in 8D-2.	12. Viscometer data obtained, sludge washing simulated, settling rate measured, particle and bulk densities measured; updated sludge solids composition based on additional analytical work; wash solution composition determined.
13. Performed 8D-2 temperature profiling (vault/tank annulus).	13. Verified that potential concrete temperatures/differentials were within specifications for STS construction.
14. Performed temperature probe of 8D-2 sludge.	14. Soft layer near supernatant temperature - thermal convection is controlling; hard layer follows math model for conduction in a heat-generating flat plate insulated at the bottom; thermal conductivity calculated.
15. Performed 8D-3 & 8D-4 in-tank video inspection.	15. 8D-3 tank in good condition for use in STS process. Verified presence of crystalline thorium phase in 8D-4.
16. Sampled 8D-1 solids.	16. Material was mostly sand with low iron content.

Method of Sampling

It was decided that multiple samples at different depths were needed to verify homogeneity and improve analytical precision. Other constraints that were applied to the sampling operation were:

1. The sampling was to take place through a 200 mm riser opening (a result of removing the shield plug in the tank's only accessible riser).

2. There was to be no transferring of liquid to the surface other than the contained sample volume (~8 mL) from each level.

3. There was to be no transfer of liquid after obtaining the sample, i.e., the sample was to be taken in the "to be shipped" container.

4. A minimum amount of equipment was to contact the liquid. That which did make contact was to be capable of decontamination by a water flush prior to bringing it to the surface.

5. The apparatus was to be able to take representative samples at a given depth.

A drawing of the device used is shown in Figure 1.

The key component is a Penberthy* air jet eductor, which uses a 689-kPa air supply as the motive force. This eductor has a hydraulic connection through a support block to a 15-gage hypodermic needle. A second 15-gage hypodermic needle has hydraulic connection through the same block to a manifold with two lengths of tubing attached for taking samples at different depths. The two needles are spaced such that they can both be inserted through a neoprene plenum into a sample vial. Operation of the eductor sets up a circulation from the tank into the vial and then out through the eductor. The tubing is attached to a weighted cable which is hung from the support block. The entire device was lowered into the riser with a winch.

In order to simplify procedures, only two lengths of tubing were used, which were valved to the manifold. They were precut, such that four depths could be sampled by using two marks on the cables, which were lined up with the top of the riser flange. Samples were taken at 0.3 and 1.5 m below the vapor/solution interface at one depth setting and 4.6 and 5.8 m below the interface at the second depth setting.

After each sample was taken, a special set of tongs was used to remove the sample vial (10-mL "pyramid" bottle) and reload a second one. One problem that was discovered during mock-up testing was incomplete sealing of the neoprene after removal from the needles. To seal the openings, a vinyl coating was sprayed over the top. This was not completely successful, and on subsequent samples, caps were replaced before transporting off-site.

* Penberthy Division of Houdaille Industries, Prophetstown, IL

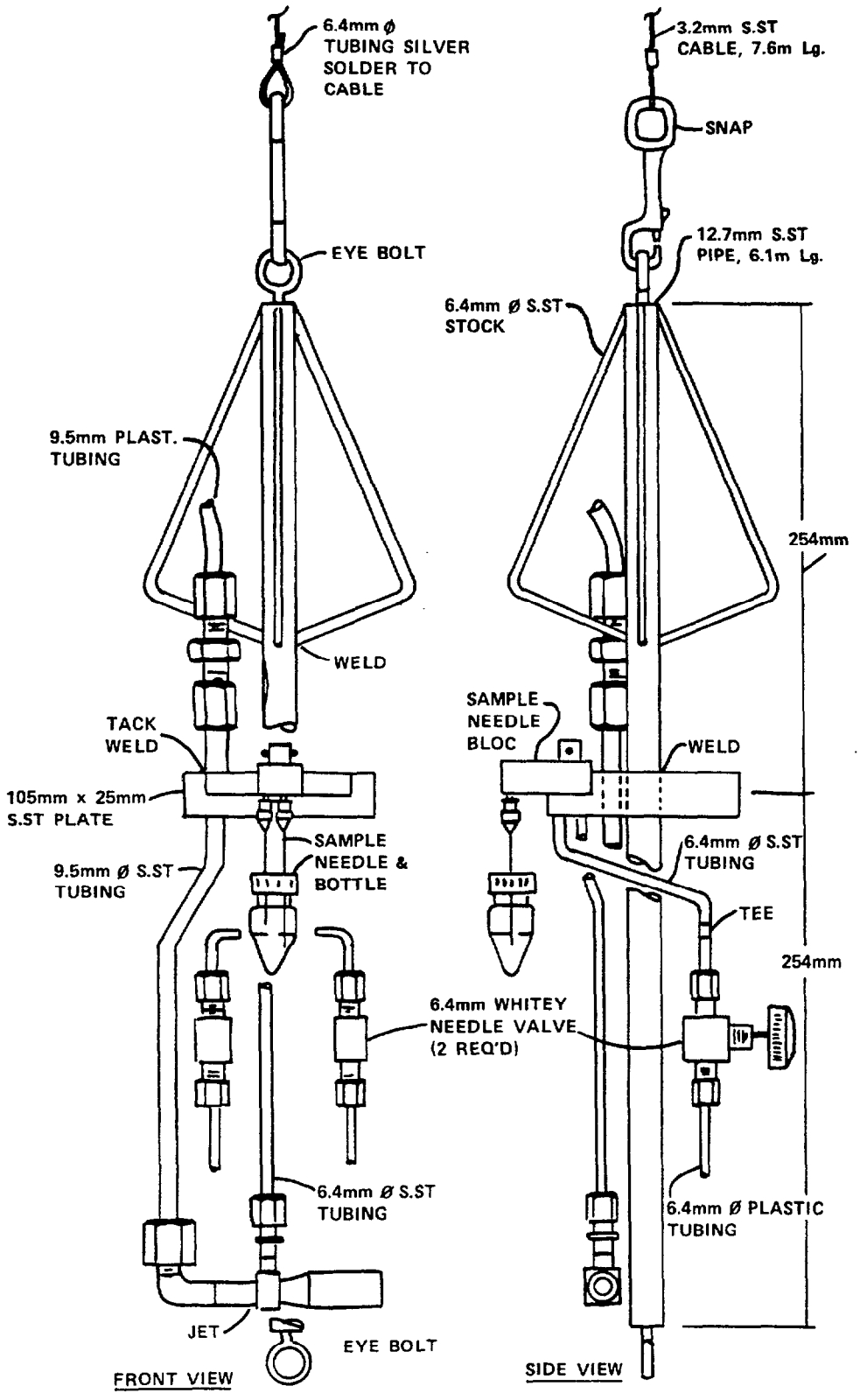

FIGURE 1
Supernatant Sampling Device

After the last sample was removed, a clean bottle was placed over the needle, and the needle block removed, bagged, and placed in a shielded container. A water flush block was installed on the sampler, the samples lowered about 61 cm into the riser, and the block, valves, tubing, and eductor water-flushed. A water spray ring was fashioned to wash the externals of the apparatus when it was brought to the surface. The items that were in contact with the liquid (weighted cable and tubes) were cranked into a wooden box (for beta shielding) which was equipped with a false bottom. (See Figures 2, 3, and 4.)

This basic device and procedure turned out to be very successful - there was no spread of contamination and minimal personnel exposure - and consequently has been used several times to draw liquid samples from the HLW tanks.

Supernatant Analytical Work

The flow sheets for the analytical work as performed by Westinghouse Laboratories are shown in Figures 5 and 6. A detailed description of the analytical methods is beyond the scope of this report.

The specific gravity of the three samples was found to be 1.320 ± 0.004 at 20°C. An average of 84 ppm of suspended solids were found in the samples. The concentration did not appear to be a function of depth. A later resampling was made to determine if these suspended solids were the result of the operation of air spargers in the tank for hydrogen purging. The second set of samples (taken after the air spargers had been off for approximately two months) yielded the same results. Since these solids settled in the samples, it was hypothesized that their suspension was a result of convection currents in the tank due to radioactive self-heating.

In order to aid in the preparation of simulated solutions, the chemical compositional data was converted to various salts. Some assumptions had to be made regarding the form of some of the elements. For example, chromium was assumed to be in the form of the chromate ion, $CrO_4^=$, because of the distinctive yellow color of the solution. Table 2 gives the chemical compositional data (average of three samples) in weight percent salt and kilograms of this salt in the tank. Independent data (See Section 5) was used to determine total kilograms in the tank.

In order to derive this table, it was necessary to resolve the cation/anion imbalance. This was done by "adjusting" the Na^+, NO_3^- and NO_2^- in proportion to the percent relative standard deviation (RSD) of the analysis. The adjustment did not exceed percent RSD for these components. Tellurium (Te as TeO_4^{2-}) and selenium (Se as SeO_4^{2-}) were not determined analytically but were included in the indicated amounts (See Table 2) to be consistent with fission yield calculations[2].

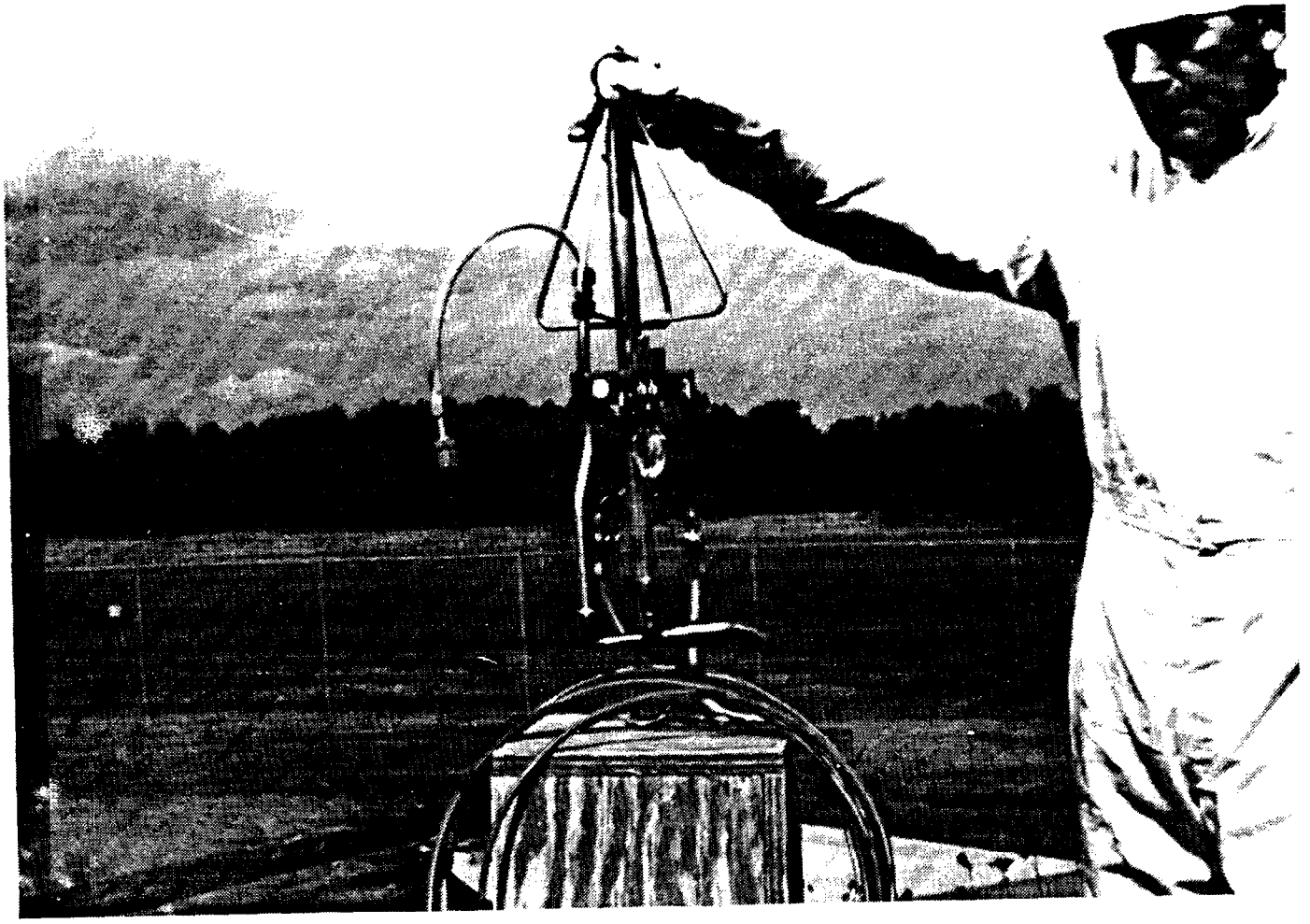

FIGURE 2
Supernatant Sampling Equipment

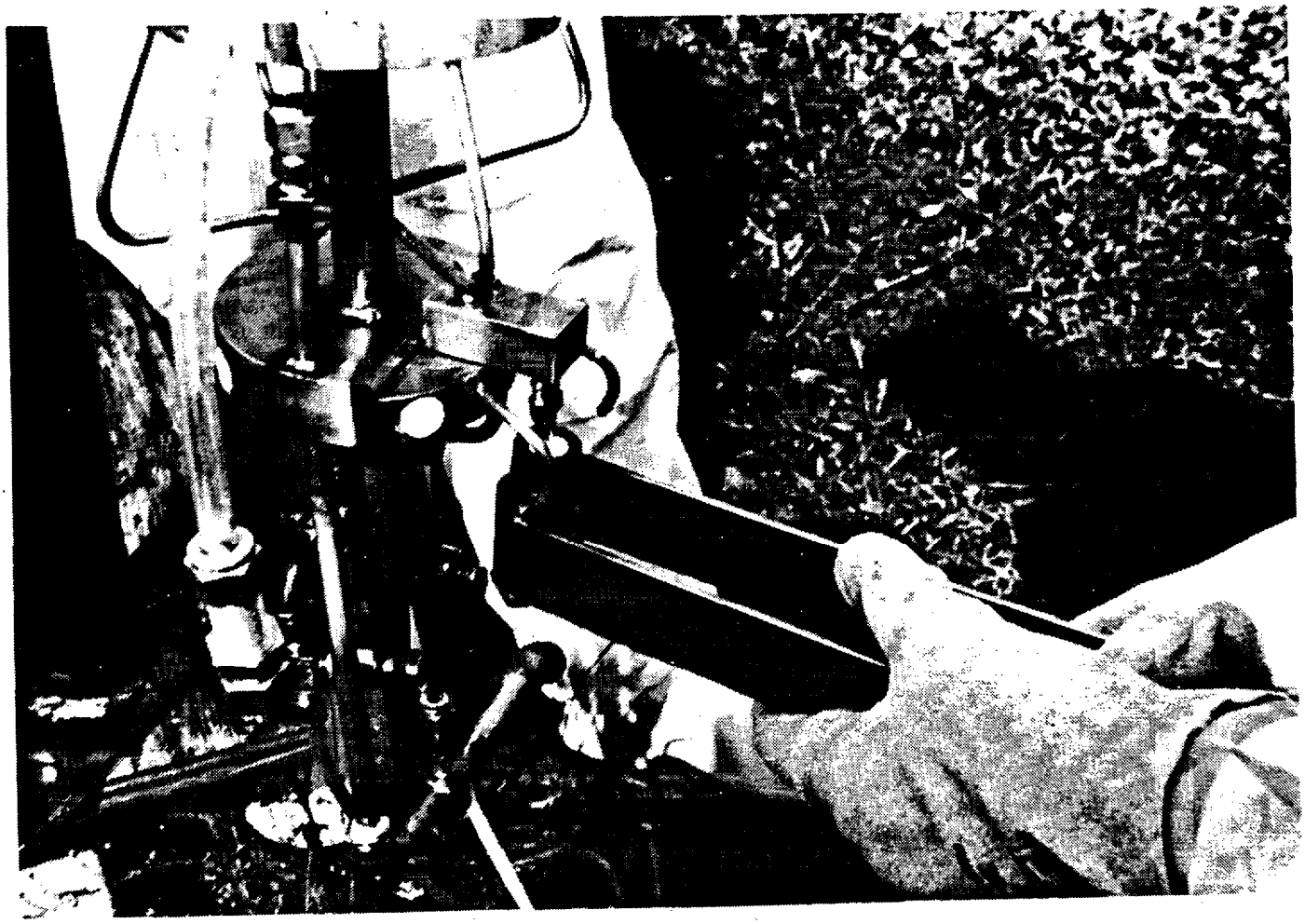

FIGURE 3
Demonstration of Sample Vial Replacement

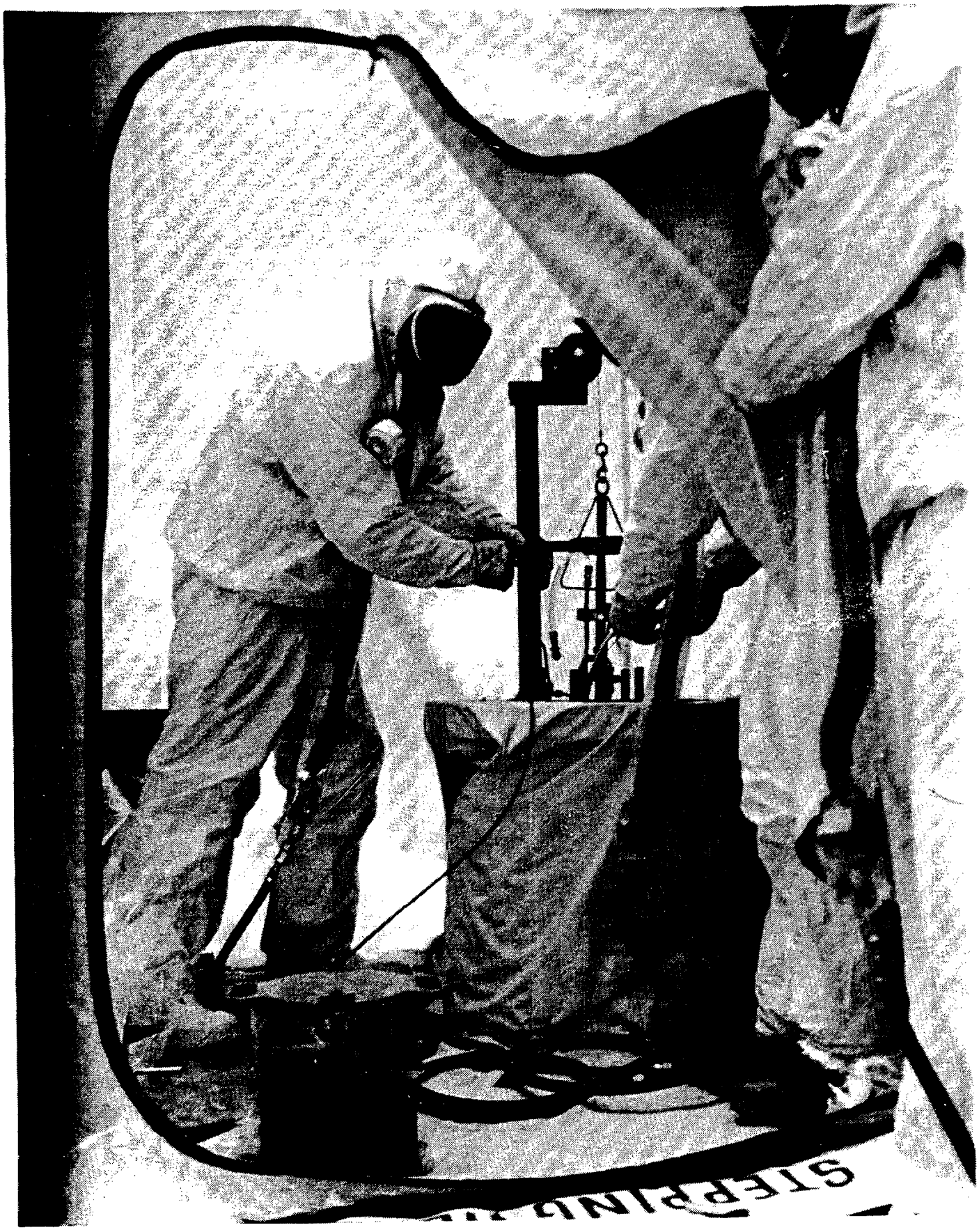

FIGURE 4
Supernatant Sampler Being Lowered into Riser

Sample Receipt

Filtration and Solution Density Determination

Status Report

Dilution	Species measured
Spectrometry	Elemental Impurities Rare Earths Noble Metals
Atomic Absorption	Na, K, Cs, Sr
Ion Chromatography	F, Cl, NO_2, Po_4, NO_3, SO_4, Oxalate
Acid Titration after Carbonate Precipitation	OH
Titration with pH Monitoring	H_2CO_3, HCO_3, CO_3
Radiochemistry	See Radiochemistry flow sheet

Status Report

Final Report

Figure 5 Supernatant Analytical Flow Sheet

Sample

Dilute

Diluted Sample	Species Measured
Gamma Spectrometry	^{137}Cs, ^{134}Cs, ^{125}Sb, ^{106}Ru
Ruthenium Separation	^{106}Ru
Antimony Separation	^{125}Sb
Rare Earth Separation	Gamma Count, ^{144}Ce Beta Count, Total Rare Earth
Strontium Separation	^{90}Sr, ^{90}Y
Alpha Spectrometry	All Significant Alpha Emitters
Am, Cm Separation	^{241}Am, ^{242}Am, ^{244}Cm
Mass Spectrometry	Uranium, Plutonium, and Neodymium
Other Determinations	^{3}H, ^{14}C, ^{99}Tc, ^{29}I

Figure 6 Radiochemistry Flow Sheet

TABLE 2: 8D-2 SUPERNATANT CHEMICAL COMPOSITION

Compound	Wt. % Wet Basis	Wt. % Dry Basis	Total Kg in Supernatant
$NaNO_3$	21.10	53.38	602,659
$NaNO_2$	10.90	27.57	311,326
Na_2SO_4	2.67	6.76	76,261
$NaHCO_3$	1.49	3.77	42,557
KNO_3	1.27	3.21	36,274
Na_2CO_3	0.884	2.24	25,249
NaOH	0.614	1.55	17,537
K_2CrO_4	0.179	0.45	5,113
NaCl	0.164	0.42	4,684
Na_3PO_4	0.133	0.34	3,799
Na_2MoO_4	0.0242	0.06	691
Na_3BO_3	0.0209	0.05	597
$CsNO_3$	0.0187	0.05	534
NaF	0.0176	0.04	503
$Sn(NO_3)_4$	0.00859	0.02	245
$Na_2U_2O_7$	0.00808	0.02	231
$Si(NO_3)_4$	0.00806	0.02	230
$NaTcO_4$	0.00620	0.02	177
$RbNO_3$	0.00416	0.01	119
Na_2TeO_4	0.00287	0.007	82
AlF_3	0.00271	0.007	77
$Fe(NO_3)_3$	0.00152	0.004	43
Na_2SeO_4	0.00054	0.001	15
$LiNO_3$	0.00048	0.001	14
H_2CO_3	0.00032	0.0008	9
$Cu(NO_3)_2$	0.00022	0.0005	6
$Sr(NO_3)_2$	0.00013	0.0004	4
$Mg(NO_3)_2$	0.00008	0.0002	2
TOTAL	39.53	100.00	1,129,038
H_2O (by difference)	60.47		1,727,164

NOTE: pH = 10.0

The main components are those that can be identified with the PUREX process as applied to West Valley (See Table 3). The processing wastes were neutralized with sodium hydroxide before transfer to the tank. This produced insoluble hydroxides of fission products and metals which settled forming a sludge layer. The volume of the sludge is about seven percent of the total waste volume.

The main constituent of the supernatant is sodium nitrate. Reaction with hydrogen formed by radiolytic degradation resulted in conversion of about one-third of the nitrate to nitrite:

$$NaNO_3 + H_2 \rightarrow NaNO_2 + H_2O$$

Sulfate resulted from the use of ferrous sulfamate [$Fe(NH_2SO_3)_2$] as a reducing agent. Phosphate came from destruction of the tributyl phosphate (TBP) used as the organic solvent. Sodium carbonate was used for removal of degradation products in the TBP. Potassium cations resulted from the use of potassium permanganate ($KMnO_4$) as a decontamination agent. Chloride probably resulted primarily from impurities in the caustic used. Fluoride was added by the use of ammonium fluoride (NH_4F) to dissolve zirconium fines in dissolver cleaning campaigns and to unplug lines. The oxalate anion was looked for, since it was thought to be the largest organic addition. Its absence (below detection limits) lends credence to the belief that any organic input has since decomposed.

Radiological Composition

The results of the gamma spectrometry together with the ruthenium, antimony, strontium, and rare earth separations are given in Table 4. Since all cesium salts are soluble, chemical and radioactive cesium was able to be used as a tracer together with U-235 fission yield data[2] to calculate the effective decay time of the U-235 fission products. An effective total calculated decay time of 19.1 years (basis 7/1/87) is in reasonable agreement with processing data. Based on these tracer calculations, Table 5 summarizes fission product elemental components.

Checks on other soluble components were reasonably close:

Element	Calculated (µg/g)	Analytical (µg/g)
Mo	128	113
Rb	18	24
Tc	32	33

Although solubility of most of the fission metal hydroxide/sulfate/carbonate/fluoride was assumed to be negligible, this could not be confirmed in many cases because of detection limits. In the case of the rare earths, separation and beta counting of the isotopes compared to fission yield totals inferred a solubility of the rare earth hydroxides of <0.02 percent of the total. The low solubility of the rare earths was further confirmed by separation and determination of Nd-148. A detection limit of <0.02 µg/g of supernatant translates to <0.15 percent of total Nd-148 in solution.

TABLE 3: CHEMICALS AND MATERIALS USED BY WEST VALLEY REPROCESSING FACILITY

Process/System	Chemicals/Materials Used
Chop-leach	Mild steel
	$Hg(NO_3)_2$
	HNO_3
Solvent Extraction	$Fe(SO_3NH_2)_2$
	$NaNO_2$
	HSO_3NH_2
	NaOH
Solvent & treatment	Tributyl phosphate (TBP)
	Na_2CO_3
	Dodecane, $C_{12}H_{26}$
D & D	$HNO_3 + H_2C_2O_4$
	$NaOH + H_6C_4O_6$
	$NH_4F + Al(NO_3)_3$
	$KMnO_4$
Zirflex Declad	$NH_4F + NH_4NO_3$
	$HF + HNO_3$
	$Al(NO_3)_3$
Metal X Fire system	$NaCl + MgCl_2$
Lab chems	Misc.
Maintenance	Molykote (MoS_x)
	Oils and greases

TABLE 4: GAMMA-RAY SPECTROMETRY AND SEPARATION

Species	Filtered Solution (mCi/g)	Error*(%)
^{137}Cs	2.83	0.2
^{134}Cs	2.34×10^{-2}	3.0
^{90}Sr	1.13×10^{-3}	1.0
^{125}Sb	5.5×10^{-5}	12
^{106}Ru	$<1.5 \times 10^{-5}$	N/A
^{144}Ce	$<7.6 \times 10^{-7}$	N/A
Rare earth, β^-	2.1×10^{-4}	3.0

* Percent error for radioactive elements is based on the 95 percent error and is equal to 1.96 x percent RSD.

TABLE 5: FISSION PRODUCT CONTENT OF TANK 8D-2

Element*	At. wt. (av)	Element in Supernatant (kg)	Assumed Form	Element in Sludge (kg)	Assumed† Form	Comments
Se	81.0	6.5	$SeO_4^{=}$	0.0		Assumed 100% soluble
Rb	86.3	68.7	Rb^+	0.0		Analytical; assumed 100% soluble
Sr	89.1	1.6	Sr^+	103.0	$SrSO_4$	
Y	89.0	~0		65.7	$Y(OH)_3$	
Zr	93.2	~0		465.2	$Zr(OH)_4$	< 9.1 kg in supernatant (detection limit)
Mo	97.5	322.0	$MoO_4^{=}$	0.0		Analytical; assumed 100% soluble
Tc	99.0	94.1	$Tc_2O_7^{=}$	0.0		Assumed 100% soluble
Ru	101.2	~0		274.2	$Ru(OH)_4$	<456 kg in supernatant (detection limit)
Rh	103.0	~0		48.2	$Rh(OH)_4$	<456 kg in supernatant (detection limit)
Pd	105.6	~0		25.9	$Pd(OH)_2$	<456 kg in supernatant (detection limit)
Ag	109.0	~0		0.6	AgOH	< 0.9 kg in supernatant (detection limit)
Cd	113.1	~0		1.3	$Cd(OH)_2$	< 9.1 kg in supernatant (detection limit)
In	115.0	~0		0.2	$In(OH)_3$	< 4.6 kg in supernatant (detection limit)
Sn	120.7	~0		1.6	$Sn(OH)_4$	Analytical shows 79.3 kg in supernatant‡
Sb	122.1	~0		0.5	$Sb(OH)_3$	< 9.1 kg in supernatant (detection limit)
Te	129.5	44.3	$TeO_4^{=}$	0.0		Assumed 100% soluble
Cs	134.8	365.0	Cs^+	0.0		Assumed 100% soluble
Ba	137.8			178.4	$BaSO_4$	< 9.1 kg in supernatant (detection limit)

* Only those >0.1 kg listed.

† No firm basis for these assumptions; may also be carbonates and fluorides present.

‡Evidently there was Sn input other than fission product.

FIGURE 8
WEST VALLEY HLW
PROCESSING FLOW SHEET

TABLE 5: FISSION PRODUCT CONTENT OF TANK 8D-2 (Continued)

Element	At. wt (av)	Element in Supernatant (kg)	Assumed* Form	Element in Sludge (kg)	Assumed† Form	Comments
La	139.0	~0		135.2	$La(OH)_3$	<48.7 kg in supernatant (detection limit)
Ce	141.0	~0		260.3	$Ce(OH)_3$	<48.7 kg in supernatant (detection limit)
Pr rare	141.0	~0		125.1	$Pr(OH)_3$	<48.7 kg in supernatant (detection limit)
Nd earths	144.7	~0		458.8	$Nd(OH)_3$	< 0.06 kg in supernatant (detection limit)
Pm	147.0	~0		1.1	$Pm(OH)_3$	<48.7 kg in supernatant (detection limit)
Sm	148.6	~0		106.3	$Sm(OH)_3$	<48.7 kg in supernatant (detection limit)
Eu	152.6	~0		4.9	$Eu(OH)_3$	<48.7 kg in supernatant (detection limit)
Gd	155.7	~0		1.3	$Gd(OH)_3$	< 4.8 kg in supernatant (detection limit)
Total		808.1		2349.9		

* Only those >0.1 kg listed.

† No firm basis for these assumptions; may also be carbonates and fluorides present.

‡ Evidently there was Sn input other than fission product.

For the transuranic (TRU) components, analytical results were able to give the amount of plutonium in solution and the isotopic breakdown. Less-than detectable amounts of Am-241 ($<1.5 \times 10^{-7}$ mCi/g), Am-243 ($<2 \times 10^{-7}$ mCi/g), and Cm-244 ($<6 \times 10^{-8}$ mCi/g) were found.

Based on a combination of analytical and theoretical considerations, a reference radionuclide content of the supernatant was generated (See Table 6). Some highlights of the radionuclide determination:

1. Radionuclide content was such that solidification, e.g., in cement would make a class "C" LLW form as defined by 10 CFR Part 61[3].

2. Cesium-137 together with its short-lived daughter product, Barium-137m, accounted for 99.9 percent of the curie activity.

3. Production of a class "A" waste form could be accomplished by a large decontamination factor (DF) (~10,000) on cesium together with some removal of Sr-90, Tc-99, and plutonium (DFs ~10).*

It was later decided that the decontamination necessary to produce a class "A" waste form was not cost-effective and that a target DF of 1,000 for cesium to produce a "low curies" Class "C" waste form would be the goal.

The supernatant sampling/analysis work was also used to give an initial reference chemical and radiological composition for the sludge. This was done by using the analytical data in conjunction with NFS processing data, chemical purchasing records, and theoretical fission yield/actinide production calculations. This initial reference was later refined by sampling and analysis of the sludge solids (See Section 5).

Supernatant In-Cell Work

Once adequate data existed on the chemical and radiological makeup of the supernatant, Battelle Pacific Northwest Laboratories (PNL) was designated the lead research organization to develop a reference process for supernatant decontamination.[4] Their work with spiked, simulated supernatant was supplemented by in-cell work done with real supernatant at WVNS. Batch equilibrium tests were done with several candidate decontamination reagents. Inorganic ion exchangers (Union Carbide Linde Ionsiv® IE-95, IE-96 and Durasil®, from the Duratek Corp.), organic precipitation agents (sodium tetraphenyl boron and sodium titanate), organic ion exchangers (Duolite® CS-100 and Amberlite® IRC-718), and the use of phosphotungstic acid and nickel and copper ferrocyanides as precipitation agents were screened[5]. In doing this work, it was necessary to use master slave manipulators (MSMs) that were not in good mechanical condition and only partially functional (they have since been replaced). Consequently, specialized equipment was designed and fabricated to compensate for their deficiencies (See Figure 7).

* Since classification is based on a "sum of fractions" rule, class "A" could be achieved by various combinations of DFs.

TABLE 6: SUPERNATANT RADIONUCLIDE COMPOSITION
(as of 7/1/86)

Isotope	$T_{1/2}$ (Half Life)	Ci	Method of Decay Correction
H-3	12.3 yr	103	$x\ e^{-\lambda\tau *}$
C-14	5,730 yr	137	$x\ e^{-\lambda\tau}$
Ni-63	92 yr	895	$x\ e^{-\lambda\tau}$
Se-79	6.5×10^4 yr	37	$x\ e^{-\lambda\tau}$
Sr-90	29 yr	2,956	$x\ e^{-\lambda\tau}$
Y-90	64 hr	2,956	Same as Sr-90 (short-lived daughter)
Zr-93	1.53×10^6 yr	0.23	$x\ e^{-\lambda\tau}$
Nb-93m	13.6 yr	0.14	From decay chain Zr-93 →Nb-93m →Nb-93
Tc-99	2.13×10^5 yr	1,599	$x\ e^{-\lambda\tau}$
Ru-106	368d	2.8	$x\ e^{-\lambda\tau}$
Rh-106	30s	2.8	Same as Ru-106 (short-lived daughter)
Pd-107	6.5×10^6 yr	1.2×10^{-2}	$x\ e^{-\lambda\tau}$
Cd-113m	14.6 yr	21	$x\ e^{-\lambda t}$
Sn-121m	50.0 yr	1.5E-3	$x\ e^{-\lambda t}$
Sb-125	2.73 yr	72	$x\ e^{-\lambda\tau}$
Te-125m	58d	16.6	23% of Sb-125 (short-lived daughter, 23% of Sb-125 → Te 125m)
Sn-126	1.05×10^5	0.40	$x\ e^{-\lambda\tau}$
Sb-126m	19m	0.40	Same as Sn-126 (short-lived daughter)
Sb-126	12.5d	0.16	40% of Sb-126m based on 40% of Sb-126m→ Sb-126
I-129	1.59×10^7 yr	0.21	$x\ e^{-\lambda\tau}$
Cs-134	2.06 yr	1.94×10^4	$x\ e^{-\lambda\tau}$
Cs-135	2.3×10^6 yr	156	$x\ e^{-\lambda\tau}$
Cs-137	30.0 yr	7.43×10^6	$x\ e^{-\lambda\tau}$

TABLE 6: SUPERNATANT RADIONUCLIDE COMPOSITION (CONTINUED)

(as of 7/1/86)

Isotope	$T_{1/2}$ (Half Life)	Ci	Method of Decay Correction
Ba-137m	2.5m	6.98×10^{6}	94% of Cs-137 (short-lived daughter, 94% of Cs-137 → Ba-137m)
Ce-144	284d	7.23×10^{-5}	$\times e^{-\lambda\tau}$
Pr-144	17m	7.23×10^{-5}	Same as Ce-144 (short-lived daughter)
Pm-147	2.62 yr	217	$\times e^{-\lambda\tau}$
Sm-151	93 yr	1.11	$\times e^{-\lambda\tau}$
Eu-152	13.4 yr	4.47×10^{-2}	$\times e^{-\lambda\tau}$
Eu-154	8.2 yr	14.9	$\times e^{-\lambda\tau}$
Eu-155	4.76 yr	2.73	$\times e^{-\lambda\tau}$
U-233	1.59×10^{5} yr	0.5	$\times e^{-\lambda\tau}$
U-234	2.44×10^{5} yr	0.3	$\times e^{-\lambda\tau}$
U-235	7.04×10^{8} yr	6.5×10^{-3}	$\times e^{-\lambda\tau}$
U-236	2.34×10^{7} yr	2.0×10^{-2}	$\times e^{-\lambda\tau}$
U-238	4.47×10^{9} yr	5.8×10^{-2}	$\times e^{-\lambda\tau}$
Pu-238	87.7 yr	130	$\times e^{-\lambda\tau}$
Pu-239	2.4×10^{4} yr	25	$\times e^{-\lambda\tau}$
Pu-240	6,537 yr	19	$\times e^{-\lambda\tau}$
Pu-241	14.4 yr	1.58×10^{3}	$\times e^{-\lambda\tau}$
Pu-242	3.8×10^{5} yr	2.50×10^{-2}	$\times e^{-\lambda\tau}$

* $\lambda = \frac{\ln 2}{T_{1/2}}$

τ = Time from reference (may be negative)

$T_{1/2}$, τ in same units

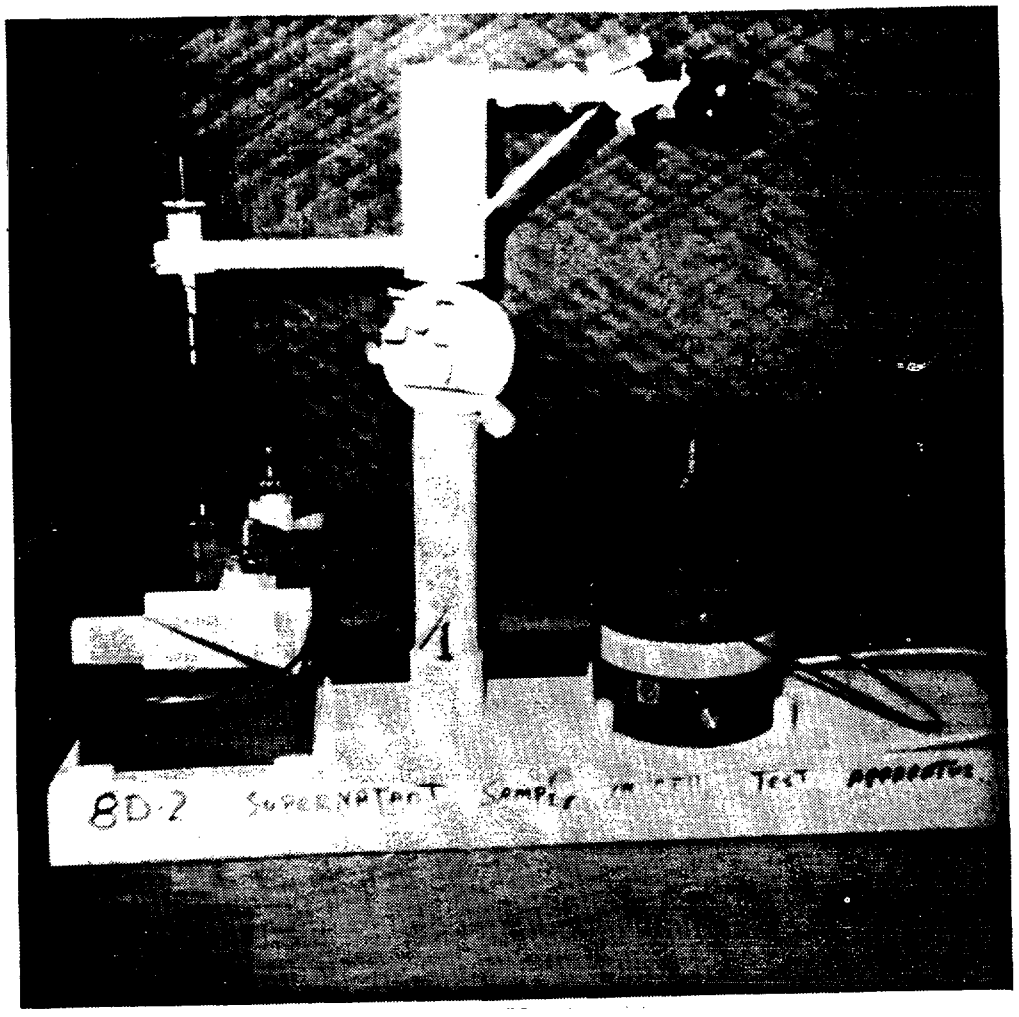

FIGURE 7
Supernatant In-Cell Test Apparatus

The detailed evaluations that were done on each of these processes are beyond the scope of this report. For preliminary design purposes, an inorganic ion exchange process was selected as a reference. Column tests performed both at PNL and WVNS narrowed the selection down to the IE-96 reference. Basic considerations in this selection were a high selectivity for cesium and compatibility of the loaded ion exchange media with the borosilicate glass form (the zeolite will be blended with the rest of the HLW streams (washed PUREX sludge solids, and THOREX) waste and with glass former chemicals to produce the feed to the slurry fed melter (See Figure 8).

The in-cell supernatant work culminated in a test in which ~500 mL of supernatant (obtained with the same apparatus as described earlier, except that 50 mL bottles were used rather than 10 mL vials) were run through three columns in series, each containing 12.86 gms of dry zeolite. After filtering through a 0.2 micron Gelman Acrodisc® filter, the feed bottle was fitted with a rubber stopper, such that it could be pressurized with nitrogen which forced the supernatant through the three columns in series. The overall flow rate was adjusted by a needle valve in the first column feed line, and was based on the "drip rate" from the third column. This control method was very effective and little trouble was encountered in maintaining a 0.2 cv/hr (column volume/hour) flow rate (See Figures 9 and 10).

The relative amount of supernatant/exchanger was such as to insure full loading of the first column and the start of breakthrough on the third column. At that point, in the reference process, the first column would be taken out of service, and the third column in the series replaced with a freshly charged column (Shanks process). The main conclusions resulting from this test were:[6]

1. A four-column system (three operating in series at all times with a fourth column off-line for recharging) is necessary in order to minimize zeolite usage and operating time and maximize the chemical cesium DF. A chemical DF $>2 \times 10^5$ with a theoretical zeolite utilization >95 percent (percent of saturation loading when in equilibrium with starting feed) can be theoretically obtained with this system.

2. If only two columns were operated in series, there would be a sacrifice of either DF, zeolite utilization, or both. For example, a DF of 2×10^5 would be obtainable with a zeolite utilization of 82 percent (See Table 7 and Figures 11 and 12) or a zeolite utilization of 92 percent would be possible with a DF of 3×10^3. Another option would be to stop throughput while the loaded column was recharged, thus increasing processing time.

3. Based on (1) and (2), it was concluded that the four-column design was conservative (a loss of one column would not be "catastrophic") and would have a high probability of meeting the target of a DF greater than 1,000.

4. As can be seen from the loading curve (Figure 13), the capacity of the IE-96 based on simulated supernatant is ~20 percent greater than with real supernatant. This has been a consistent result in batch equilibrium and column tests with both IE-95 and IE-96. We have not been able to come up with an explanation for this, but are convinced that it is real.

TABLE 7: COLUMN LOADING SUMMARY

No Operating Columns	Total CV Throughput	Percent Loading 1	2	3	Average DF
3	25	92.4	16.6	0.3	5×10^6
3	30	97.4	32.7	1.3	2×10^5
3	35	99.8	49.7	4.1	1×10^4
2	20	82.0	29.6	---	2×10^5
2	25	92.4	16.6	---	3×10^3

WEST VALLEY HLW PROCESSING FLOW SHEET

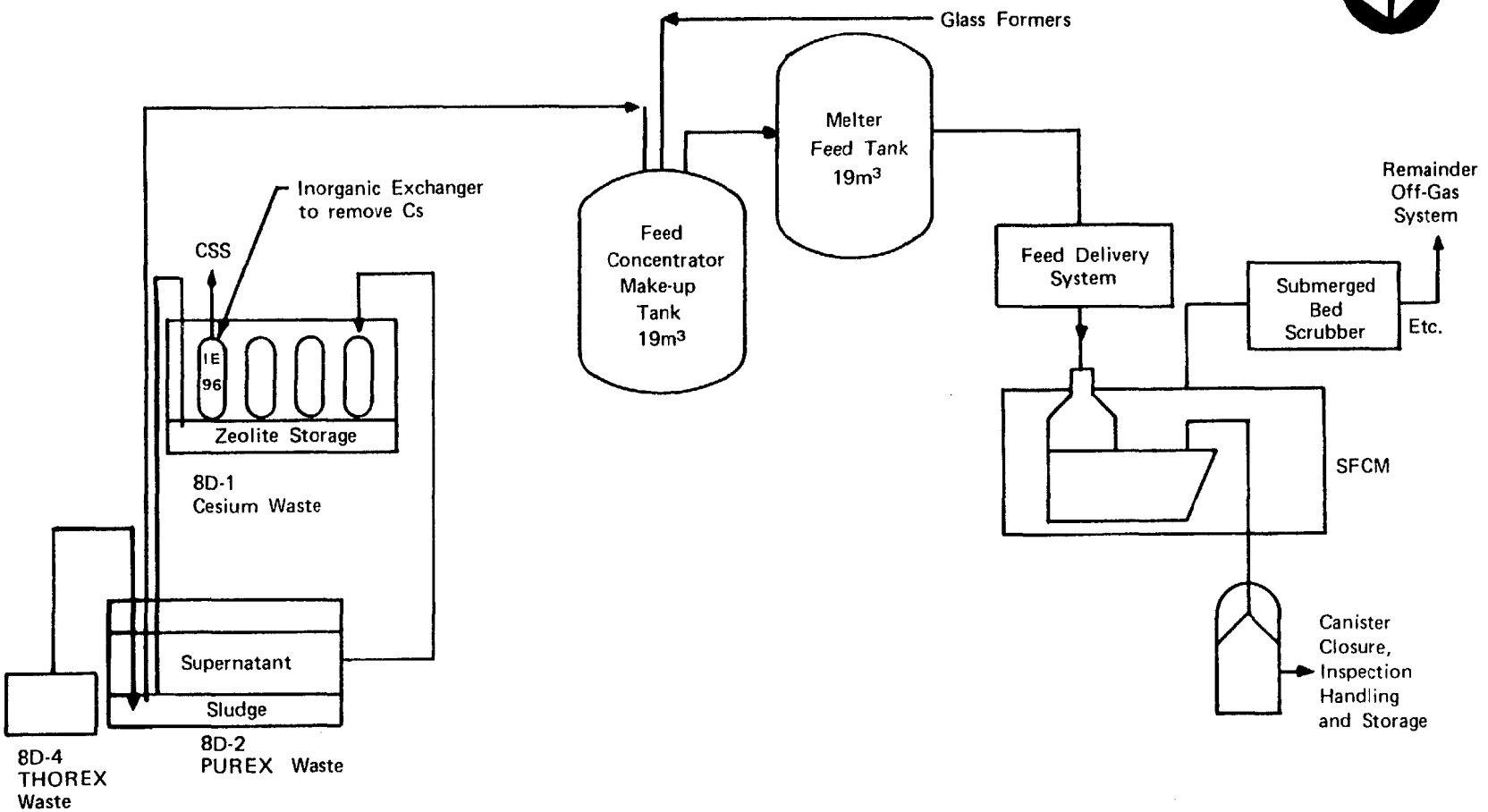

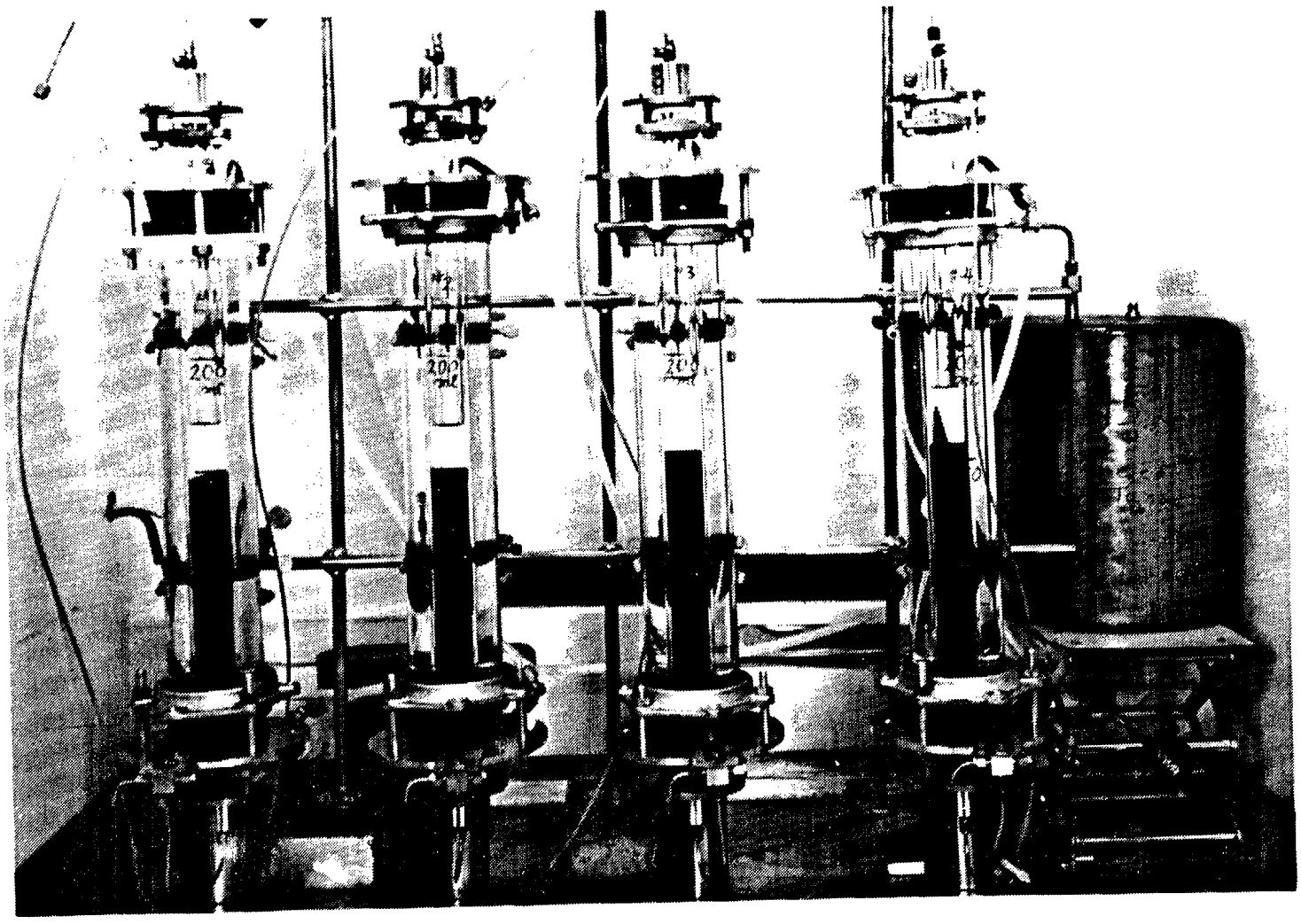

FIGURE 9
PNL Column Test Apparatus (Tracer Studies)

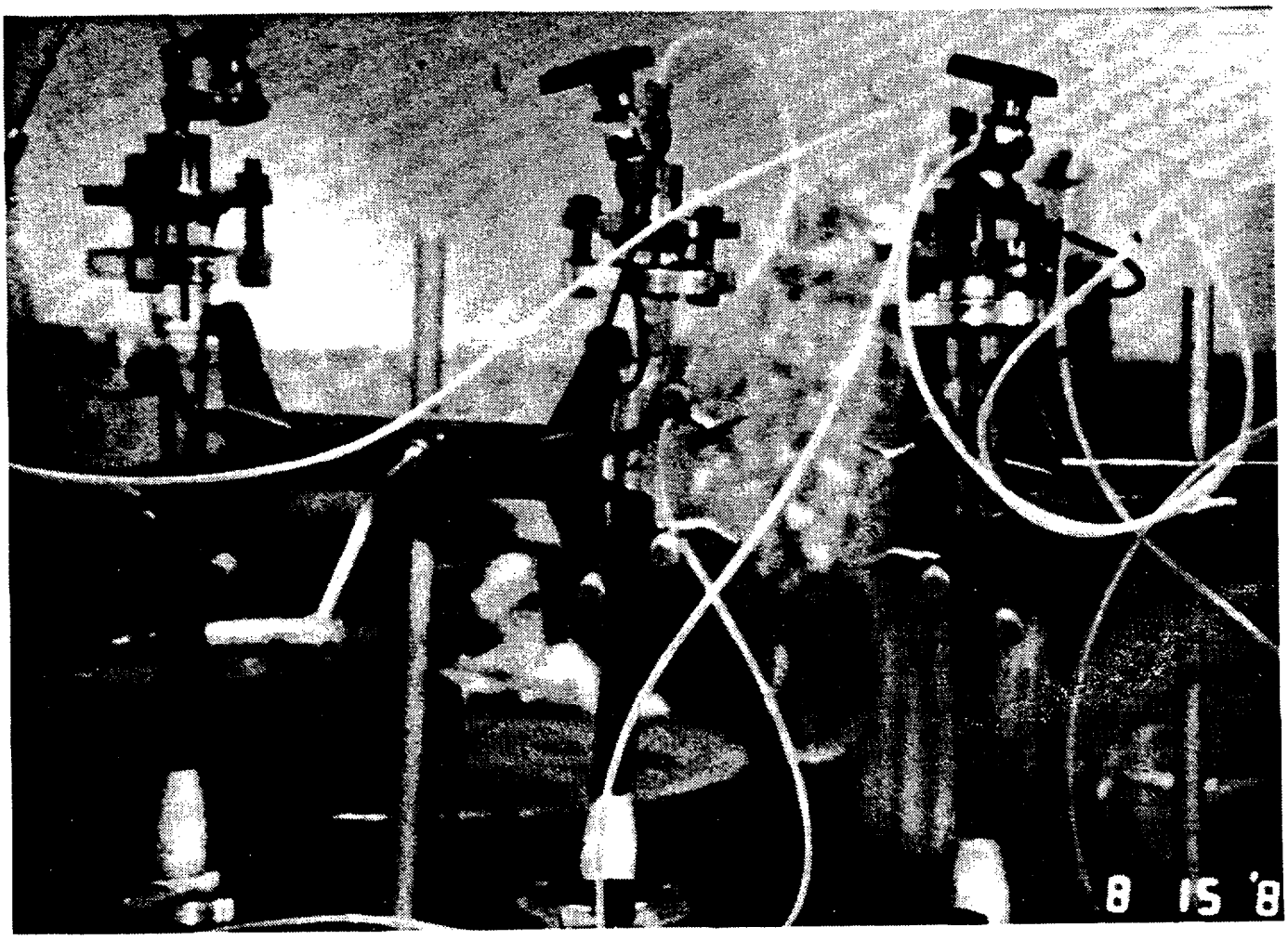

FIGURE 10
WVNS In-Cell Column Test Apparatus

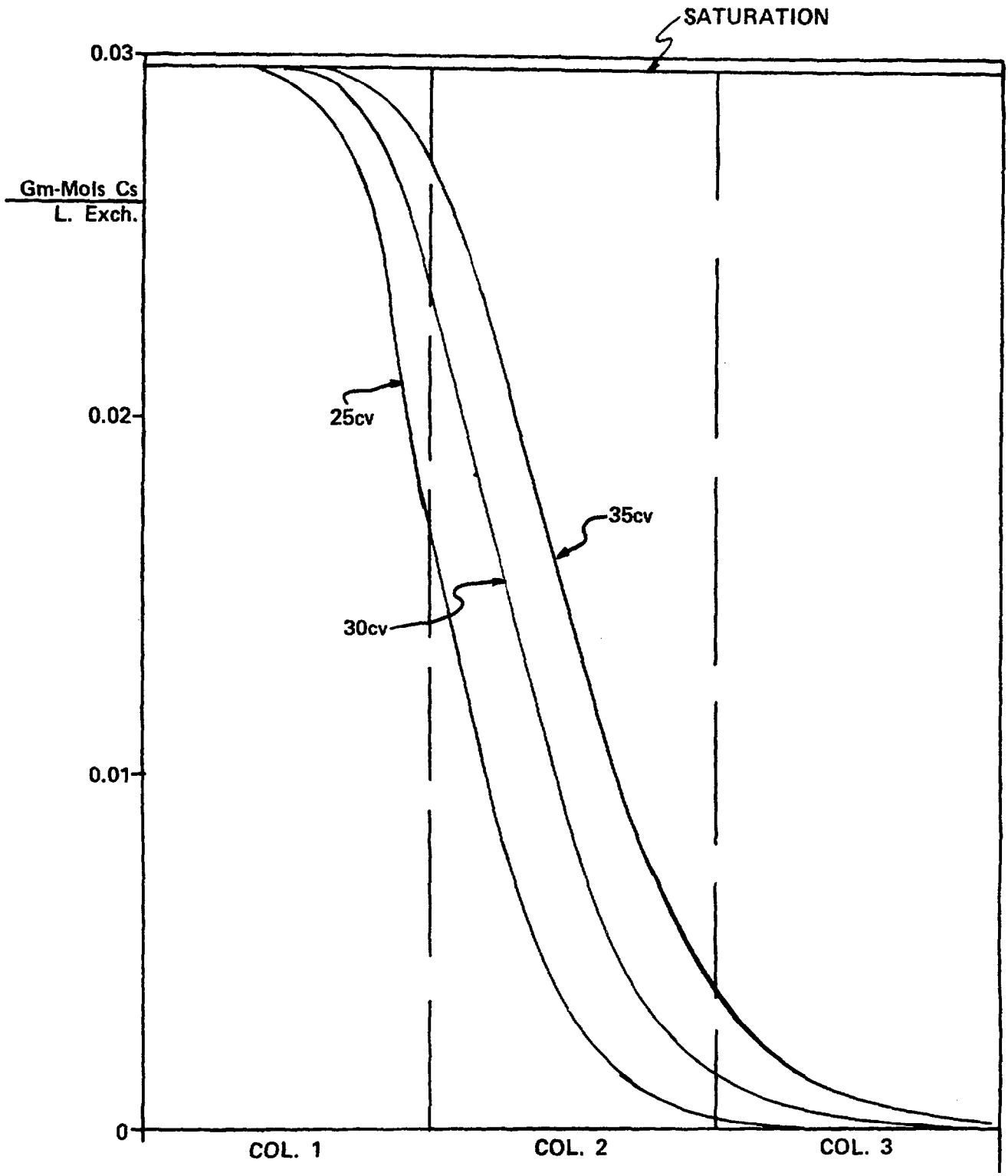

FIGURE 11
Column Loading Profiles
(3 Columns)

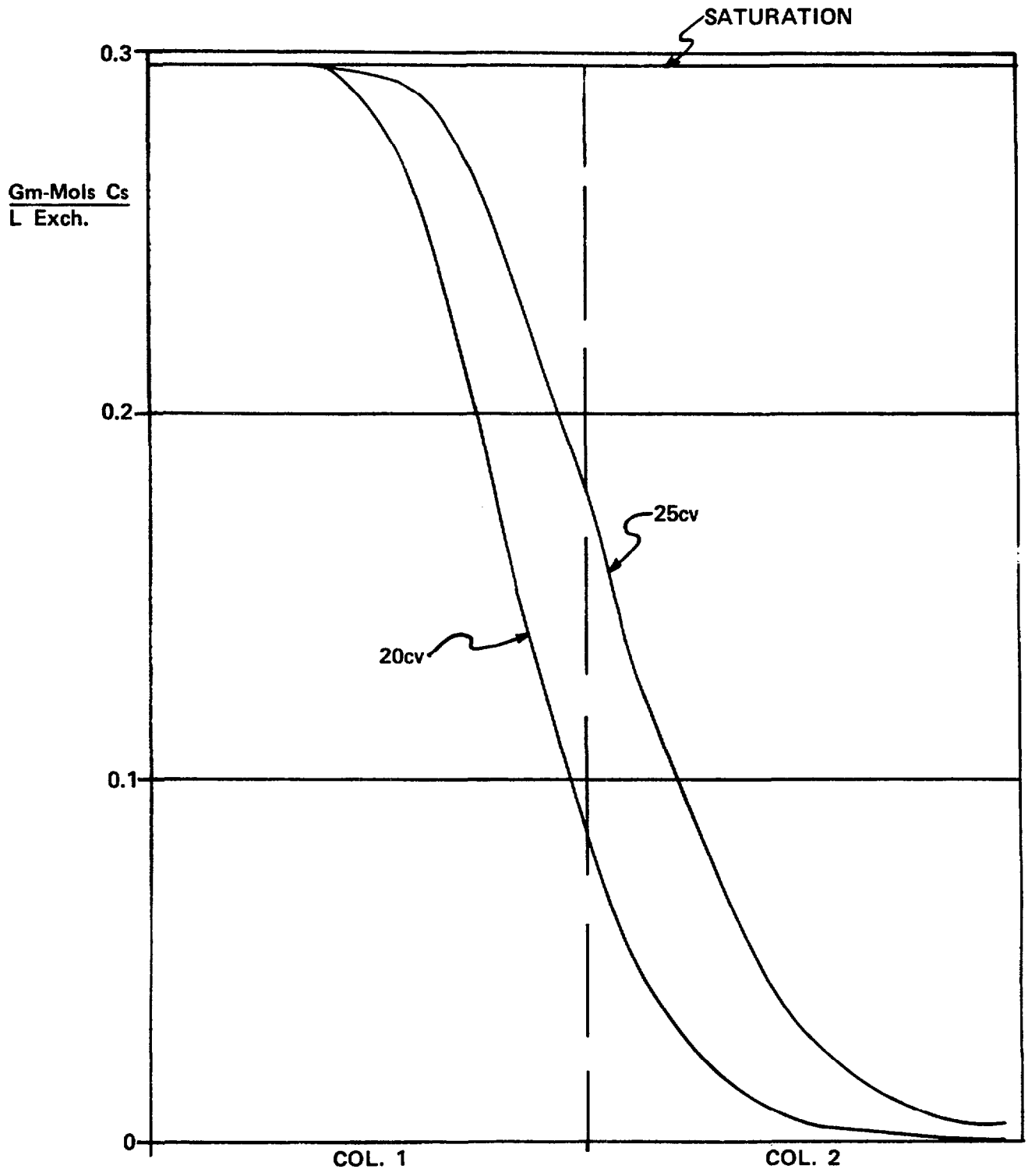

FIGURE 12
Column Loading Profiles
(2 Columns)

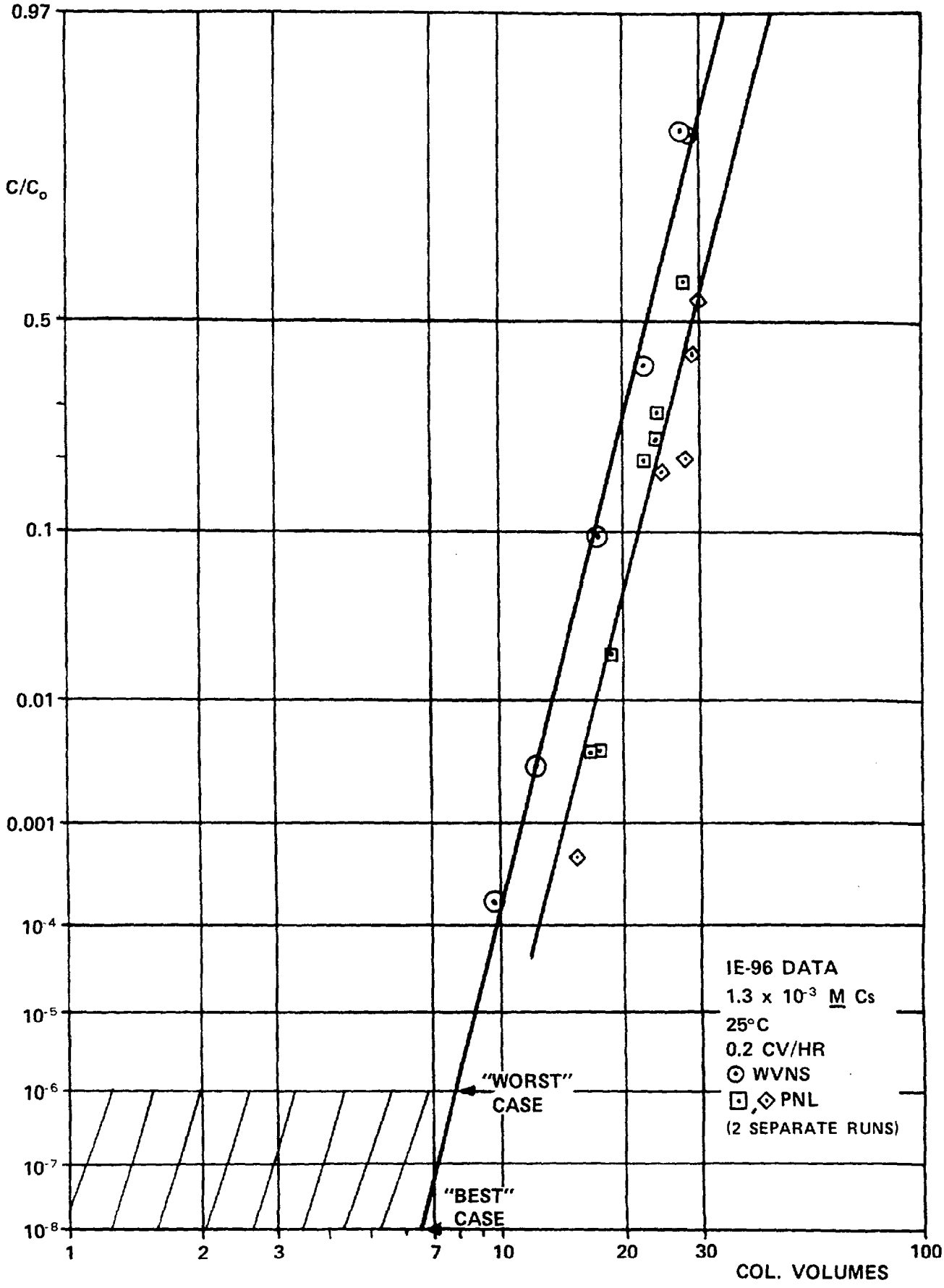

FIGURE 13
Column Loading Curves

As inferred above, one of the criteria for the STS design was to minimize the use of zeolite, i.e., maximize utilization. This was based mainly on glass compositional requirements. In addition to the four-column design, it was discovered that supernatant dilution and cooling would minimize zeolite use by increasing its capacity.

The effect of dilution was verified by in-cell work, but not the temperature (See Figure 14). However, based on the good correlations obtained from previous tests between WVNS and PNL, it was felt that the risk of accepting their relative improvement numbers was minimal. The practical limitations based on equipment design was deemed to be 6°C and 3:1 dilution (two parts water to one part supernatant). This doubles the capacity of the zeolite (See Table 8) and was the basis for the STS design.

Testing with Decontaminated Supernatant

An additional objective of the three-column test was to obtain a relatively large quantity of decontaminated supernatant for work that could be done outside the cell. This supernatant is virtually identical with the actual supernatant except that a small amount of Cs^+ (1.3×10^{-3} M) was exchanged with Na^+. (To a lesser extent, exchange also involves K^+ and Rb^+ cations, but this is also assumed to have a negligible effect on the properties in question.)

Leach Testing

A portion of this decontaminated supernatant was used to make cement cylinders for leach testing (See Figure 15). Both unconcentrated (~41 weight percent) and concentrated (~58 weight percent) supernatant were used. American Nuclear Society (ANS) Procedure 16.1[7] was used for the tests. Cement recipes were those developed by Westinghouse R&D and used by them in an earlier study using simulated supernatant[8]. The leachability of three components - cesium, strontium, and plutonium - were followed by means of the radioactive isotopes Cs-137, Sr-90, and the sum of Pu-238, 239 and 240 respectively. Leachability indices, which are proportional to the negative logarithm of the diffusivity, were determined. Index averages are tabulated and compared with Westinghouse R&D results in Table 9.

Based on these tests, it was concluded[9]:

1. The Westinghouse R&D simulant that was used for their tests appears to be a good surrogate. The results of their leachability testing are considered valid. It can be strongly inferred that their additional waste form qualification tests (e.g., compressive strength tests) are also valid.

2. The leachability indices of both waste forms exceeded 6, which is the level required by the Nuclear Regulatory Commission (NRC)[10] for the disposal of Class B and Class C radioactive wastes. Since the index is proportional to the negative logarithm of the diffusivity, the "worst case" indices represent an "improvement" by a factor of ~5 - 6 over the minimum required.

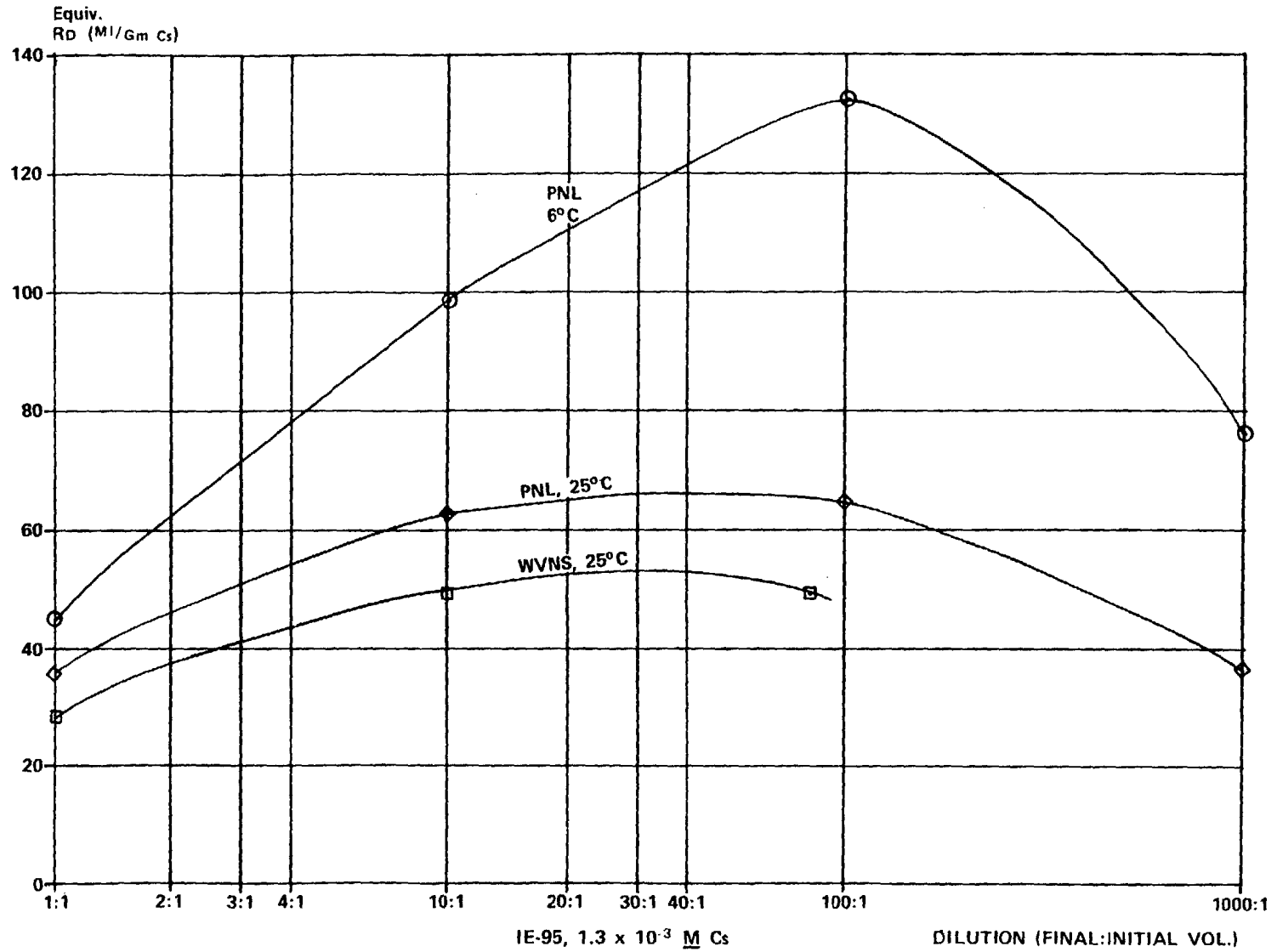

FIGURE 14
Dilution and Temperature Correlations for Cesium Loading on IE-95

TABLE 8: SUMMARY: DILUTION/TEMPERATURE DATA

Temp.	Dil'n*	Base R_D**	Temp. Factor	Dil'n Factor	Conv. Factor	CV***
25°C	1:1	31	1.0	1.0	0.73	23
6°C	1:1	31	1.25	1.0	0.73	28
25°C	2:1	31	1.0	1.31	0.73	30
6°C	2:1	31	1.31	1.37	0.73	41
25°C	3:1	31	1.0	1.45	0.73	33
6°C	3:1	31	1.41	1.45	0.73	46

* Dilution is final volume over initial volume

** R_D is a dimensional number (mL/g) which is the ratio of the cesium absorbed on the zeolite (g/g) over the concentration of the cesium in solution (g/mL) in equilibrium with it. It is a measure of capacity and can be determined from either batch equilibrium tests or column loading tests.

*** The amount of Cs in this amount of supernatant (1.3×10^{-3} M) would saturate one column volume of exchanger.

TABLE 9: LEACHABILITY INDEX AVERAGES

Component	Unconcentrated Supernatant		Concentrated Supernatant	
	WVNS	Westinghouse R&D (Avg. of 3)	WVNS	Westinghouse R&D (Avg. of 3)
Cs	6.76	6.60*	6.76	6.79
Sr	7.46	----	7.30	----
Pu	>15.32**	----	>15.89**	----
NO_3/NO_2	TBD***	6.57*	TBD***	6.49

* Data not calculated beyond two weeks because ~100% of cesium had leached out.

** Several samples were below detectability level.

*** To Be Determined.

FIGURE 15
Leach Testing of Cement Cylinders made from Decontaminated Supernatant

3. The leachability of strontium in the cement form was an order of magnitude lower than the cesium, while plutonium was extremely leach resistant.

Physical Property Correlations

In addition to the cement cylinder leach tests, decontaminated supernatant was used to measure several other properties such as density, viscosity, boiling point rise, crystallization point, freezing point, total dissolved solids (TDS) and pH. Sufficient data were taken to enable correlations to be made so that these properties (where applicable) could be determined as a function of temperature and dilution. Correlations were also derived for the 8D-2 sludge wash solutions based on a reference mathematical model which gave the chemical composition of three reference wash solutions as a mixture of water, supernatant, and sodium sulfate (See Section 6). As an example of these correlations, Figure 16 correlates viscosity data while Table 10 tabulates density data. All the chemical, radiological, and physical property data were compiled in one document which was an attachment to the STS design criteria[11] (See Appendix A).

As an example of the use of Table 10: the supernatant density is calculated from the formula:

$$(1) \quad \rho_{Super} = \frac{(\rho_{H_2O})\ (\rho_{Salts})}{(0.6057)\ \rho_{Salts} + (0.3953)\ \rho_{H_2O}}$$

The density of diluted supernatant is then calculated by the following formula (assumes no volume change of dilution):

$$(2) \quad \rho_{Dil\ Super} = (\Phi_{Super})\ \rho_{Super} + (1 - \Phi_{Super})\ \rho_{H_2O}$$

where Φ_{Super} is the volume fraction of supernatant.

For example, the density of 3:1 diluted supernatant at 6°C is calculated. A 3:1 dilution is defined as two parts water to one part supernatant. Therefore:

Φ Super = 0.333; Φ_{H_2O} = 0.667; from Table 13:

$$\rho\ Super = \frac{(0.99997)\ (2.6392)}{0.6047\ (2.6392) + 0.3953\ (0.99997)} = 1.325\ g/mL$$

From equation (2): $\rho_{3:1\ Super}$ = 0.333 (1.325) + 0.667 (0.9997) = 1.108 g/mL (@6°C)

TABLE 10: SUPERNATANT DENSITY/TEMPERATURE CORRELATION

Temp. (°C)	ρ_{H_2O}(g/mL)	ρ_{Salts}(g/mL)	ρ_{Super}(g/mL)
0	0.99987	2.6542	1.327
5	0.99999	2.6416	1.326
10	0.99973	2.6291	1.323
15	0.99913	2.6165	1.322
20	0.999823	2.6040	1.320
25	0.99707	2.5915	1.317
30	0.99567	2.5789	1.315
35	0.99406	2.5664	1.312
40	0.99224	2.5538	1.309
45	0.99025	2.5413	1.305
50	0.98807	2.5287	1.302
55	0.98573	2.5162	1.298
60	0.98324	2.5036	1.294
65	0.98059	2.4911	1.290
70	0.97781	2.4785	1.292
75	0.97489	2.4660	1.281
80	0.97183	2.4535	1.277
85	0.96865	2.4409	1.272
90	0.96534	2.4284	1.267
95	0.96192	2.4158	1.262
100	0.95838	2.4033	1.257

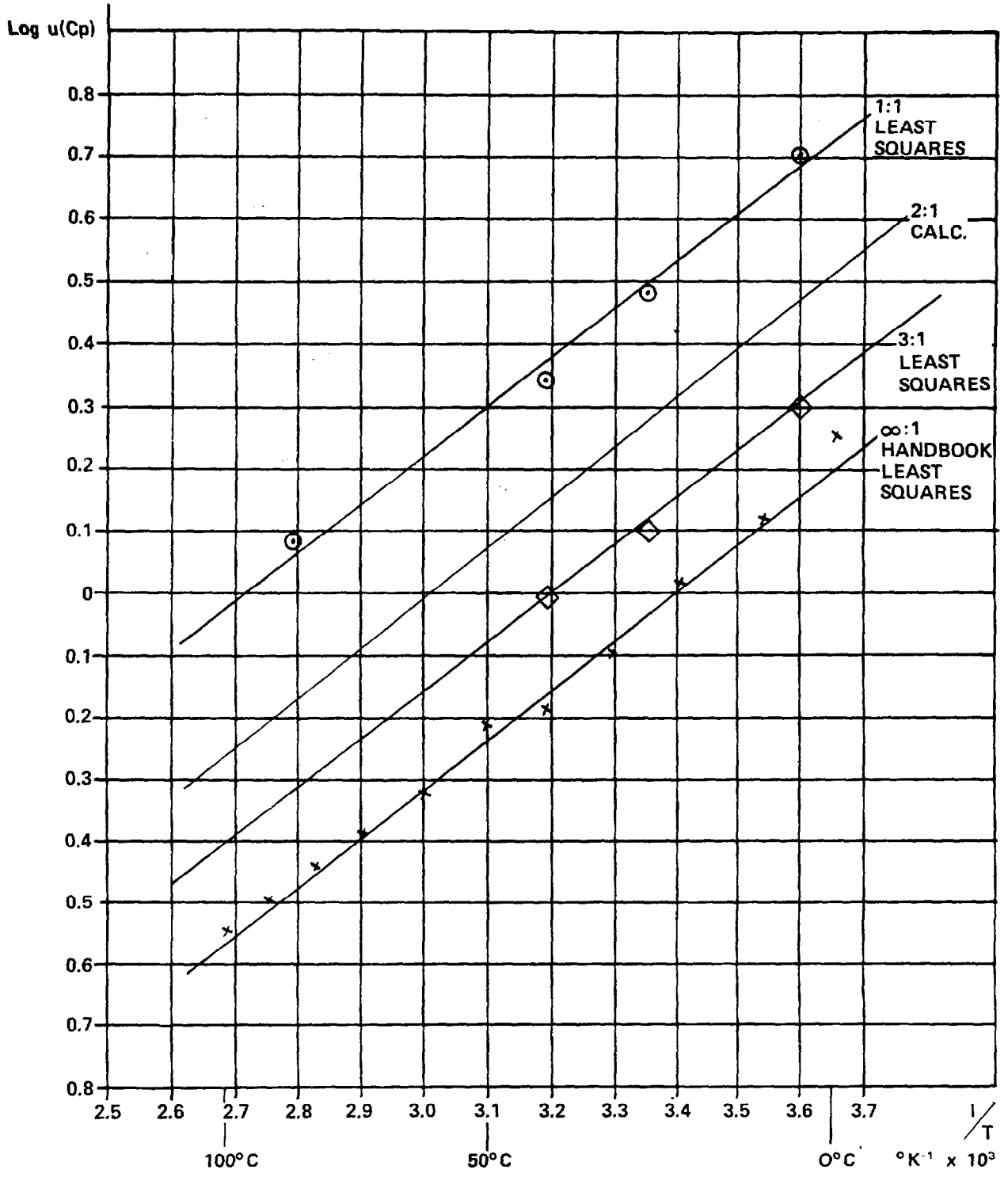

FIGURE 16
8D-2 Supernatant Viscosity Data

4. THOREX WASTE CHARACTERIZATION

Sampling and Analytical Work

Although only about ~2 percent of the total high level waste volume, the THOREX waste has ~6 percent of the total curie content, and the unrecovered thorium is an important consideration in the formulation of the reference borosilicate glass. Sampling of the 8D-4 (THOREX) waste tank was done with the same equipment used to sample the 8D-2 tank. Three samples were taken at a nominal 0.30, 1.5, and 2.7 metres below the vapor/liquid interface (the total liquid depth was ~3.0 metres). The analytical work was performed by the Westinghouse AESD Laboratories. Although the original volume of solution was ~45,000 litres, evaporation had reduced this volume to ~31,380 litres. Another analyses had been performed by Oak Ridge National Laboratories (ORNL) in 1978. The volume at that time was about the same as for the WVNS sample so that the data were directly comparable (water was added to 8D-4 in 1979). Both the ORNL and the Westinghouse AESD analyses could account for less than one-half of the total thorium in the tank, based on input as documented by NFS.

Qualitative observation of the small amount of solids in the three samples indicated that saturation had been reached with respect to thorium nitrate (probably the pentahydrate form, see Figure 17)[12]. The saturated solution was a viscous liquid with a measured density of 1.844 g/cm^3 at 23°C. It consisted of ~71 weight percent salts. An average of 810 ppm of water-insoluble solids were found at the three depths, with each level having approximately the same amount. Beta and gamma scanning of the solids gave results which were consistent with zirconium oxide and insoluble fission product fines transferred to the tank during the campaign.

To facilitate preparation of simulated solutions, the chemical composition was calculated as amounts of certain salts and acids (See Table 11). Westinghouse Laboratories reported that there were a number of unidentified peaks in the anion chromatogram which were not able to be identified. As a result, cation equivalents exceeded the anion equivalents by >8 percent. For the purpose of Table 11, additional nitrate was added to balance the cations. The total thorium was assumed to be that reported by NFS. An assumption as to the volume occupied by the thorium nitrate was necessary in order to calculate the kg of elements in solution from the solution composition.

In addition to the analytical work, an ORIGEN2[13] computer code run was made using fuel, irradiation and processing parameters obtained from NFS records. The match with most of the analytical data was satisfactory. The total liquid volume (after correcting for the solid phase) was computed by using the average of Cs-137 and Sr-90 as a tracer. This volume agrees closely with that calculated by assuming a thorium nitrate pentahydrate solid phase. This correction will be verified by resampling after the volume is made up and the solids redissolved. For the purpose of Table 11, the ORIGEN2 data were used for the fission products. The transuranics (Pu, Np, Cm, and Am) were in excess of the ORIGEN2 output by an order of magnitude and it was theorized that the addition of hydrofluoric acid in the dissolver to enhance fuel dissolution also resulted in the dissolution of a "heel" from previous PUREX processing campaigns. The radionuclides as determined by analysis and the ORIGEN2 run are given in Table 12.

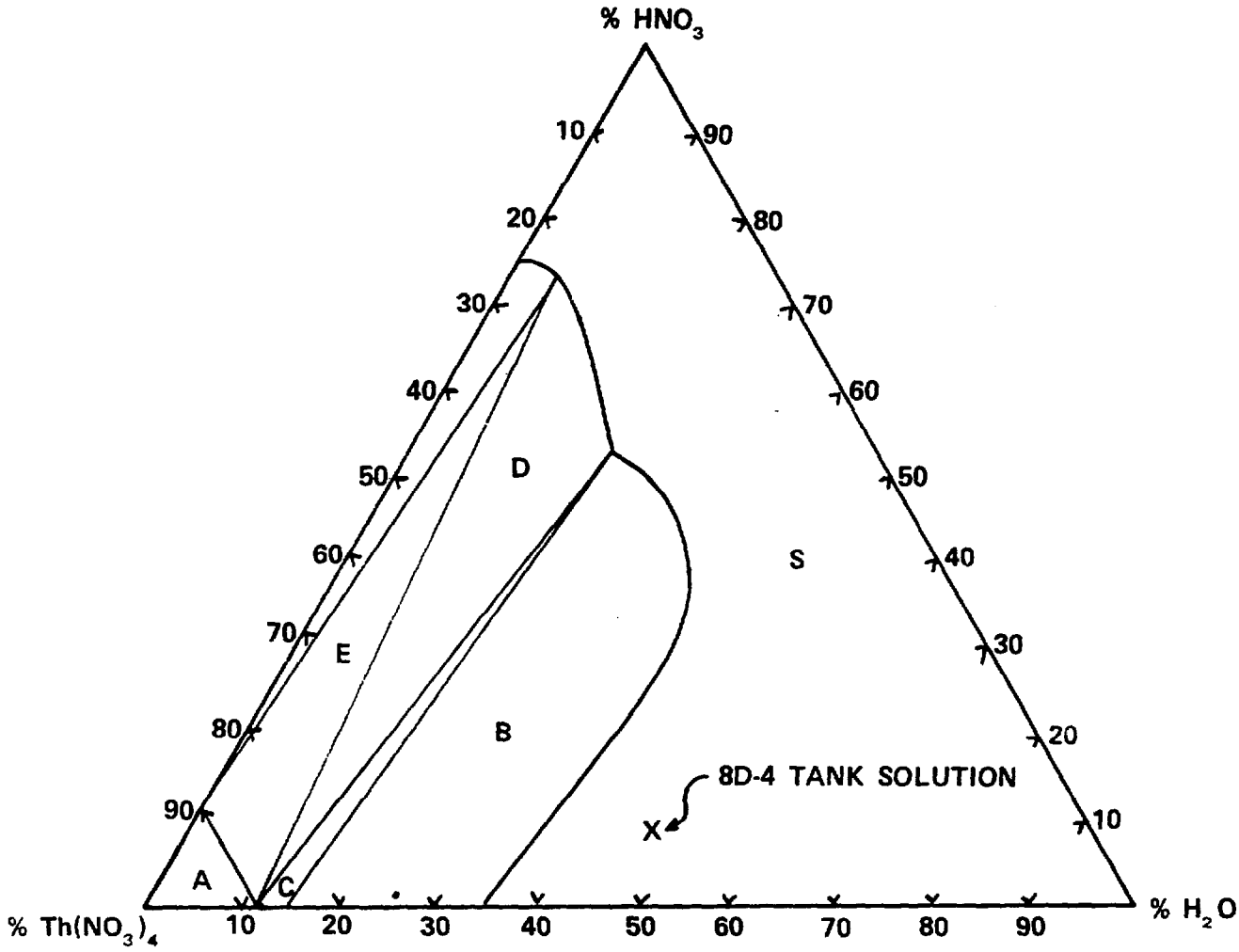

A: REGION OF HYDROLYSIS
B: PENTAHYDRATE & VARIABLE LIQUID
C: PENTAHYDRATE, TETRAHYDRATE, AND LIQUID
D: TETRAHYDRATE & VARIABLE LIQUID
E: TETRAHYDRATE, ANHYDROUS PHASE & LIQUID
S: HOMOGENEOUS SOLUTION

FIGURE 17
Equilibrium Data
($Th(NO_3)_4$ – HNO_3 – H_2O @ 25°C)

TABLE 11: THOREX WASTE CHEMICAL COMPOSITION

A. Solution

Compound	Wt. %	Mass (kg)
$Th(NO_3)_4$	26.69	11,633
$Fe(NO_3)_3$	19.41	8,462
$Al(NO_3)_3$	9.58	4,175
HNO_3	4.88	2,129
$Cr(NO_3)_3$	4.40	1,918
$Ni(NO_3)_2$	1.81	791
H_3BO_3	1.10	480
$NaNO_3$	0.521	227
Na_2SO_4	0.413	180
KNO_3	0.438	191
Na_2SiO_3	0.289	126
$KMnO_4$	0.225	98
$Mg(NO_3)_3$	0.131	57
Na_2MoO_4	0.125	54
$Nd(NO_3)_3$	0.167	73
$Ce(NO_3)_4$	0.117	51
NaCl	0.115	50
$Ru(NO_3)_4$	0.0959	42
$Ca(NO_3)_2$	0.0699	30
$CsNO_3$	0.0637	28
$Ba(NO_3)_2$	0.0619	27
$La(NO_3)_3$	0.0512	22
$Pr(NO_3)_3$	0.0473	21
$Sr(NO_3)_2$	0.0364	16

TABLE 11: THOREX WASTE CHEMICAL COMPOSITION CONTINUED

A. Solution

Compound	Wt. %	Mass (kg)
$Y(NO_3)_3$	0.0328	14
$Sm(NO_3)_3$	0.0321	14
$Zr(NO_3)_4$	0.0283	12
Na_3PO_4	0.0265	12
$NaTcO_4$	0.0263	11
$Rh(NO_3)_4$	0.0242	11
$Zn(NO_3)_2$	0.0226	10
$Pd(NO_3)_4$	0.0174	8
$UO_2(NO_3)_2$	0.0142	6
$RbNO_3$	0.0137	6
$NaTeO_4$	0.0120	5
$Co(NO_3)_2$	0.00583	3
Na_2SeO_4	0.00267	1
NaF	0.00243	1
$Eu(NO_3)_3$	0.00217	1
$NP(NO_3)_4$	0.00206	0.9
$Cu(NO_3)_2$	0.00177	0.8
$Pa(NO_3)_3$	0.00153	0.7
$Sn(NO_3)_3$	0.00165	0.7
$Pu(NO_3)_3$	0.00151	0.7
$Gd(NO_3)_3$	0.00081	0.4
$Cd(NO_3)_2$	0.00064	0.3
$Sb(NO_3)_3$	0.00034	0.1
$AgNO_3$	0.00019	0.08
$In(NO_3)_3$	0.00008	0.04
$Ge(NO_3)_4$	0.00005	0.02
$Pm(NO_3)_2$	0.00002	0.01
Total	71.12	43,587
H_2O (by diff.)	28.88	12,587

B. Solids

Insolubles	35

Video Camera Work in 8D-3 & 4

To obtain more information concerning the "missing thorium" in Tank 8D-4 and to verify the structural integrity of both the 8D-3 and 8D-4 tanks (the 8D-3 tank will be used as a surge tank for IX column effluent during STS operation), the interiors were inspected by means of a Rees R93* camera. An articulated arm assembly was designed such that the whole assembly could be lowered through a two-inch pipe and the whole tank interior surveyed up to the upper weld seam, which attaches the dished head to the tank wall (See Figure 18).

The video observations in 8D-3 showed that the tank was in excellent condition. There is no evidence of corrosion or deterioration (See Figures 19-30).

In the 8D-4 tank, observations above the liquid level were comparable to those observed in 8D-3, i.e., no signs of corrosion or deterioration (See Figures 31-38). The 8D-4 supernatant is dark brown in color and was found to be opaque to visual observations (only reflections could be observed). Seen at one side of the tank was a light-colored solid mass. It appeared to be relatively flat, extended slightly (20-50 mm) above the surface, and followed the curvature of the tank at about 0.3 m wide from the tank wall. Its dimensions are ~2 m long by 0.3 m wide (See Figures 39 and 42). From these observations and simulation work by PNL[14], it was concluded that thorium nitrate accumulated on the cooling coils (each tank has three independent cooling coils - one on the floor bottom and two on the wall) as the tank volume decreased by evaporation. Calculations indicate that if this material [as $Th(NO_3)_4 \cdot 5\ H_2O$] were uniformly distributed around the tank periphery and bottom, it would have a thickness of ~0.5 metres. It is planned to redissolve this crystalline mass before start of HLW processing.

5. 8D-2 SLUDGE SOLIDS CHARACTERIZATION

At the start of the Project, little was known about the characteristics of the sludge layer at the bottom of the tank. Although estimates of the composition and total amount of solids were available from NFS records, little was known about its consistency and topography. Since then, a considerable amount of activity has been done through the one available access riser (known as the M-1 riser, see Figure 43) at the center of the tank. Although some caution has to be used in assuming that this one location is representative of the whole, considerably more information is now available concerning this settled sludge.

In Situ Characterization

Initial sludge characterization was done using two mechanical devices which were designed to fit through a 200 mm opening in the M-1 riser. This access opening is the result of removing a shield plug from the center of the riser. The two devices were known as the buoyancy probe and the shear vane.

---

* Rees Instruments, Inc. Orange, CA

TABLE 12: REFERENCE 1987 RADIONUCLIDE CONTENT (CURIES) OF THOREX WASTE

Radionuclide	Total Curies	Radionuclide	Total Curies
3-H	<1.74E+00	216-Po	9.76E+00
14-C	1.30E-01	217-At	2.07E-01
55-Fe	5.63E+02	219-Rn	7.52E+00
60-Co	1.14E+03	220-Rn	9.76E+00
59-Ni	2.03E+01	221-Fr	2.07E-01
63-Ni	2.51E+03	223-Fr	1.04E-01
79-Se	3.35E+00	223-Ra	7.52E+00
90-Sr	4.54E+05	224-Ra	9.76E+00
90-Y	4.54E+05	225-Ra	2.07E-01
93-Zr	1.62E+01	228-Ra	1.48E+00
93m-Nb	1.02E+01	225-Ac	2.07E-01
99-Tc	1.04E+02	227-Ac	7.52E+00
106-Ru	6.24E-01	228-Ac	1.48E+00
106-Rh	6.24E-01	227-Th	7.42E+00
107-Pd	1.14E-01	228-Th	9.76E+00
113m-Cd	3.75E+01	229-Th	2.07E-01
121m-Sn	5.99E-01	230-Th	4.38E-02
126-Sn	3.11E+00	231-Th	5.17E-03
125-Sb	2.89E+02	232-Th	1.64E+00
126-Sb	4.35E-01	234-Th	7.11E-05
126m-Sb	3.11E+00	231-Pa	1.52E+01
125m-Te	7.08E+01	233-Pa	3.02E-01
129-I	<1.80E-01	234m-Pa	7.11E-05
134-Cs	3.10E+02	232-U	2.74E+00
135-Cs	5.47E+00	233-U	2.09E+00
137-Cs	4.75E+05	234-U	2.17E-01
137m-Ba	4.49E+05	235-U	5.17E-03
144-Ce	1.39E-01	236-U	9.80E-03
144-Pr	1.39E-01	238-U	7.11E-05
1.46-Pm	5.07E-01	236-Np	1.23E-01
147-Pm	9.11E+03	237-Np	3.02E-01
151-Sm	4.78E+03	239-Np	4.49E+00
152-Eu	4.82E+01	236-Pu	1.09E-02
154-Eu	2.53E+03	238-Pu	4.80E+02
155-Eu	8.44E+02	239-Pu	1.54E+01
207-Tl	7.50E+00	240-Pu	8.09E+00
208-Tl	3.51E+00	241-Pu	8.50E+02
209-Pb	2.07E-01	242-Pu	1.19E-02
211-Pb	7.52E+00	241-Am	2.41E+02
212-Pb	9.76E+00	242-Am	6.76E+00
211-Bi	7.52E+00	242m-Am	6.79E+00
212-Bi	9.76E+00	243-Am	7.83E+00
213-Bi	2.07E-01	242-Cm	5.59E+00
212-Po	6.25E+00	243-Cm	2.34E-01
213-Po	2.03E-01	244-Cm	1.37E+01
215-Po	7.52E+00	245-Cm	2.00E-02
		246-Cm	2.29E-03

FIGURE 18
Camera Assembly Being Used at 8D-3 Tank

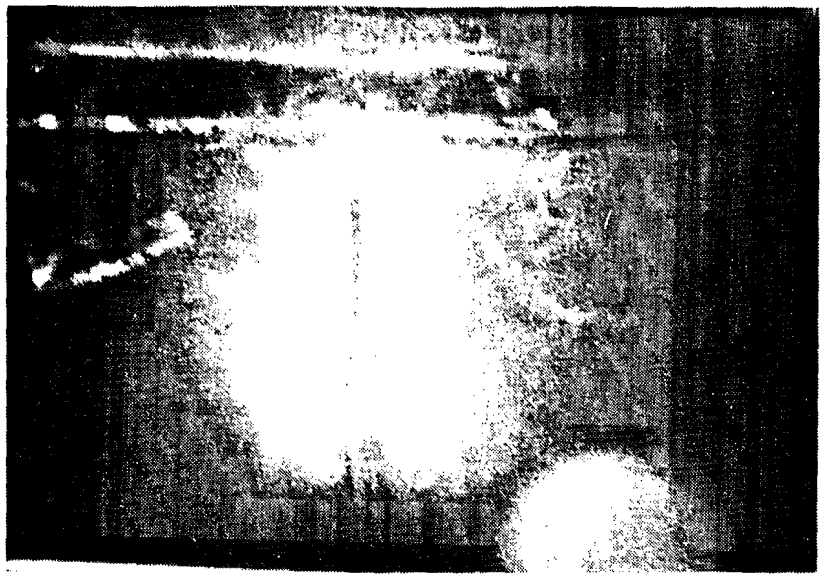

FIGURE 19
Intersection of Top and Vertical Weld Seams

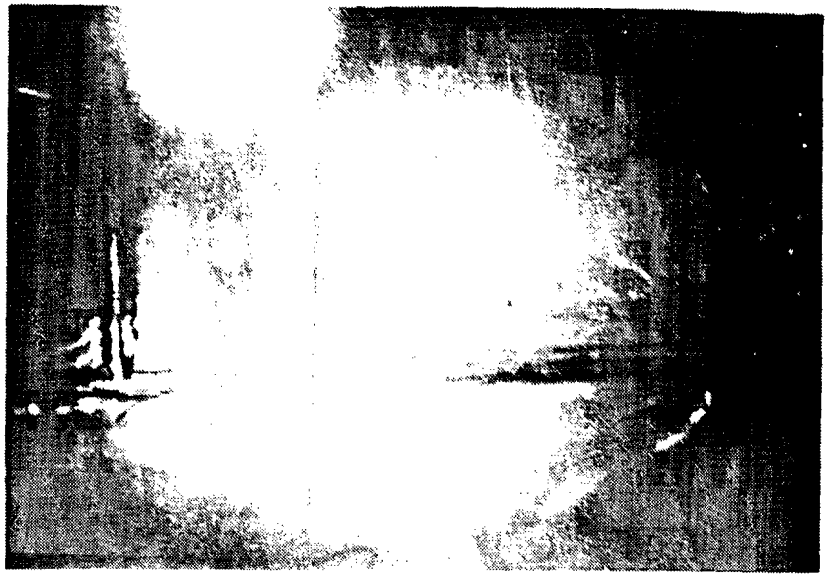

FIGURE 20
Intersection of Bottom and Vertical Weld Seams

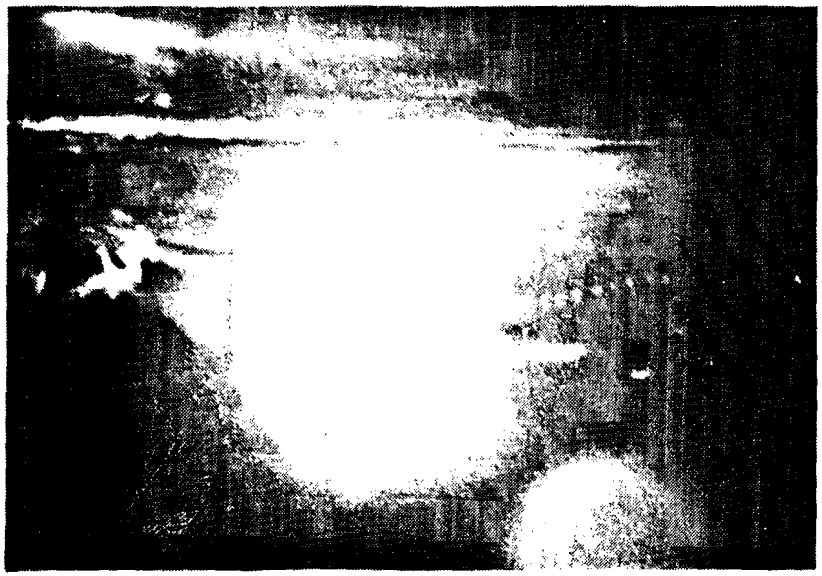

FIGURE 21
Upper Weld Seam

FIGURE 22
Upper Weld Seam; Inlet Cooling Lines

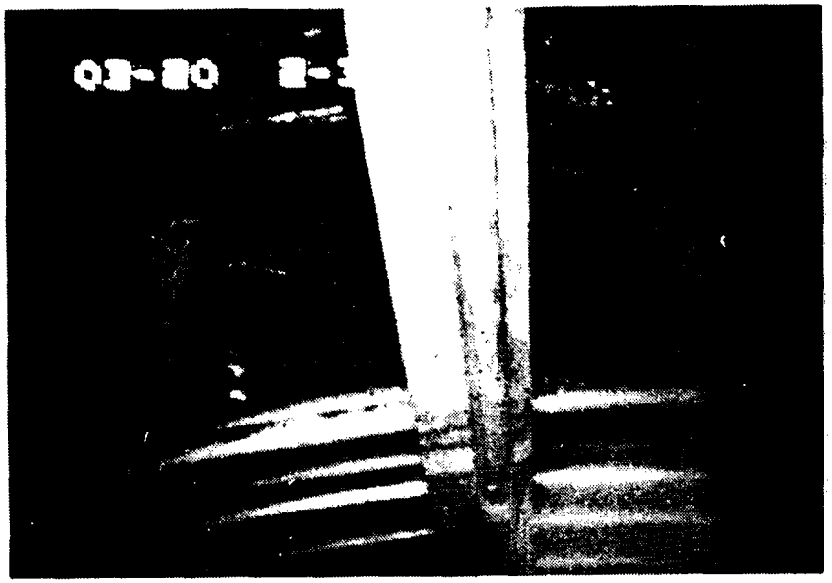

FIGURE 23
Lower Weld Seam; Top of Wall Cooling Coils;
Air Bubbler Tube and Support Bracket

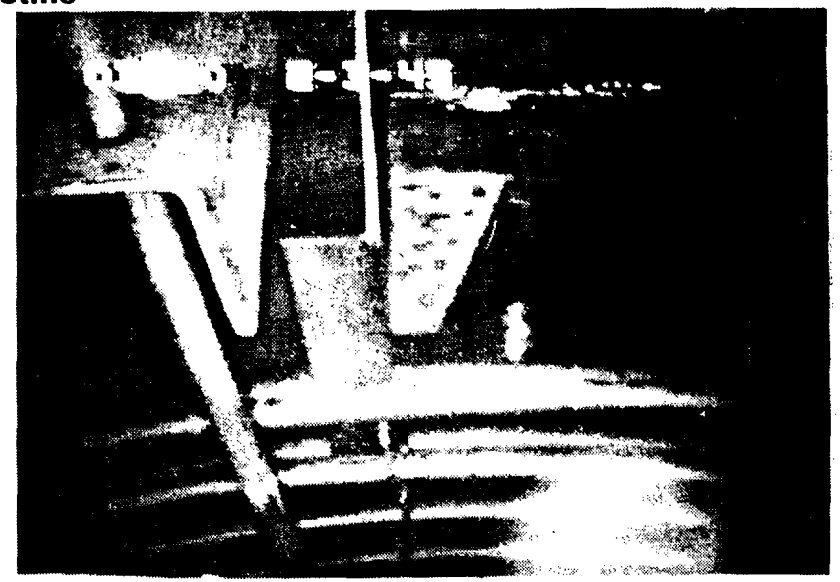

FIGURE 24
Lower Weld Seam; Top of Wall Cooling Coils;
Thermocouple Pipe and Support Bracket

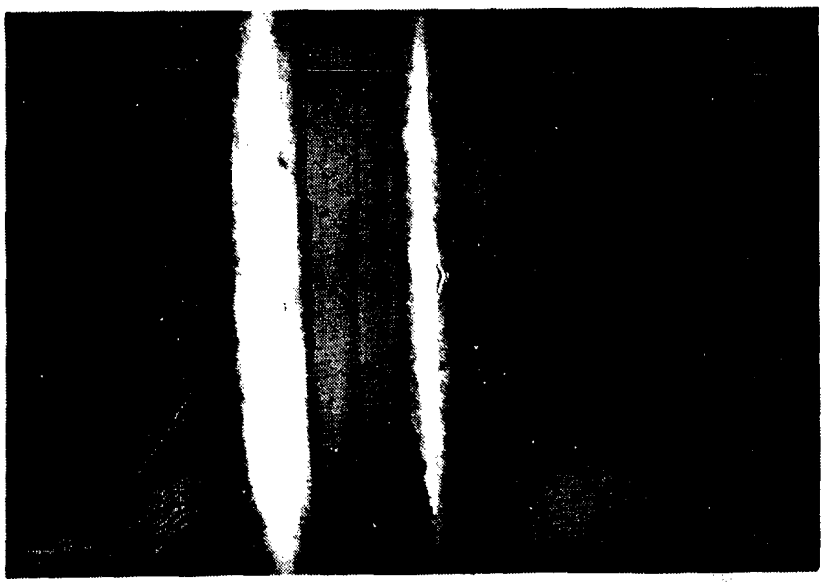

FIGURE 25
Inlet Cooling Lines Between Upper and Lower Weld Seams

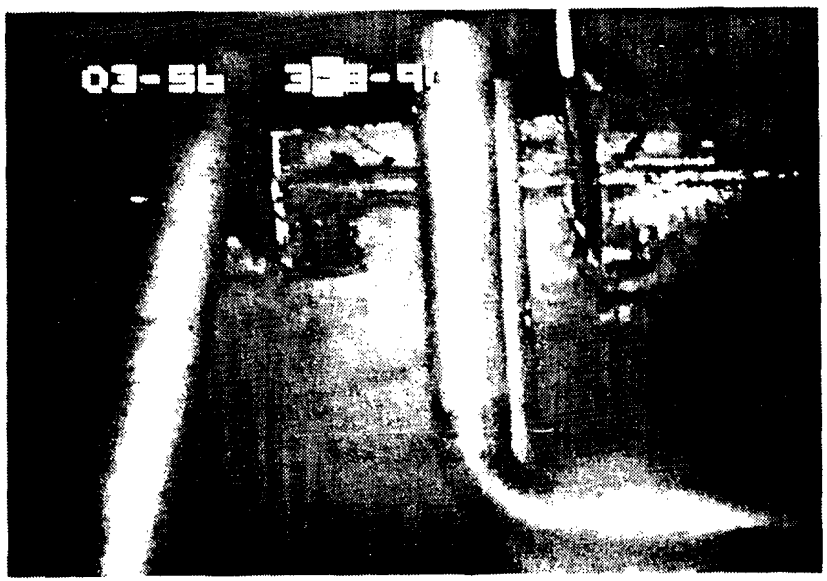

FIGURE 26
Inlet Cooling Lines at Lower Weld Seam

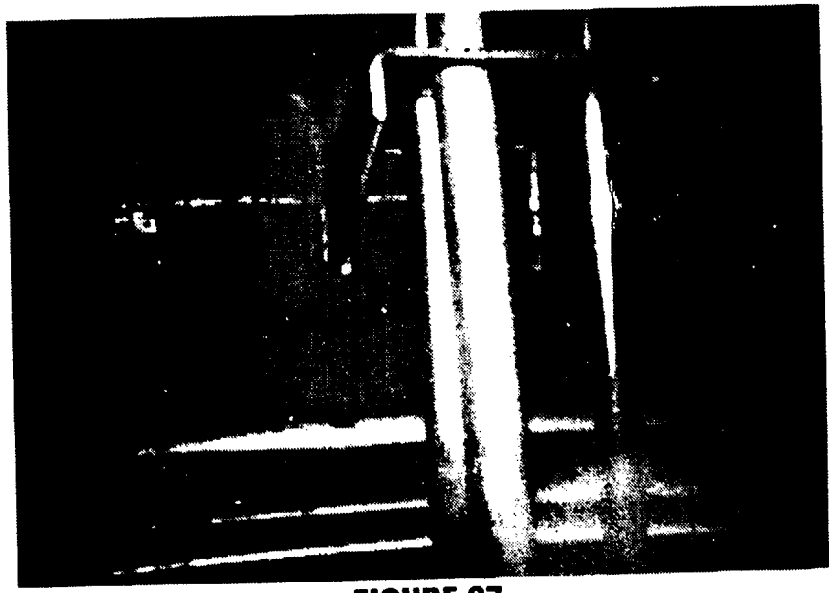

FIGURE 27
Outlet Cooling Lines at Lower Weld Seam

FIGURE 28
Wall Cooling Coils at Condensate Level

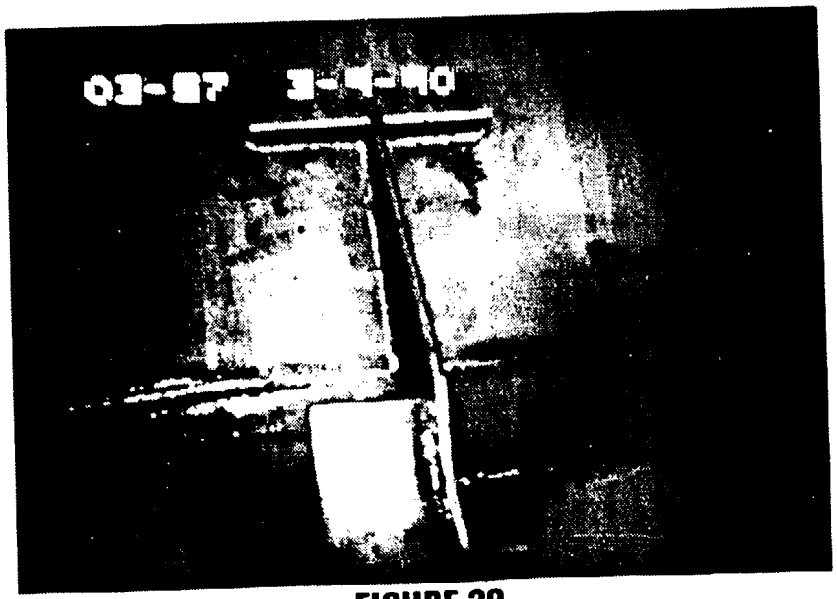

FIGURE 29
Coil Support Bracket at Lower Weld Seam

FIGURE 30
Bottom Cooling Coil Viewed Through Condensate

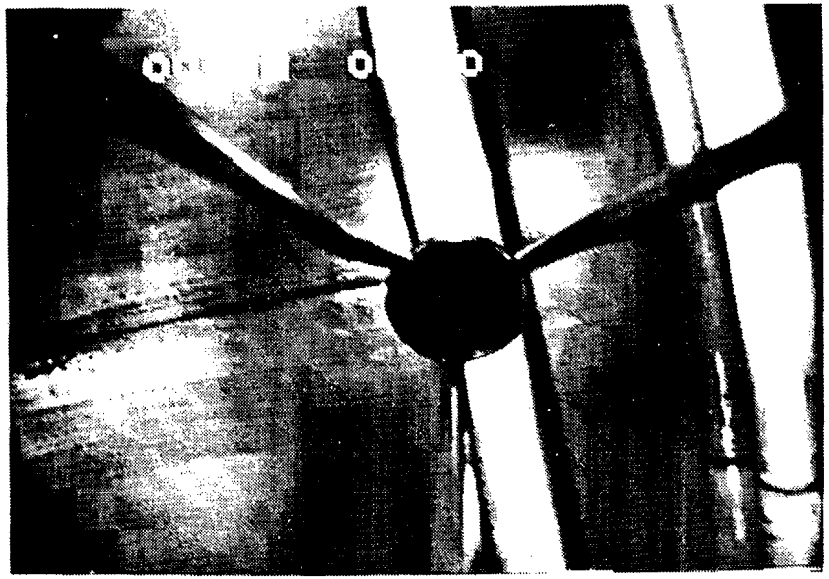

FIGURE 31
Outlet Cooling Pipes Showing Weld Seams

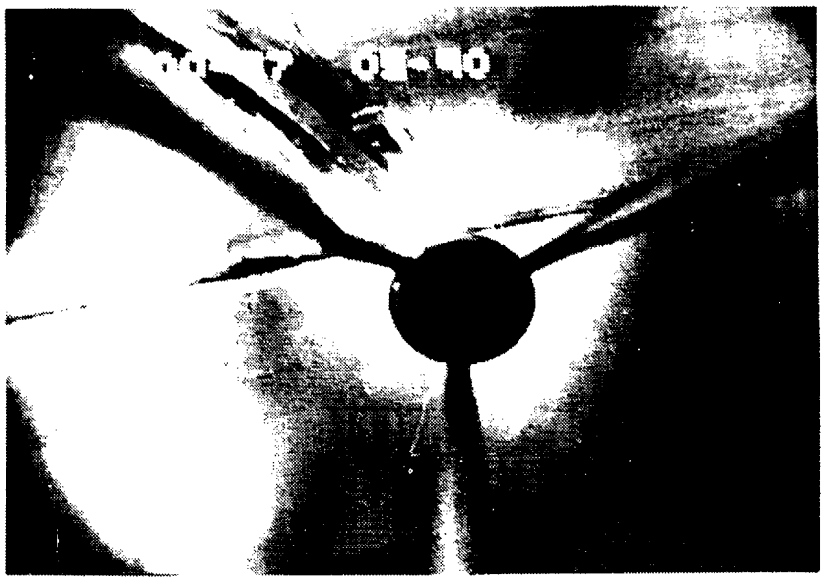

FIGURE 32
Upper Weld Seam and Roof Stiffener

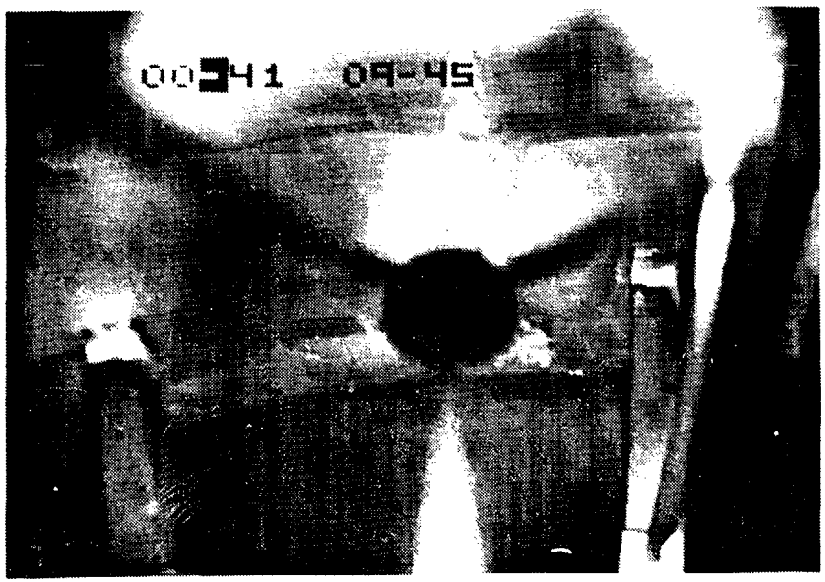

FIGURE 33
Liquid Interface; Thermocouple Pipes

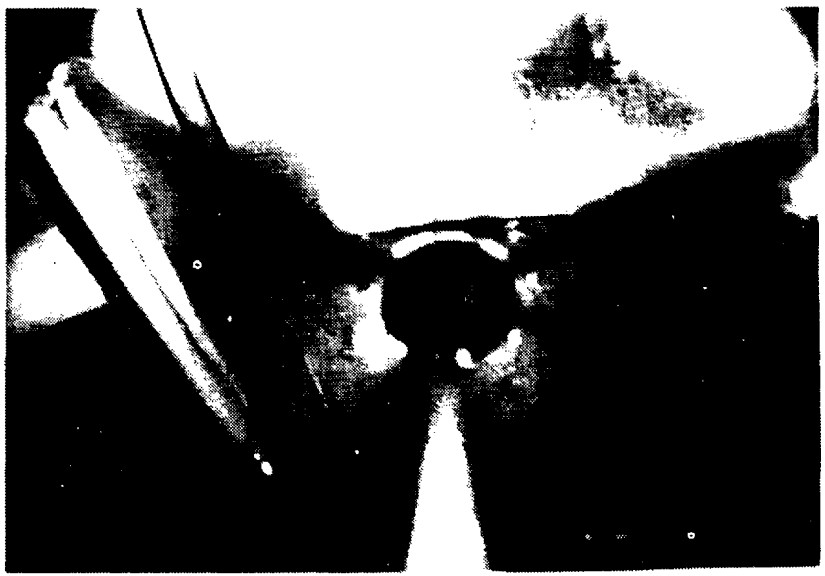

FIGURE 34
Liquid Interface; Outlet Cooling Water Lines

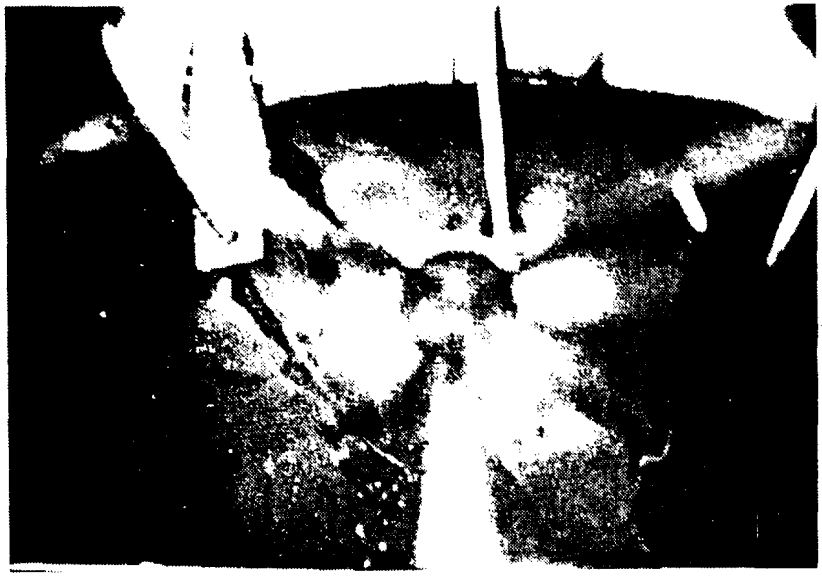

FIGURE 35
Liquid Interface; Air Bubbler
and Thermocouple Pipes

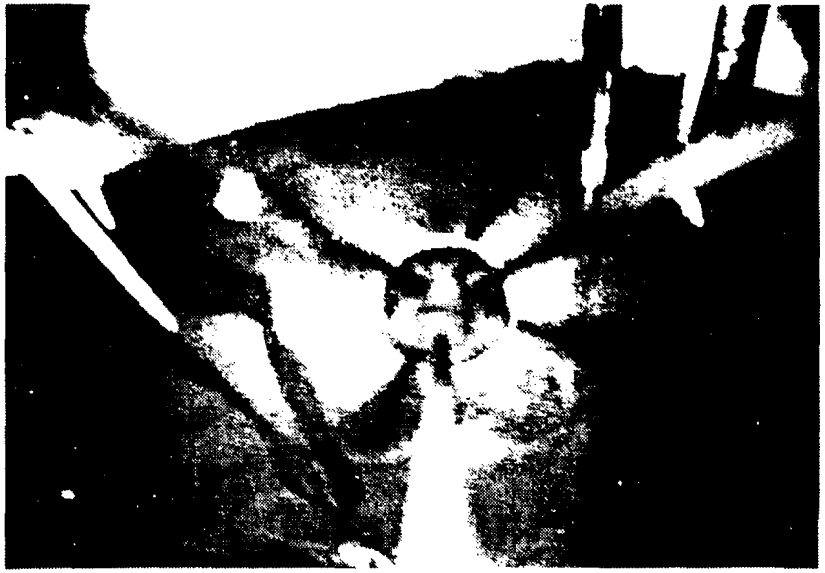

FIGURE 36
Liquid Interface; Outlet Cooling Water Lines;
Thermocouple Pipe

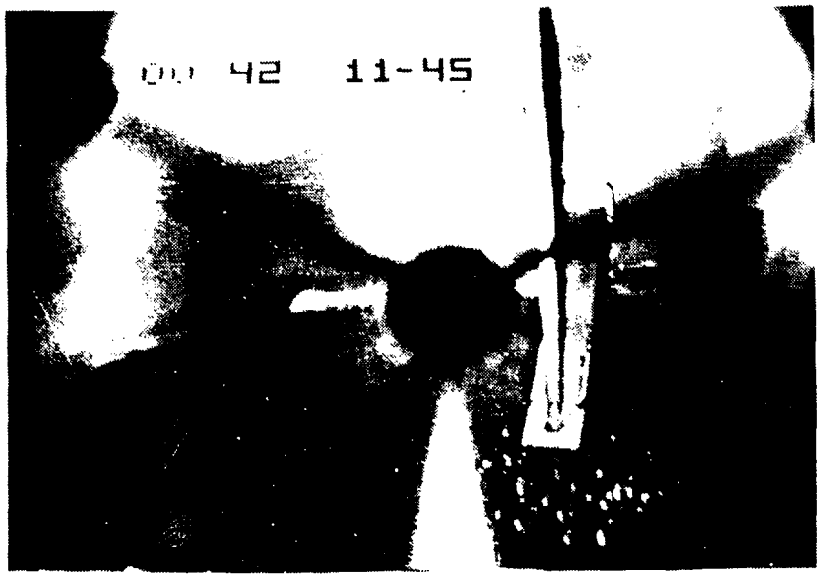

FIGURE 37
Low Pressure Air Bubbler Tube (Purging in Process?)

FIGURE 38
View Looking Straight Down Showing Solid Particles

8D-4 Video Stills - Crystalline Mass

FIGURE 39

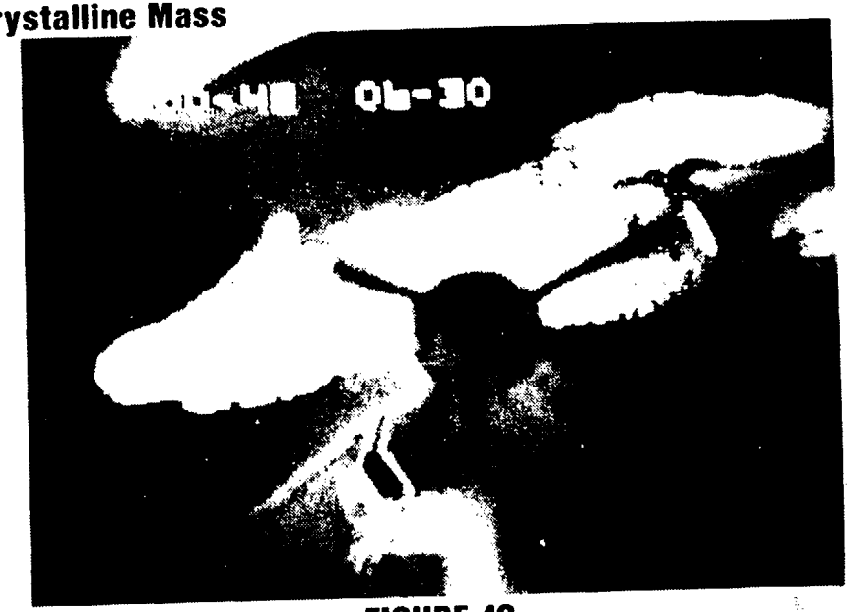

FIGURE 40

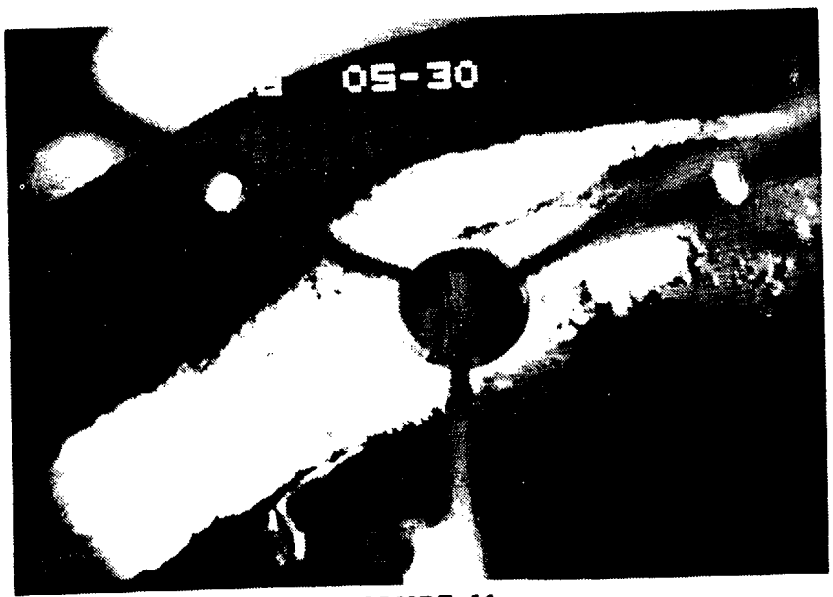

FIGURE 41

FIGURE 42

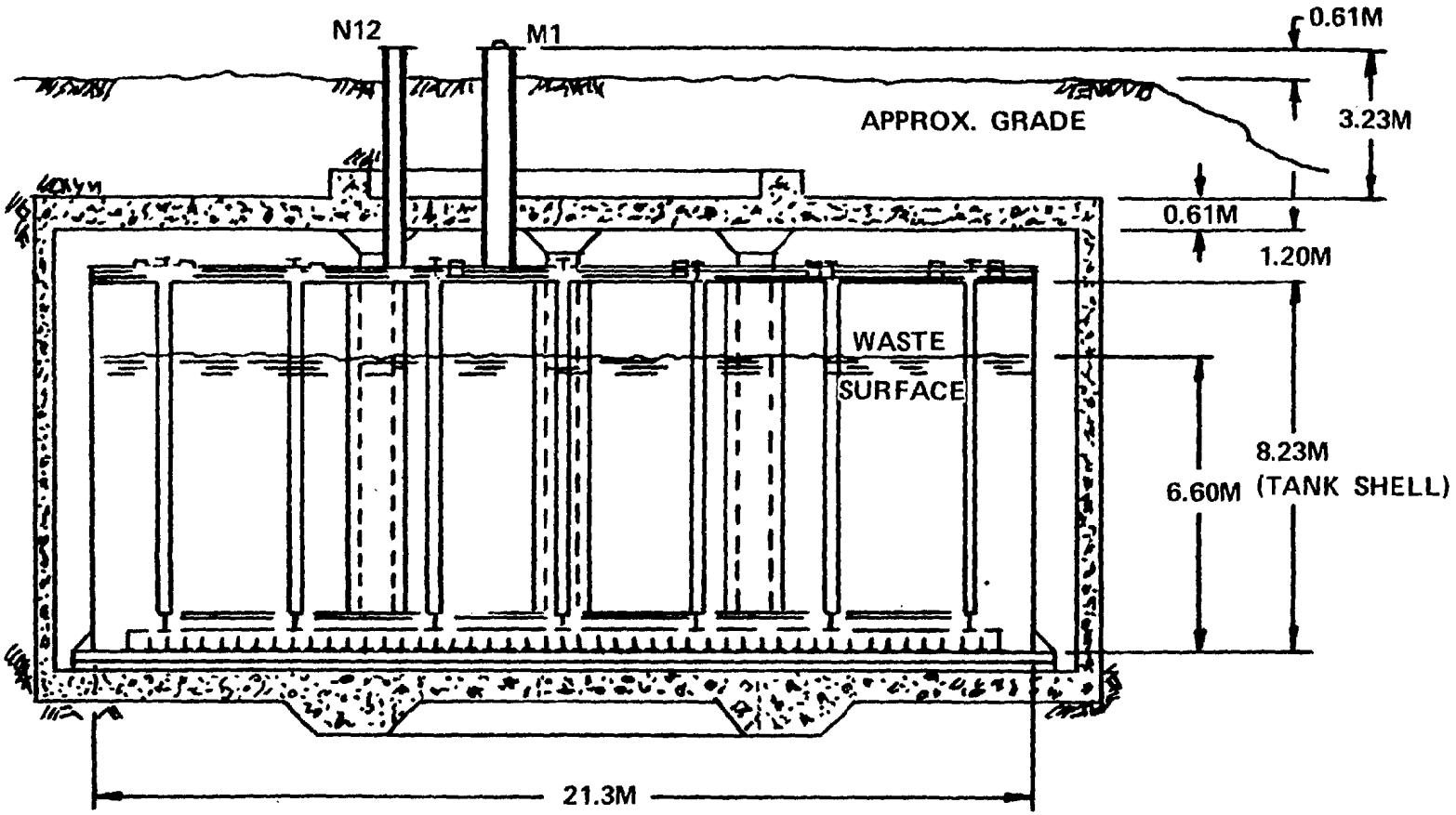

FIGURE 43
Tank 8D-2, Cross Sectional Elevation

Buoyancy Probe Tests

The buoyancy probe test is based on the simple concept of buoyancy effects on a submerged body as originally defined by Archimedes.

1) $W_A - W_L = V\gamma_L$

where W_A = weight of an object in air, W_L = weight of the same object in liquid, V = volume of object, and γ_L = density of the liquid.

The buoyancy probe device used consisted of an 8.44 kg stainless steel weight displacing a volume of 1.076 L. The probe was attached to a steel tape of uniform cross section with a per unit weight of 6.3 g/m. The tape was reeled out from a nearly frictionless pulley assembly (See Figures 44 and 45). As the probe was lowered into a liquid medium, an electric load cell measured its apparent weight. The load cell reading, R, together with the length of the reeled out tape at a certain elevation in the medium, L, was used to compute the liquid density, γ_L. Substituting these values into Eq. (1) yields

2) $\gamma_L = (8.44 - R + 0.0063L)/1.076$

in kilograms per litre.

The load cell readout was connected to an x-y plotter so that a continuous chart recording was obtained in addition to a digital readout. The top of the M-1 riser flange was used as a reference. Certified tank drawings were then used to convert the tape readings to distances from the tank bottom.

Figure 46 shows the buoyancy probe plotted to scale together with the density trend between 0.48 and 0.32 m. It was found that a loose sediment-liquid interface exists at 0.48 m above the tank bottom. The specific gravity (G_s) values computed between 0.48 and 0.32 m are thus "apparent" values, indicating an increasing influence of upward resistive "drag" type forces applied by the "loose sediment" against the penetrating surface of the probe.

When the buoyancy probe was lowered slightly below 0.32 m, a sharp drop in tension reading was observed and the probe was raised back to a height of 0.48 m. At that position, a steady reading again corresponding to a G_s of 1.27 was obtained. This procedure was repeated a few more times, and identical responses were obtained. This pattern seemed to suggest that the probe encountered a hard surface at a height of approximately 0.32 m. That surface must have had a firm support that prevented it from yielding or moving under the weight of the probe which, in turn, led to the observed abrupt loss of tension. The fact that the same tension reading was reestablished at the 0.48 m height after encountering such an unyielding surface implies a lack of "stickiness" in any of the sludge materials penetrated by the probe.

This initial probe led to the following results/conclusions[15]:

1. The vapor/liquid interface was identified at a height of 6.27 m above the tank bottom. Since this agreed with tank level instrumentation, it represented a verification of tank volume.

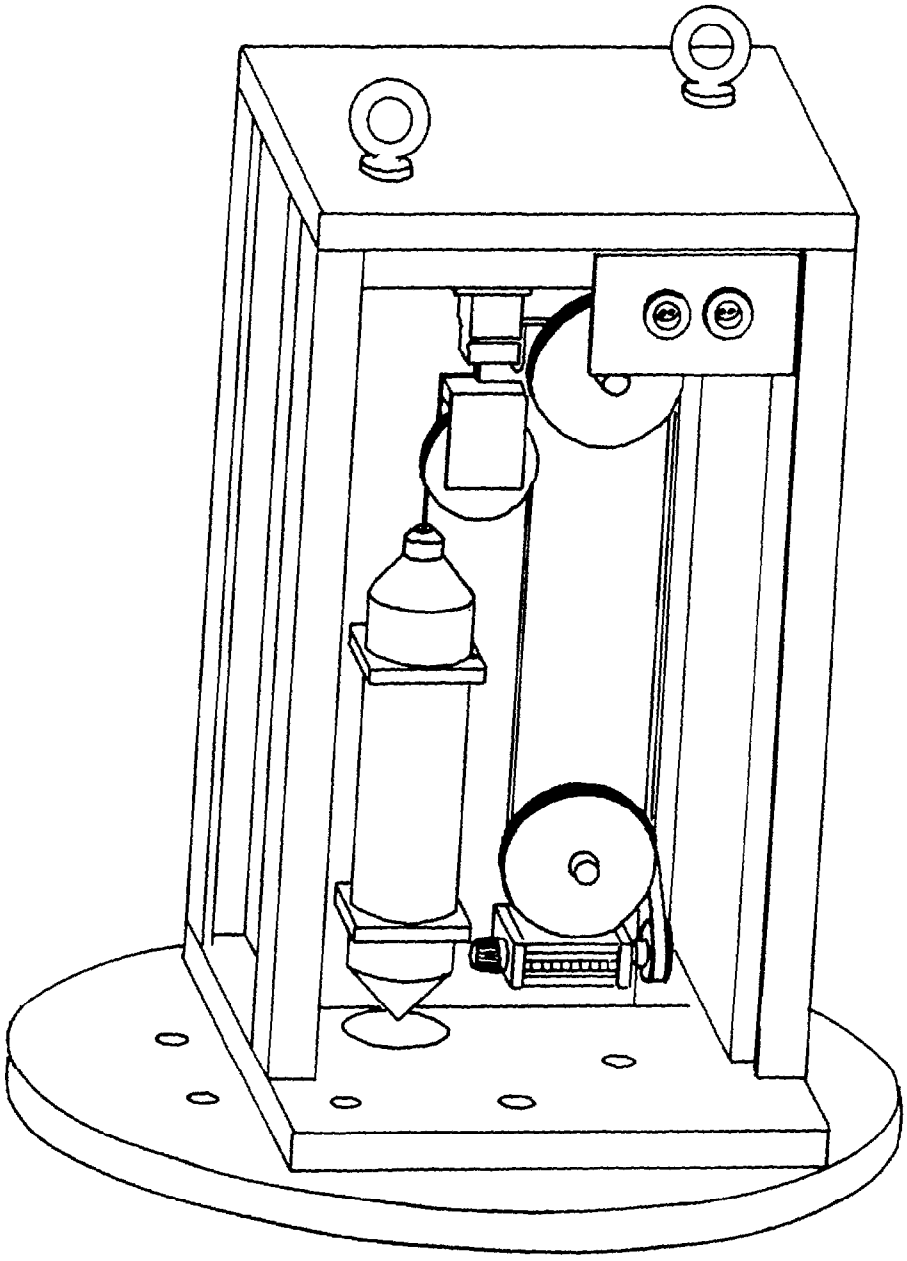

FIGURE 44
Bouyancy Probe Device

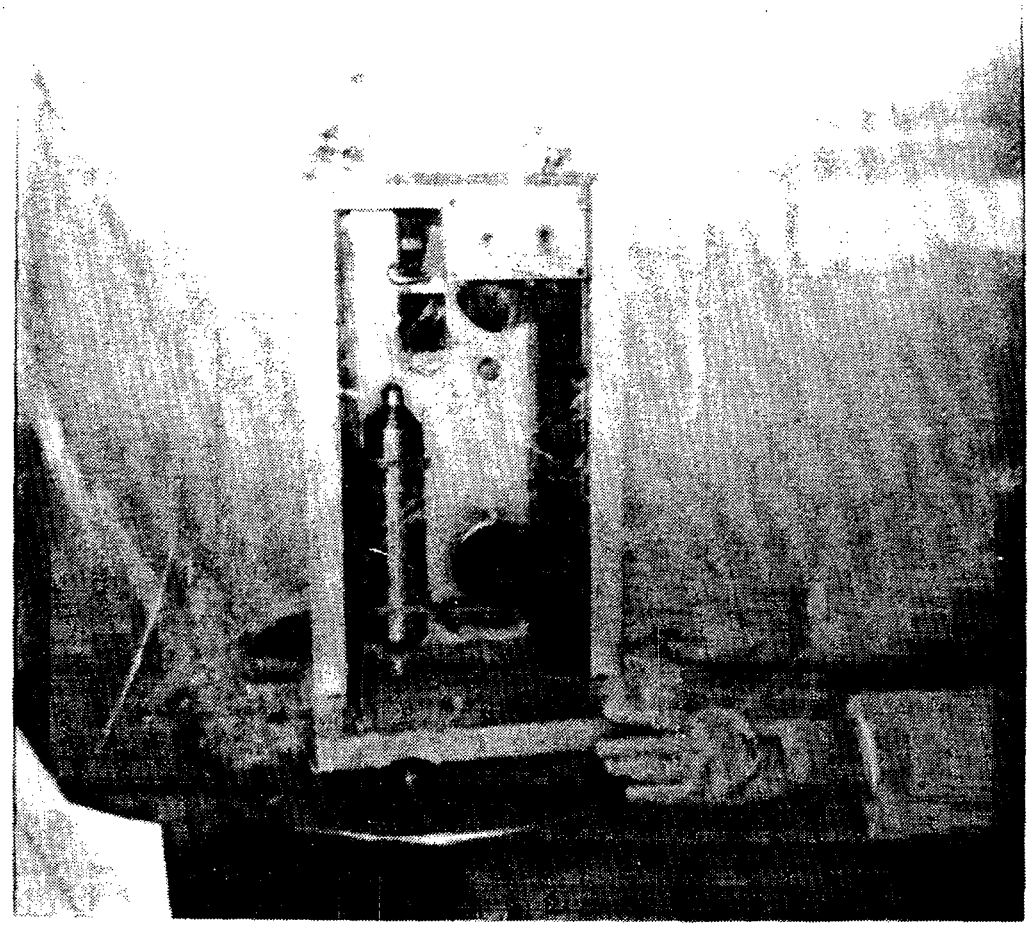

FIGURE 45
Buoyancy Probe Being Mounted on Tank Riser

2. The specific gravity (G_s) of the supernatant was constant, down to the sludge level. The precision of the apparatus was such that the value was determined to be 1.270±0.004 kg/L. This also agreed closely with tank instrumentation.

3. A slurry-like material was encountered at a height of 0.48 m above the tank bottom (henceforth referred to as the soft layer).

4. An unyielding surface (relative to the probe weight) was encountered at 0.32 m above the tank bottom (henceforth referred to as the hard layer).

Shear-Vane Tests

Shear vane testing is a widely used technique in the field of soil mechanics. The test is performed, both in the field and in the laboratory, to evaluate ultimate and remolded shear strength characteristics of cohesive soils, particularly soft clays.

The device used in this study was a four-bladed vane. Each blade was 38.1 mm wide, 76.2 mm high, and 3.2 mm thick. The blades are attached to the end of a long (>12 m) vertical shaft that is driven by a gear belt attached to a gear motor (See Figures 47 - 50). The latter is mounted on a platform that is free to rotate but is prevented from doing so by means of a link connected to a 45 kg electric load cell. When a resistance torque is applied by the medium being sheared to the vane and then to the shaft, the tension measured by the load cell is proportional to the magnitude of such torque.

As the vane is rotated within a medium, it shears it along a cylindrical surface. The expression of the shear strength of the medium along that surface as a function of the applied torque is given by the equation.

$$S = 6T/[\pi D^2(3H+D)]$$

where S = shear strength of the medium, T = applied torque, D = diameter of the sheared mass, i.e., twice the width of a blade, and H = height (length) of the blades.

In the particular case of the shear-vane device used in this testing, S in kPa can be obtained from the expression

$$S = 1.08T$$

where T is the applied torque in N·m.

Four shear-vane tests were performed at the elevations indicated in Figure 46. These four elevations were decided on the basis of the buoyancy probe test and the elevation of the tank bottom.

The scheme of each of the four tests, V-1 through V-4, is shown in Figure 51. The resulting initial shear curves obtained are shown in Figure 52 and are summarized in Table 13.

TABLE 13: SHEAR VANE TEST RESULTS

Test ID	Height (m)*	Peak Torque (N·m)	Peak Strength (kPa)	Time to Peak (min)
V-1	0.35	0.4	0.4	5
V-2	0.22	2.7	2.9	2
V-3	0.12	26.6	28.7	9.3
V-4	0.02	31.6	34.2	10.5

* Bottom of vane above tank bottom

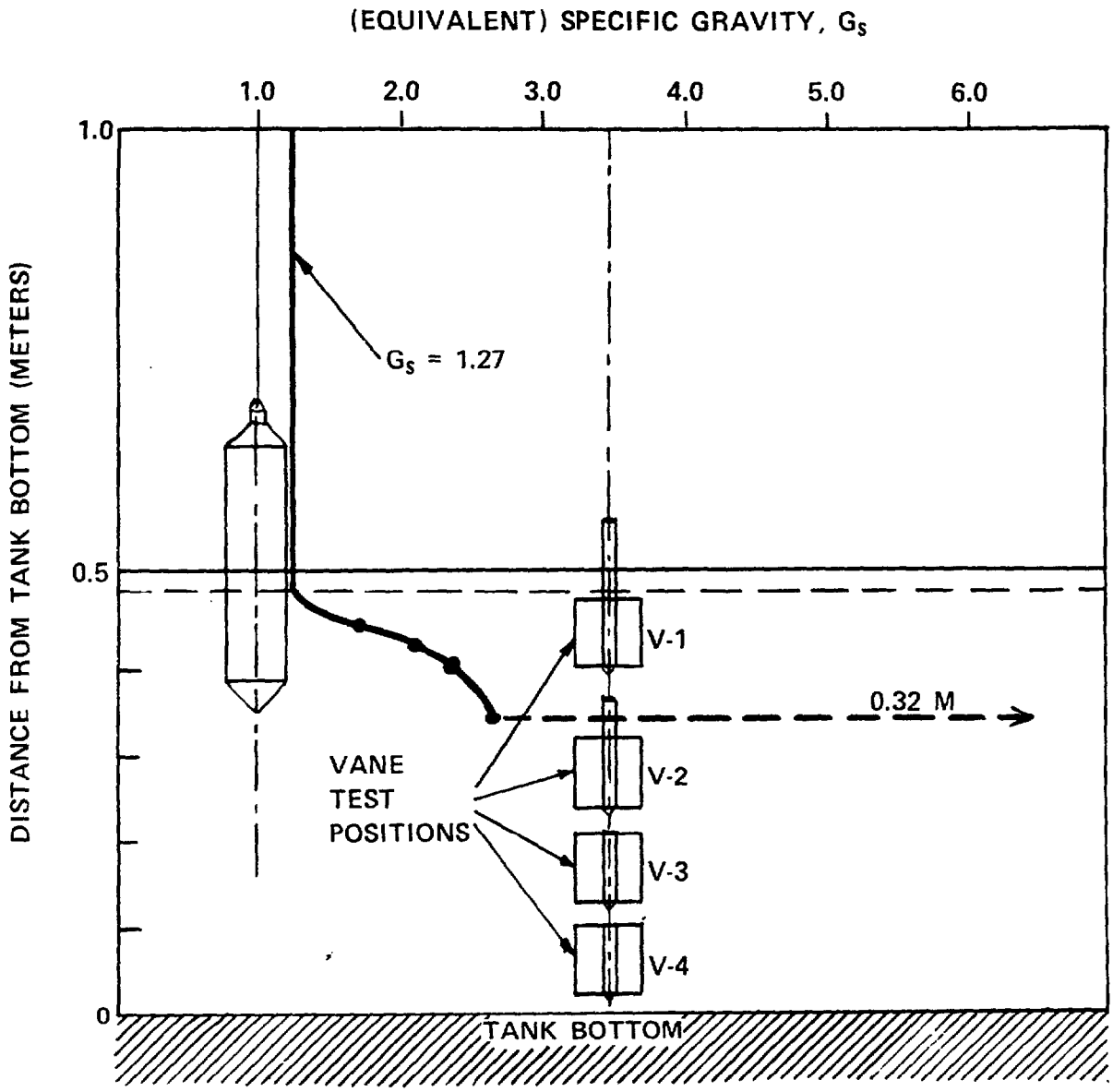

FIGURE 46
Buoyancy Probe Test Results

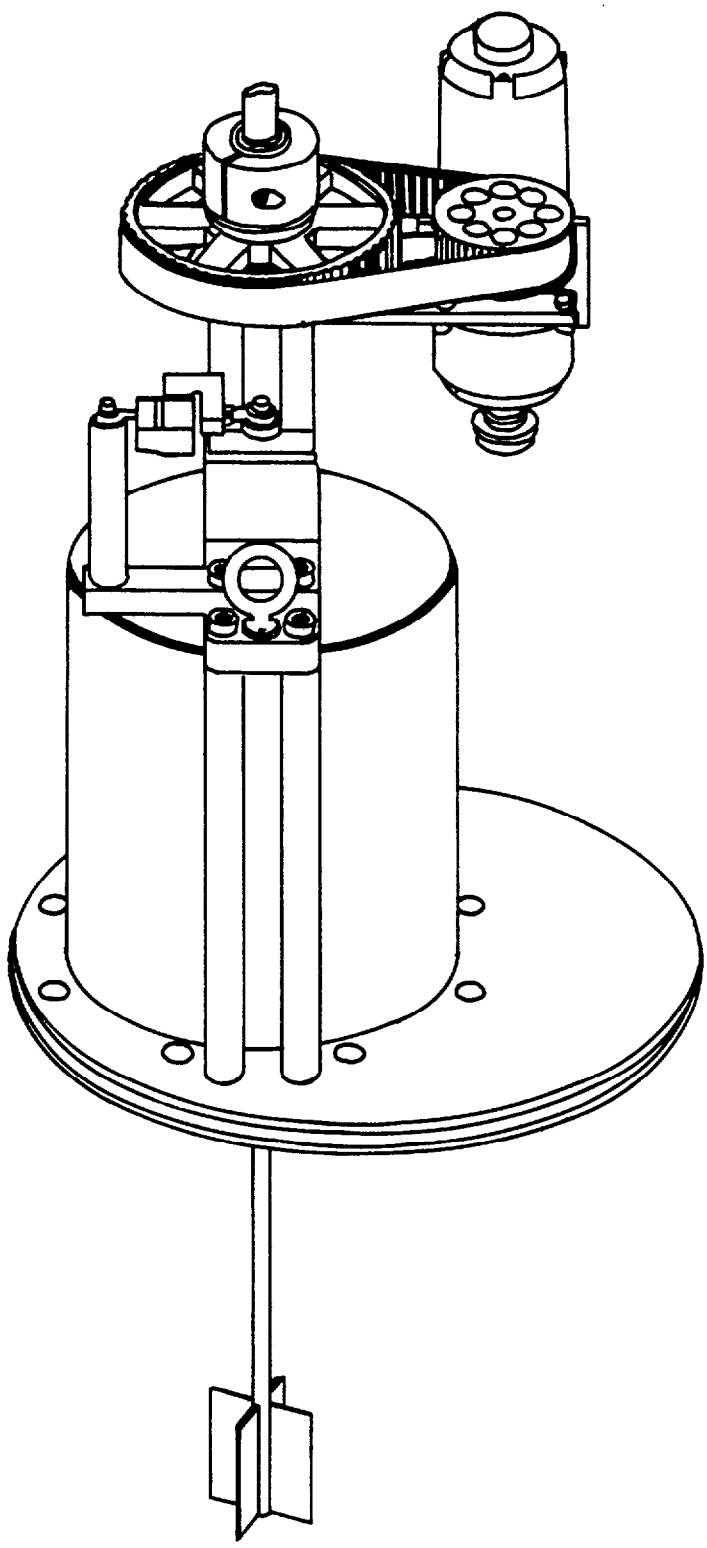

FIGURE 47
Shear Vane Device

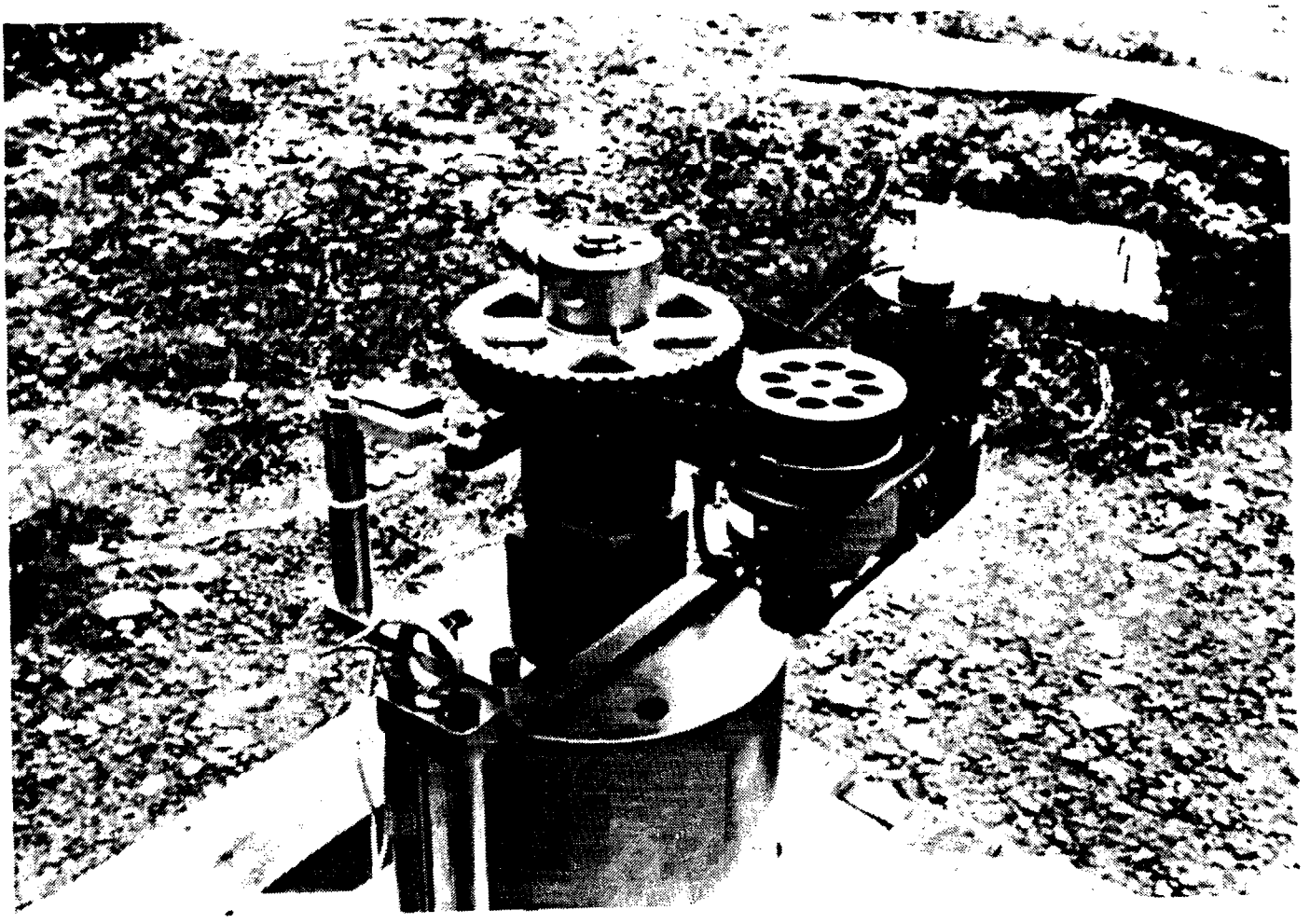

FIGURE 48
Top of Shear Vane Showing Driver and Torque Indicator

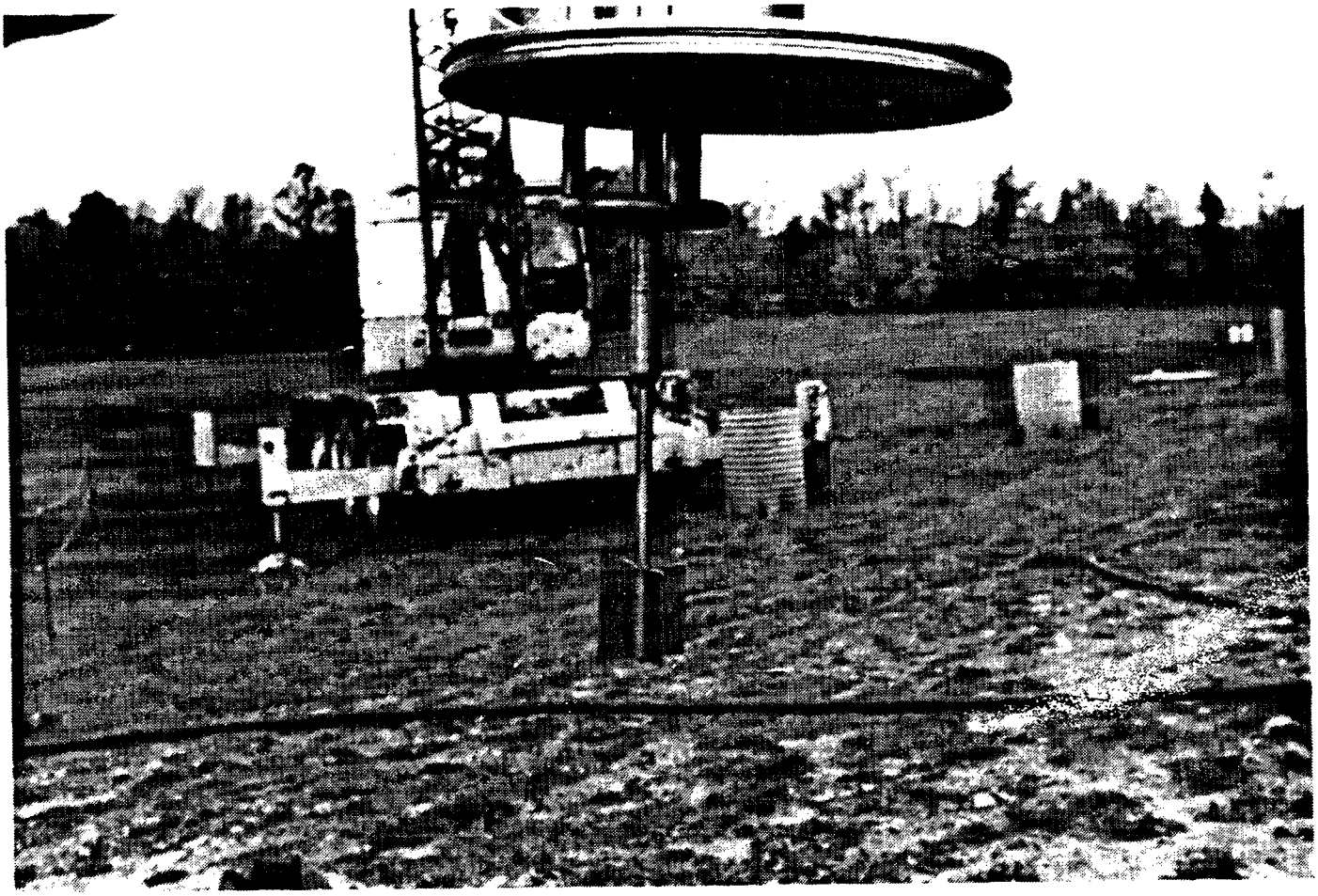

FIGURE 49
Bottom of Shear Vane Showing Shield Plate and Vane

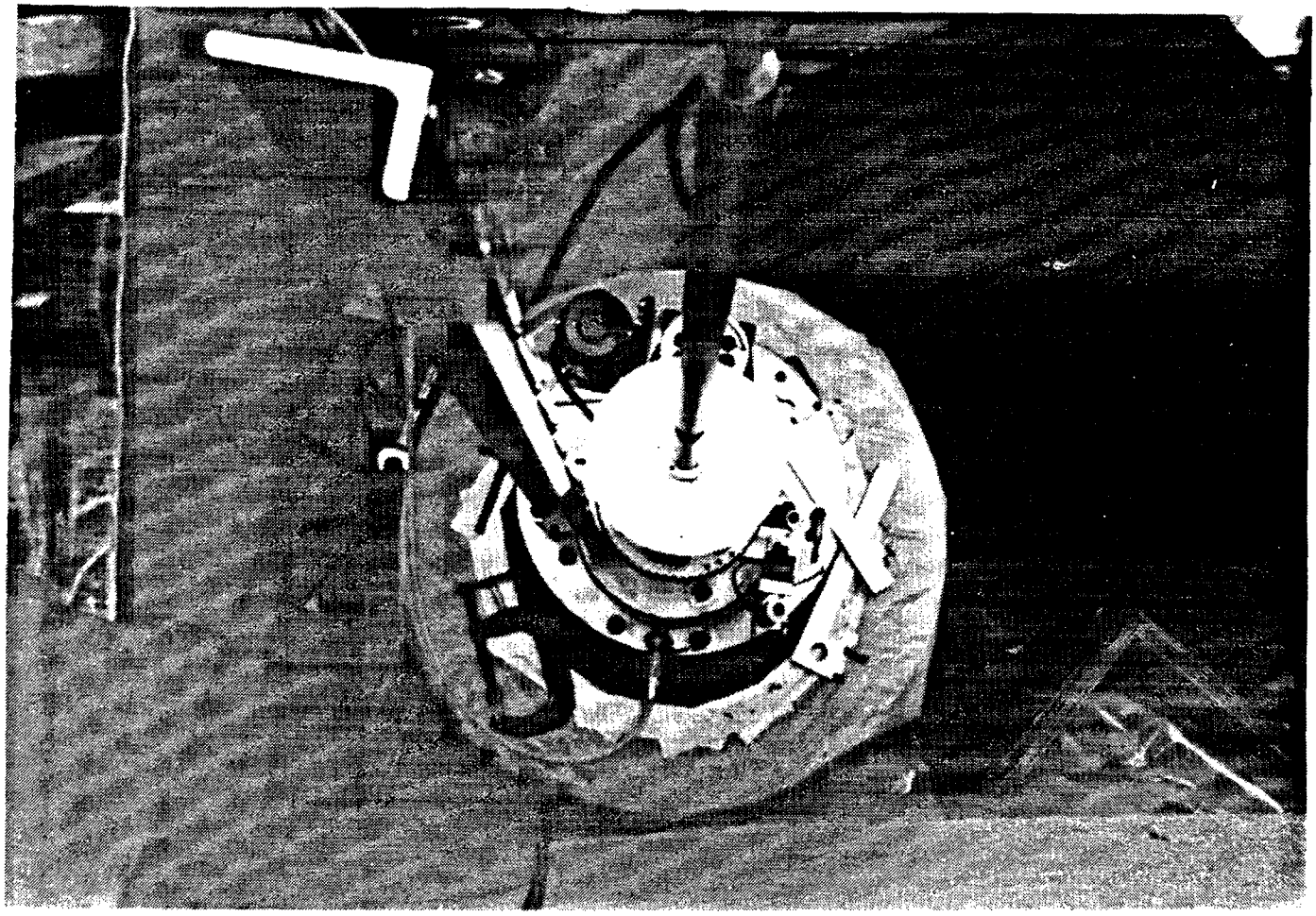

FIGURE 50
Shear Vane Mounted on Riser

The results presented in Figure 52 clearly show the striking differences in consistency between the materials sheared in tests V-1 and V-2 and those sheared in tests V-3 and V-4. To appreciate the implications of the peak strength values obtained (these are shown in parentheses next to the peak torque value for each curve), it should be noted that with a peak shear strength of 2.9 kPa, most naturally occurring "muds" would not be able to support their own weight unless contained laterally. Thus, sludge material encountered in V-1 and V-2, i.e., between depths of about 0.5 and 0.2 m from the bottom, are most likely soupy or light slurry-like in consistency.

The materials encountered in V-3 and V-4, i.e., within the bottom ~0.2 m layer of sludge, appear to be relatively cemented as they yielded peak strength values comparable to a medium stiff clay. The frictional component of their strength is probably negligible due to the lack of effective overburden applied to them vertically. In this case, such overburden is limited to about 2.5 - 5 kPa, i.e., the stress due to the buoyant weight of the ~0.3 m of sludge above it. The frictional component of their strength would be equal to the product of the effective overburden (the buoyant weight of the ~0.3 m of sludge above it) and the tangent of the angle of internal friction (ϕ). If we assume an upper loose slurry density of 1.5 kg/L and a ϕ of 0.35 rad, this is only 0.25 kPa, which is negligible compared to the measured 25 - 30 kPa.

The cohesive nature of the bottom 0.2 m layer can be further substantiated by additional examination of certain secondary characteristics of the tested sludge, specifically the following parameters (see Figure 51): residual strength ratio = $\alpha_o = S_R/S_P$ and initial shear relaxation ratio = $\lambda_o = T_B/T_R$.

Plots of both α_o and λ_o versus S_P for the sludge are shown in Figures 53 and 54 together with those obtained for five bentonite mixes and two relatively loose sand masses, all tested with the shear vane prior to actual sludge testing.

From Figure 53, it can be seen that the sludges in Tests V-3 and V-4 appear to have displayed a substantially lower tendency of strength loss after reaching a peak value with an average α_o of about 0.8, compared to 0.6 for bentonite mud. It is postulated that the limited rate of postpeak strength loss in V-3 and V-4, as compared to the bentonite tests, is attributable to the difference in the roughness of the failure surface in the two materials.

From the same plot is can be seen that the two sands had an average α_o value of about 0.4. Of interest is the remarkable loss of strength displayed in the V-1 and V-2 tests, as indicated by α_o values of 0.15 and 0.2, respectively. This is interpreted as added evidence of the "loose" nature of these sediments, since a relatively "open" particle-to-particle microfabric would have resulted in a substantial degree of structural change during shear and thus led to the observed loss of strength.

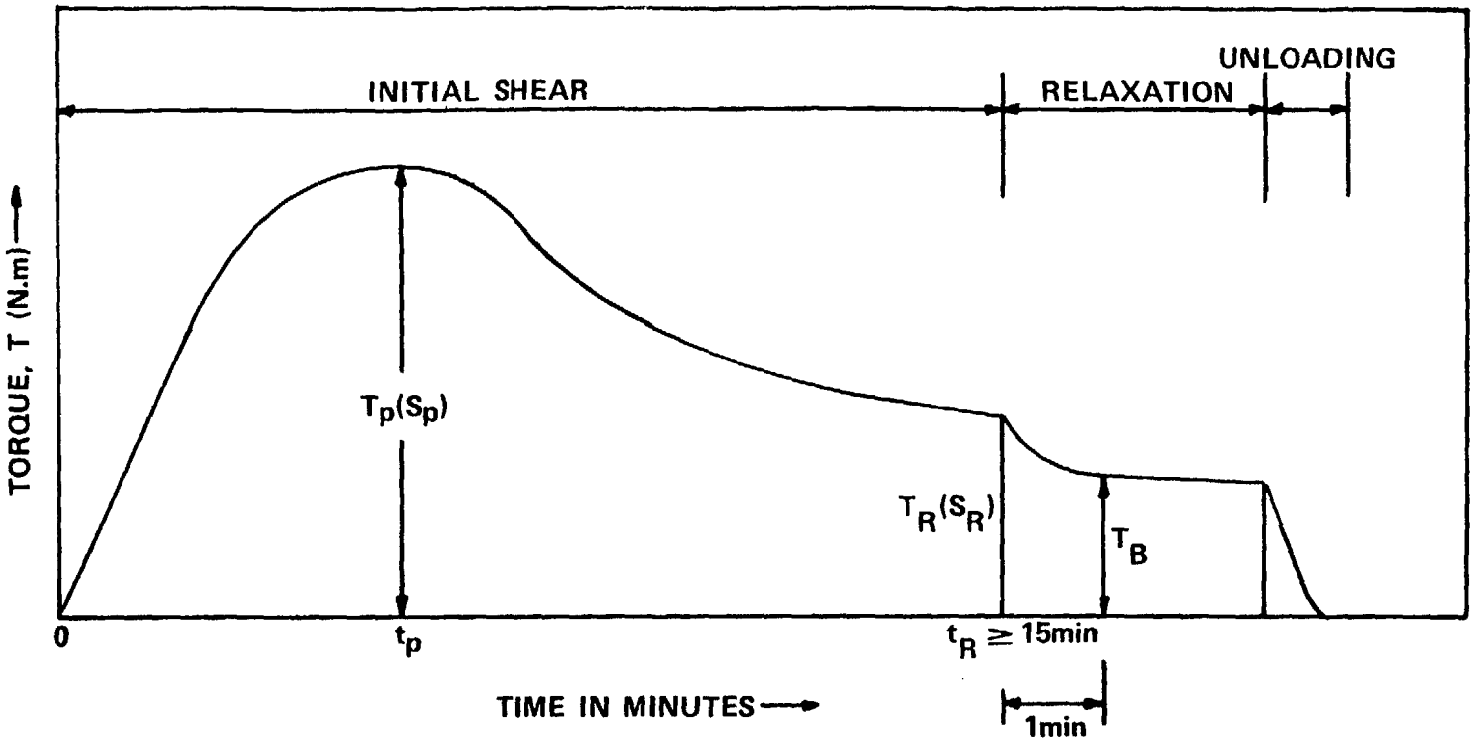

FIGURE 51
Shear Vane Test Scheme

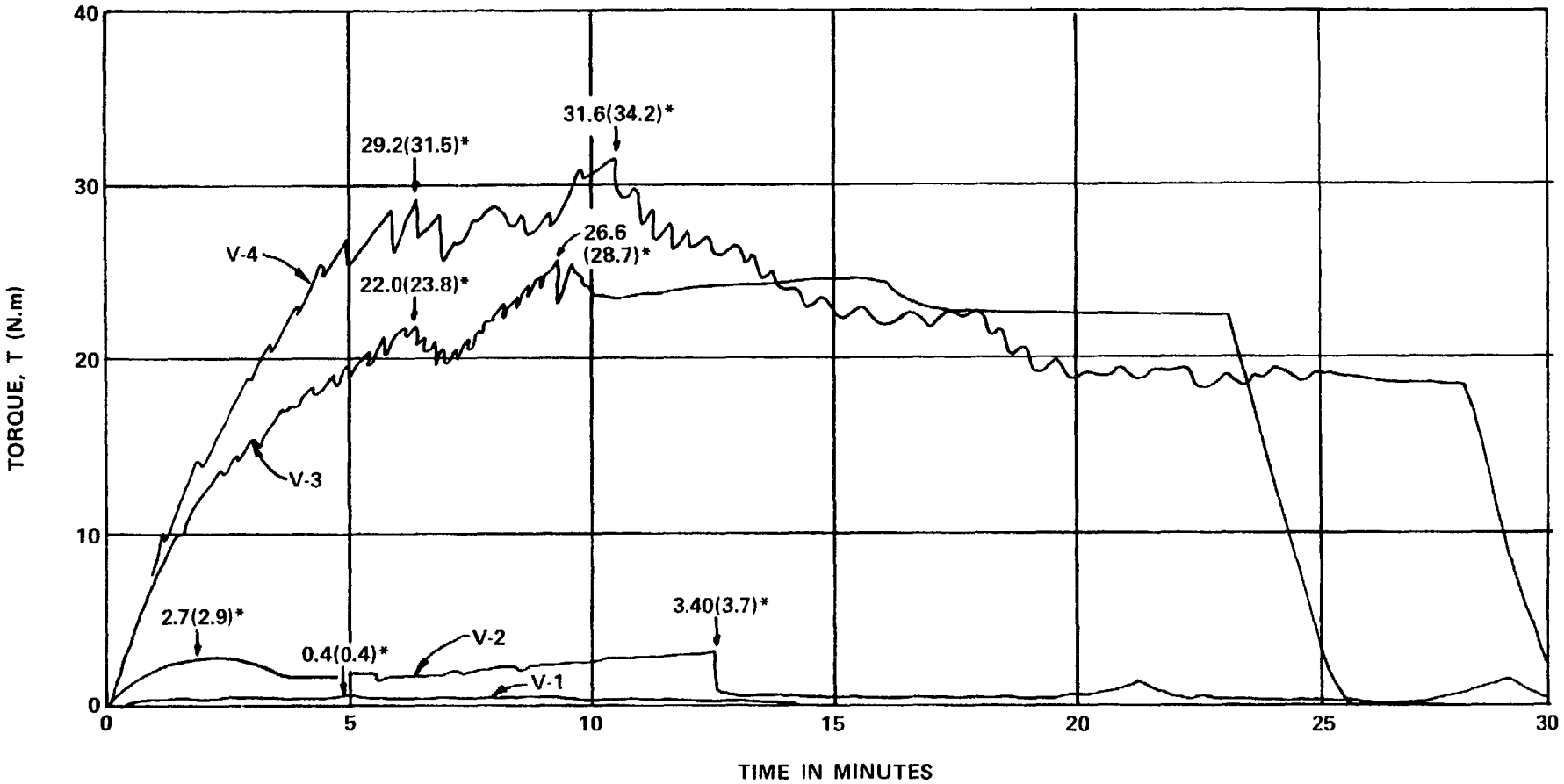

*VALUES IN PARENTHESIS REPRESENT CORRESPONDING PEAK STRENGTH

FIGURE 52
Shear Vane Test Results

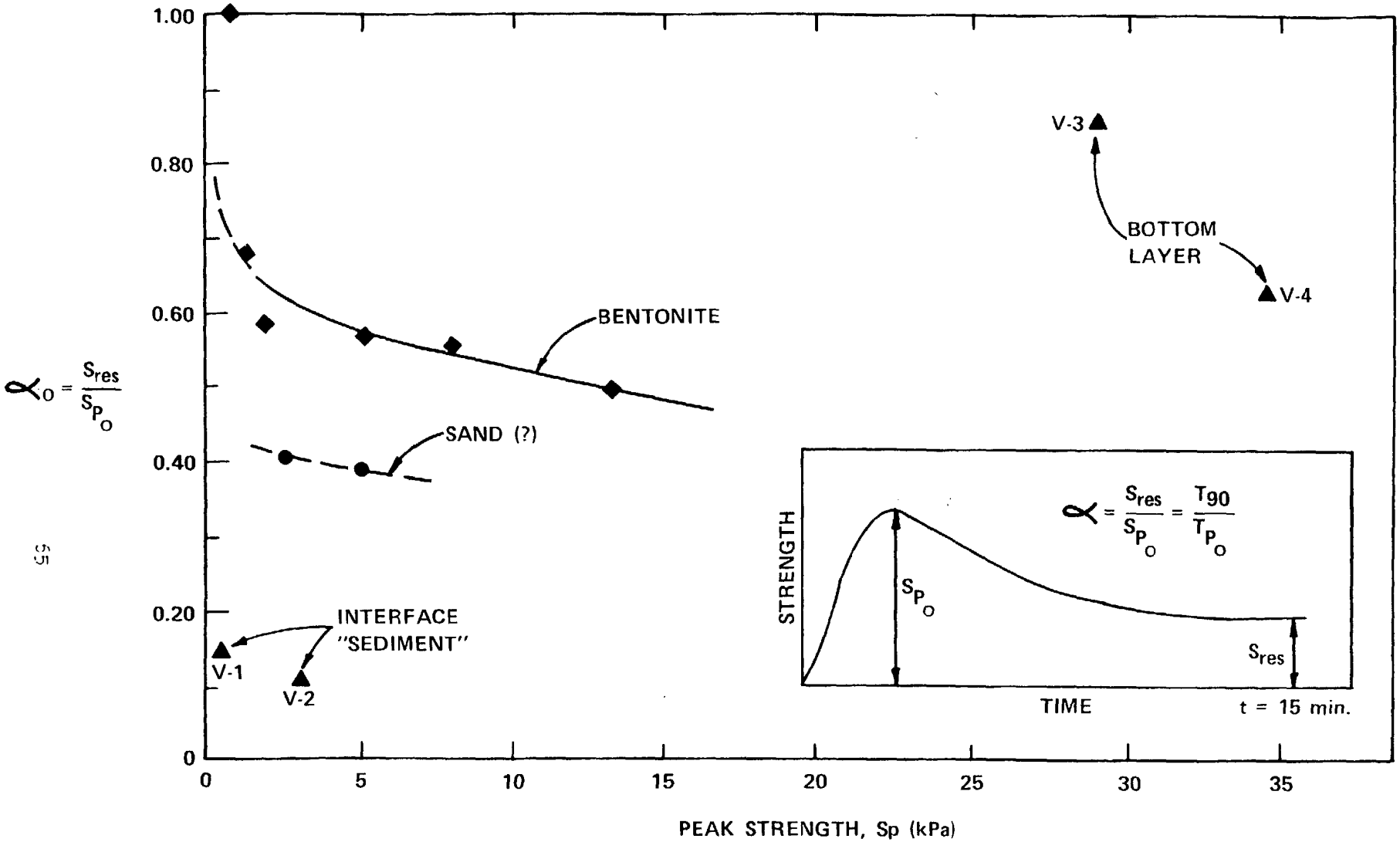

FIGURE 53
Shear Vane Test Results

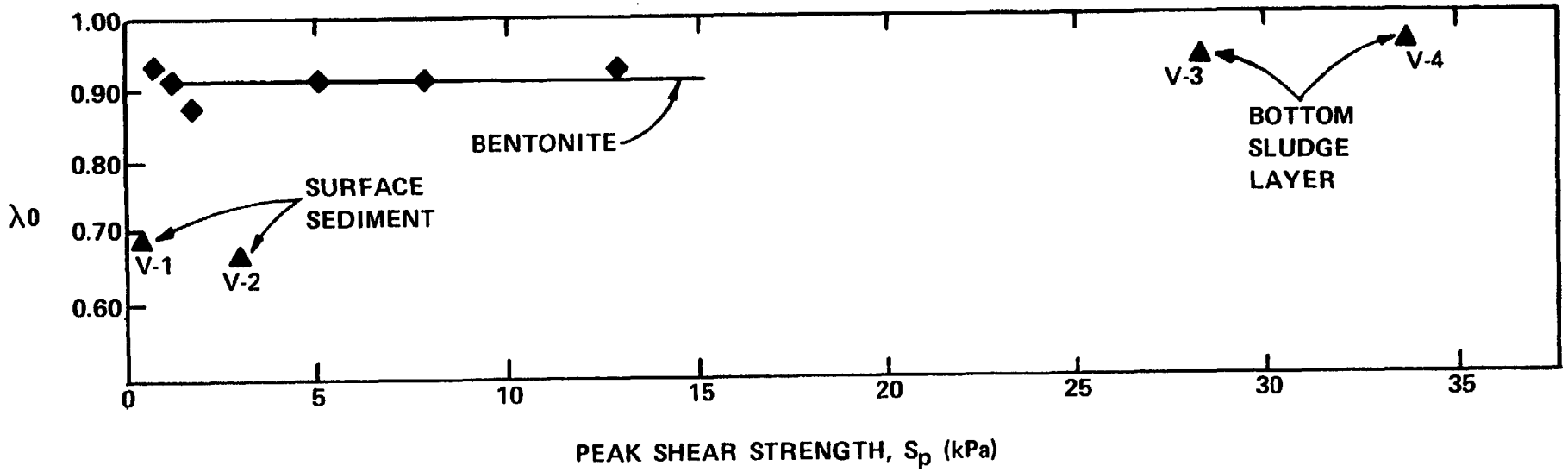

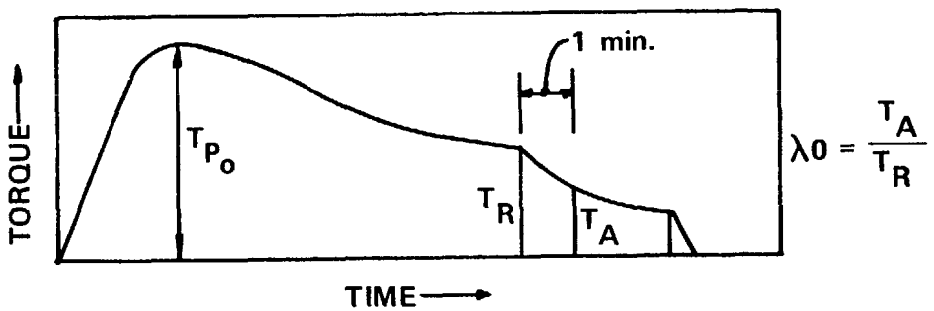

FIGURE 54
Shear Vane Test Results: Sp Versus λ0

The relaxation response of the tested sludges is defined in Figure 51 and is plotted in Figure 54 for the sludge and the five bentonite clays. The similarity of the λ_o values obtained for the V-3 and V-4 sludges and the bentonite clays is remarkable when compared to those obtained for V-1 and V-2. This trend is believed to further substantiate the interpretation that the bottom 0.2 m layer of sludge is cohesive.

Extended Topographic Measurements

As a follow-on to the initial in situ probing, an articulated arm device was designed and fabricated that would utilize and extend the range of the buoyancy probe device (See Figures 55 and 56). In these tests, the interface between the supernatant and the soft layer and that between the soft layer and the hard layer were reidentified for the location directly along the axis of the M-1 riser and were also located for eight additional points located 1.5 m from this point. In order to better evaluate the information obtained in these test, contour lines for each of the two interfaces probed and a sectional profile (See Figures 57, 58, and 59) were drawn.

6. SLUDGE CORE SAMPLING

As a follow-up to the in situ characterization tests, it was decided to obtain a vertical core sample of the sludge layer. The criteria that were used in the design of the sampling equipment were:

1. Sampling was to be performed through the 200 mm opening in the M-1 riser that had been used for all previous characterization activities.

2. The core was limited to 19 mm diameter based on exposure considerations.

3. An assurance of penetration to the tank bottom was desired.

4. A high probability of obtaining an undisturbed, i.e., nonsmeared sample was desired.

5. It was to have the capability of drawing the sample without exposure into a liquid-tight "primary containment," which in turn would be inside a transfer cask with sufficient shielding to allow contact handling (<10 mR/hr).

6. It was to have the capability of transferring the primary containment in the transfer cask to the Analytical Cells and transfer the primary containment from the transfer cask into the shielded Analytical Cells without exposure.

7. There was to be the capability of removing the samples from the primary containment and to remove the sample from the sampler with MSMs inside the Analytical Cell.

Equipment meeting the above criteria was designed, fabricated, and tested. The sample tube had a split barrel, was coated with Teflon^R and fit inside an outer stainless steel tube (See Figures 60 - 62).

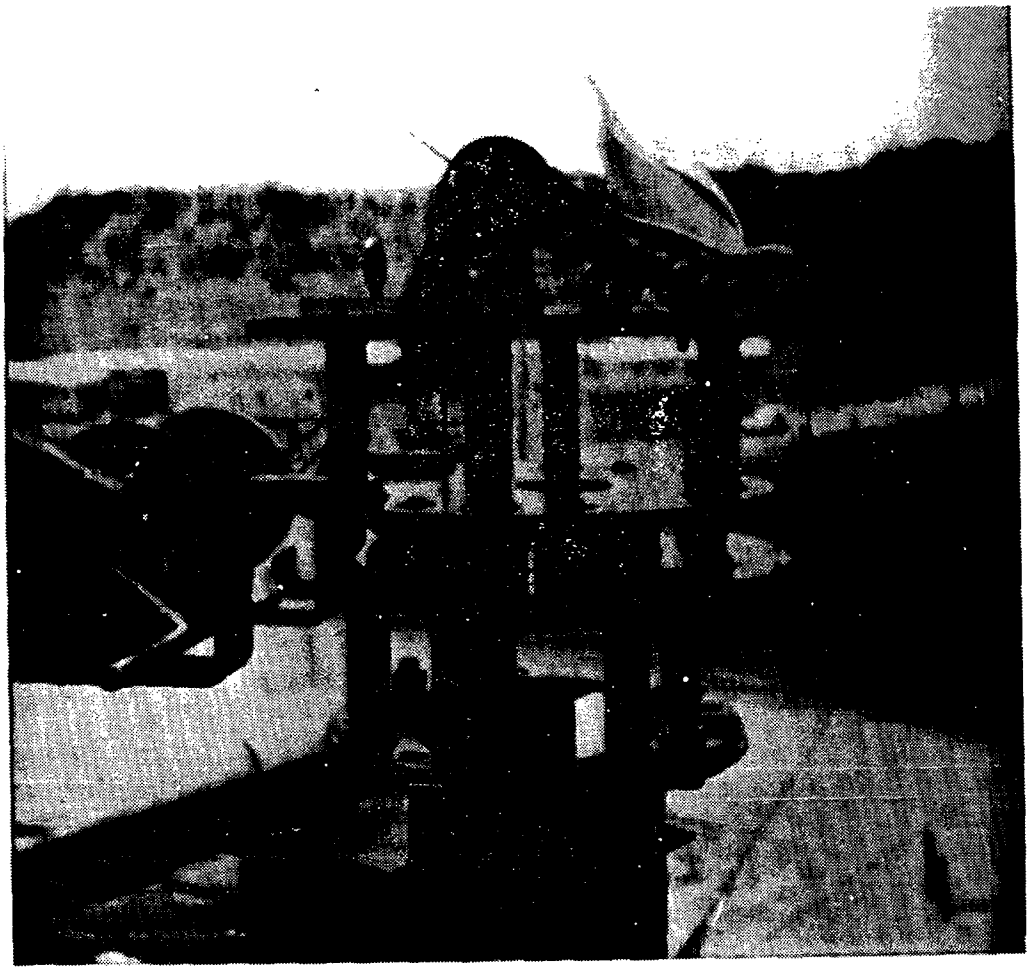

FIGURE 55
Top Assembly of Articulated Arm Device

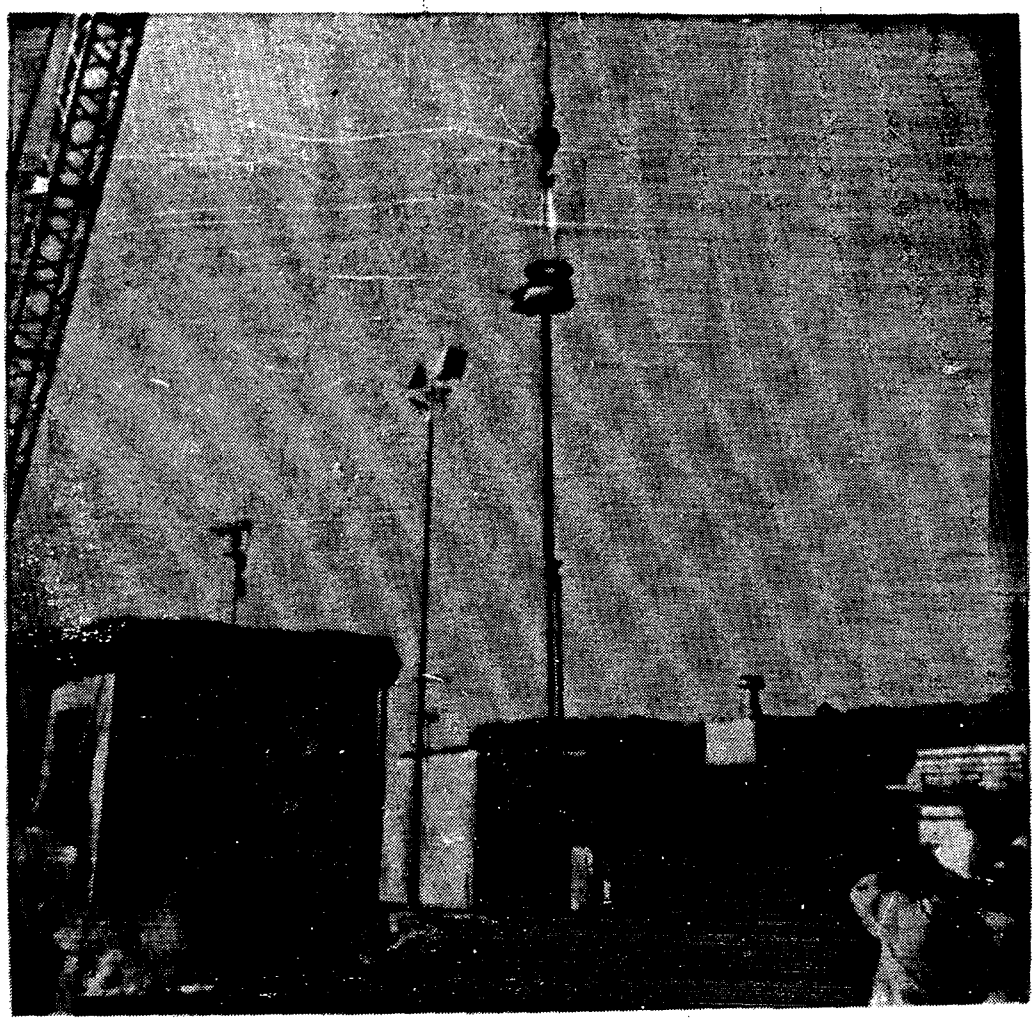

FIGURE 56
Articulated Arm Assembly Ready to be Lowered into Containment

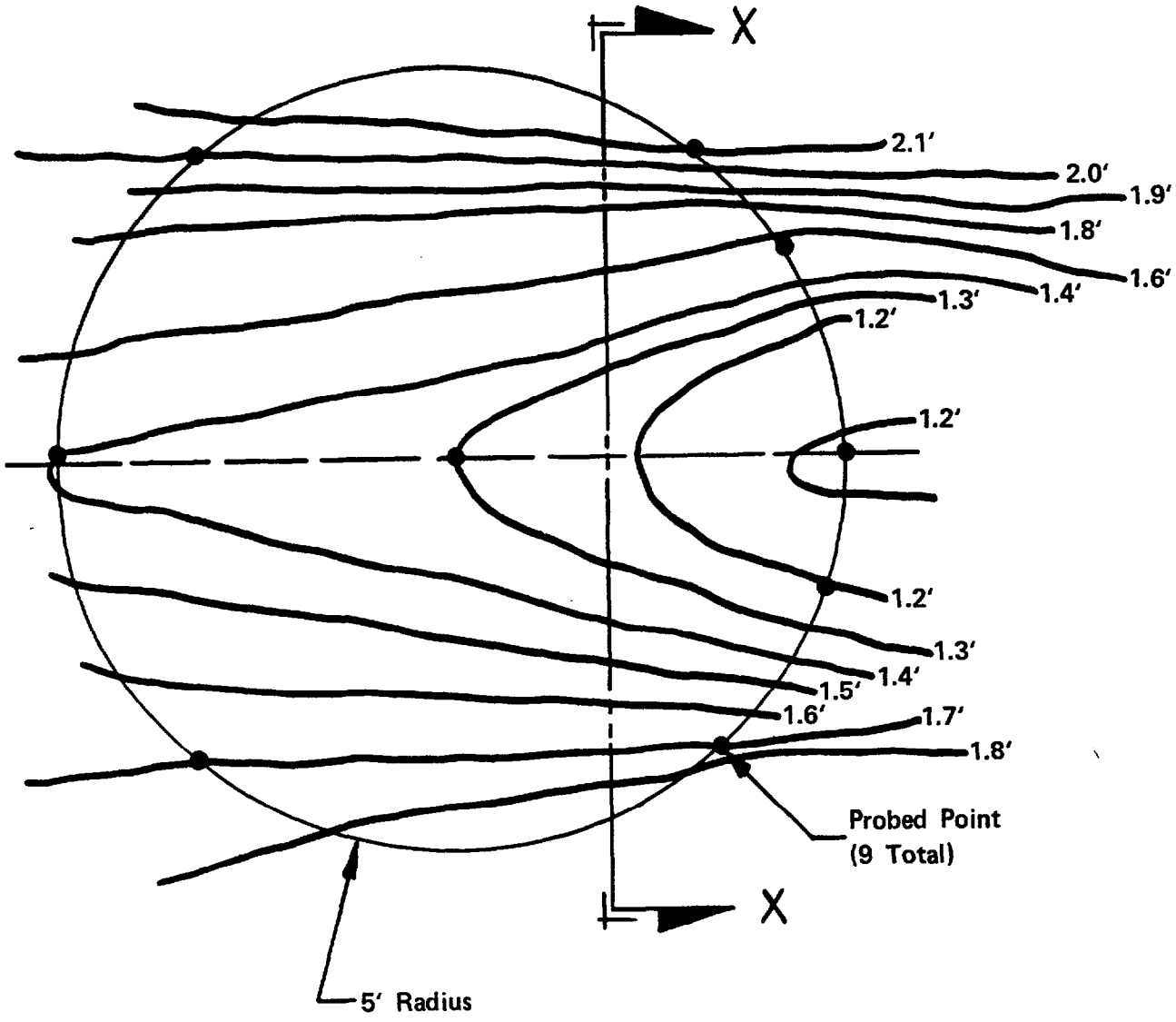

FIGURE 57
Projected Top Sludge Surface Contours Based on Probing

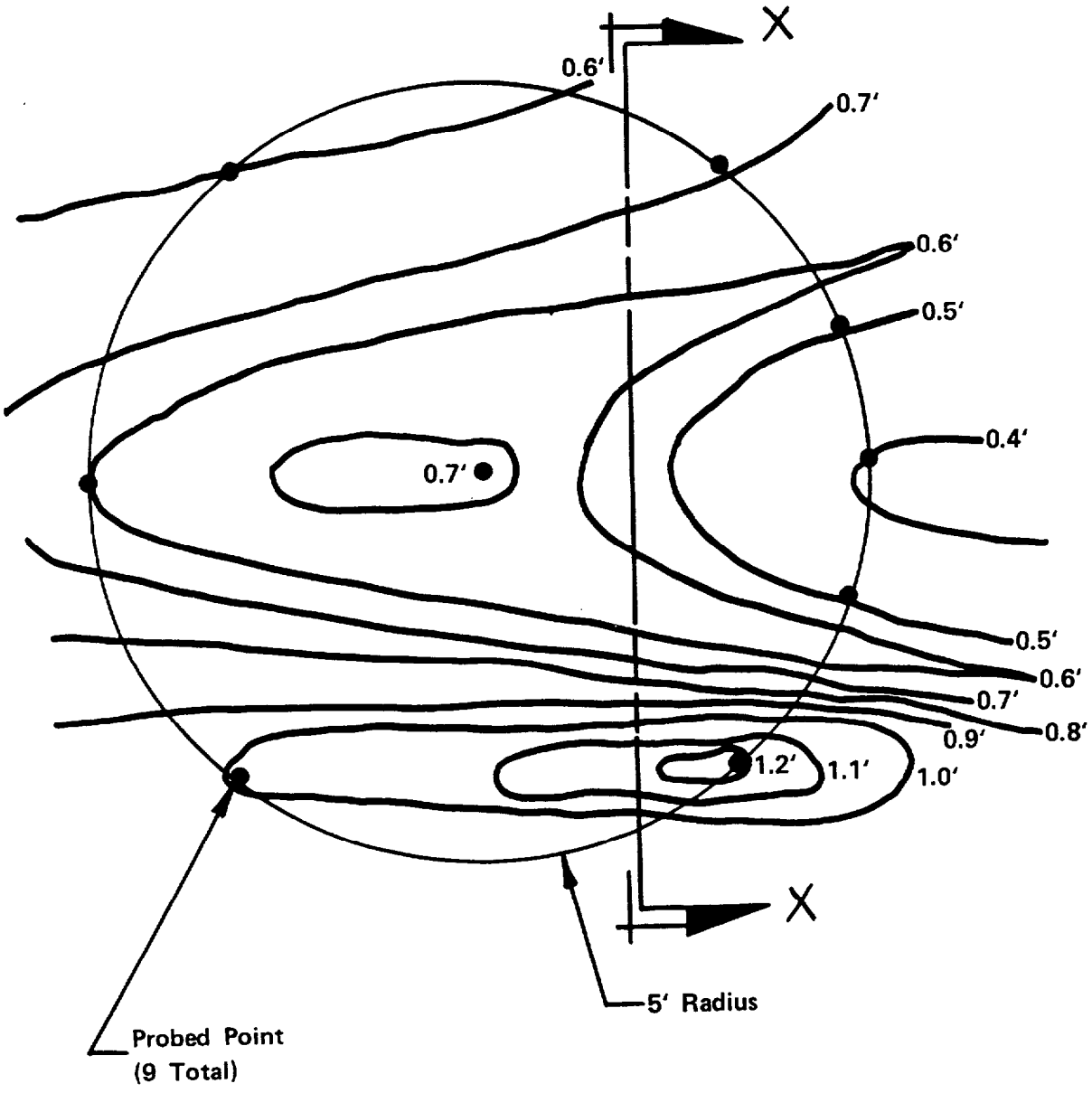

FIGURE 58
Projected Bottom Sludge Contours Based on Probing

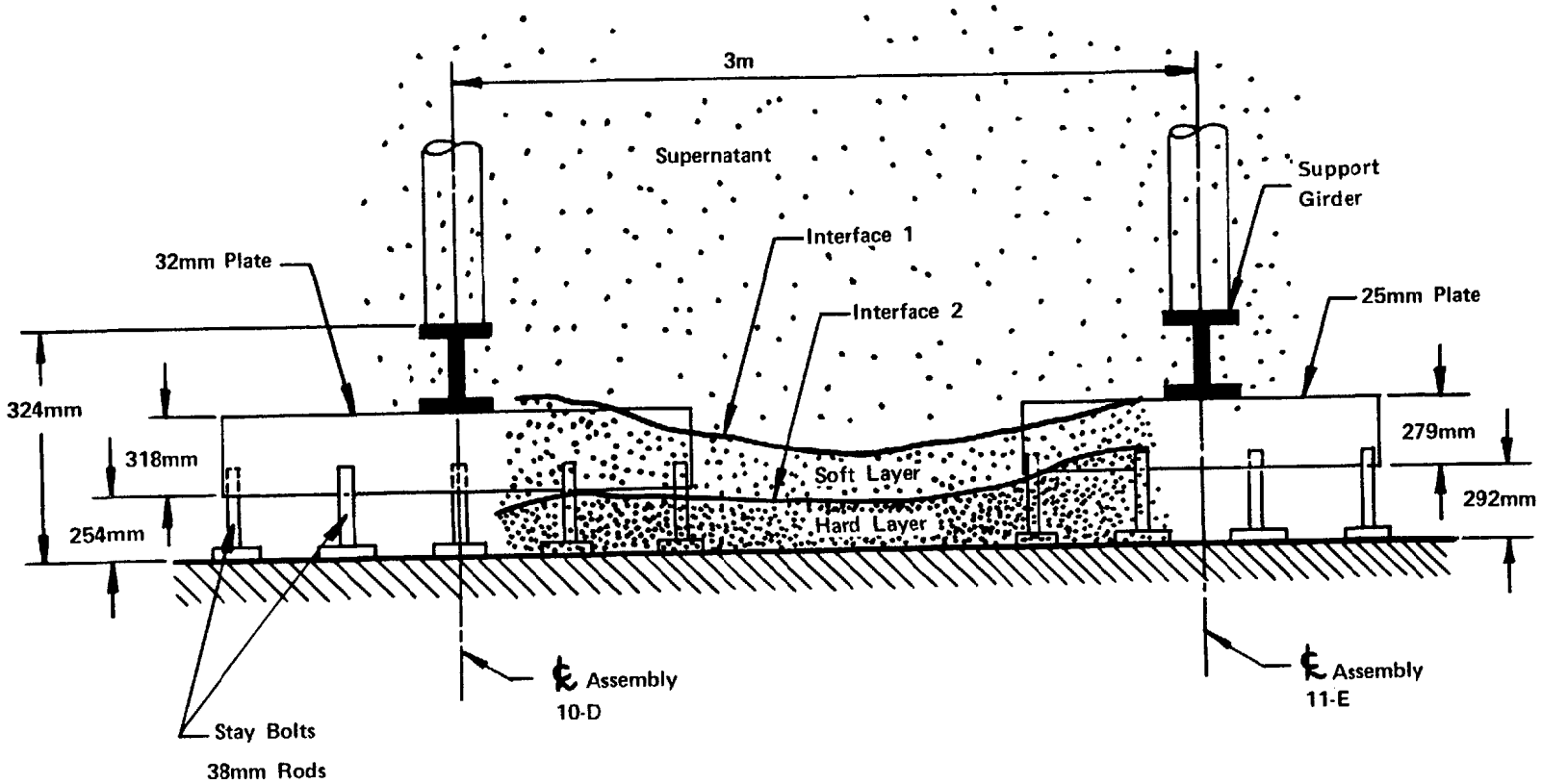

FIGURE 59
8D-2 Sludge Layering: Sectional View X-X

A piston with an O-ring seal operated inside the split-barrel sample tube. The sample tube had protrusions on each end so as to leave a 0.965 mm clearance between the sample tube and the outer tube. Twelve 4.3 mm wide x 0.25 mm deep slots were machined into one end of the sample tube. Thin stainless steel foils 0.025 mm (1 mil) in thickness were spot welded to notches milled into the piston. When assembled, the foils ran from the piston, around the notched end of the sample tubes, and fit in the annular space between the sample and outer tube. When operated, i.e., when the sample is obtained, the piston is held stationary while the outer and sample tubes move into the sludge. This forces the foils to move along the inside of the sampler. There is no relative motion between the sludge and the foil lining and this tends to prevent smearing. When the operation is complete, the foils line ~85 percent of the interior of the sample tube. In addition, relative motion of the piston and sample tubes create a suction which tends to hold the sample. Further assurance of sample retention is provided by a notched bit on the end of the outer tube which is designed to crimp when driven against the bottom of the tank. Soil sampling using the foil-lined sampler principle was developed in Sweden in the 1940s[16,17] in order to obtain undisturbed samples of the soft marine clays of Scandinavia.

The sampler is attached to a long (>14 m) 25 mm OD drive rod assembled in 1.5 m threaded sections. The rods were drilled so as to accommodate a 6.35 mm inner rod attached to the piston. By means of a framework, the whole assembly could be lowered into the riser down to the sludge level, the piston rod held stationary, and the drive rod forced down to capture the sample. The drive rod was driven by a "dynamic" driving mechanism consisting of two eccentrically-weighted shafts rotating in opposing directions on each side of the drive shaft. The rotary motion results in transmitting a gentle vertical vibrator motion which was presumed to increase the probability of high recovery.

After sampling, the assembly was lifted out of the riser. Placed on top of the riser was a transfer cask which provided 160 mm of lead shielding. Within this shielding was a Delrin^{R} primary containment vessel. The sampler was raised into the containment such that it was secured by a double O-ring seal on the top. Closing a ball valve on the bottom of the containment completed the retention of the sludge-containing sampler in the liquid tight primary containment.

The lead-shielded transfer cask was then transported to the Analytical Cell area. A 200 mm port had previously been cored in the 0.9 m thick concrete wall of the Analytical Cells and fitted with a shielded access port. By raising the cask and rotating it 90°, the transfer cask could be fitted to the access port, a lead shutter raised, and the primary containment pushed into the Analytical Cells without any exposure.

Once in the cells, the apparatus was designed such that MSMs together with relatively simple tooling could be used to remove the sampler from the containment and to disassemble the sampler to expose the sludge. After photographing, the core was placed over a compartmentalized sample tray so that the sample could be split into seven portions (each tray was 25 mm wide). Approximate 0.1 g portions were placed in sample vials for later analysis.

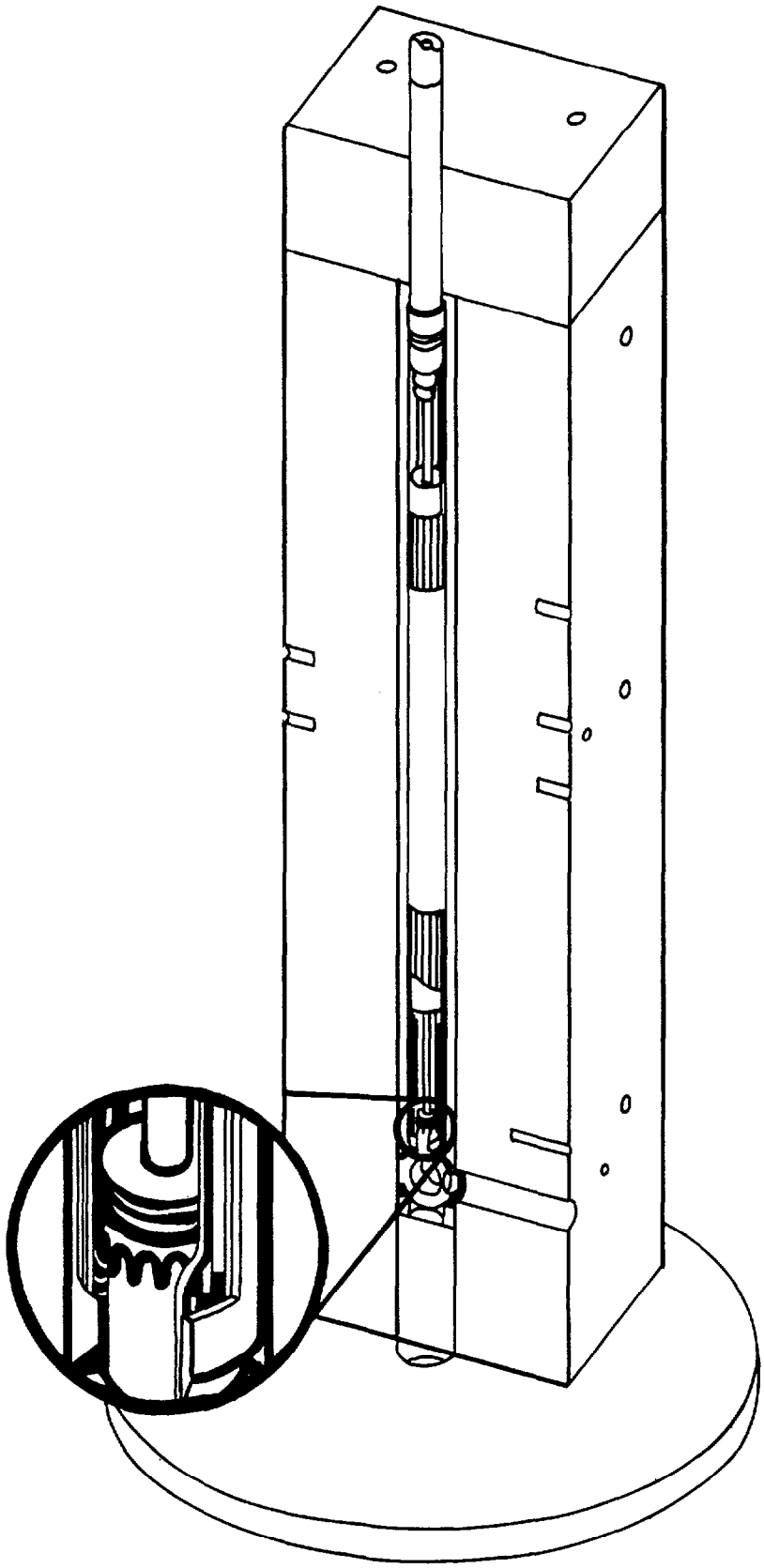

FIGURE 60
Foil Sludge Core Sampling Device

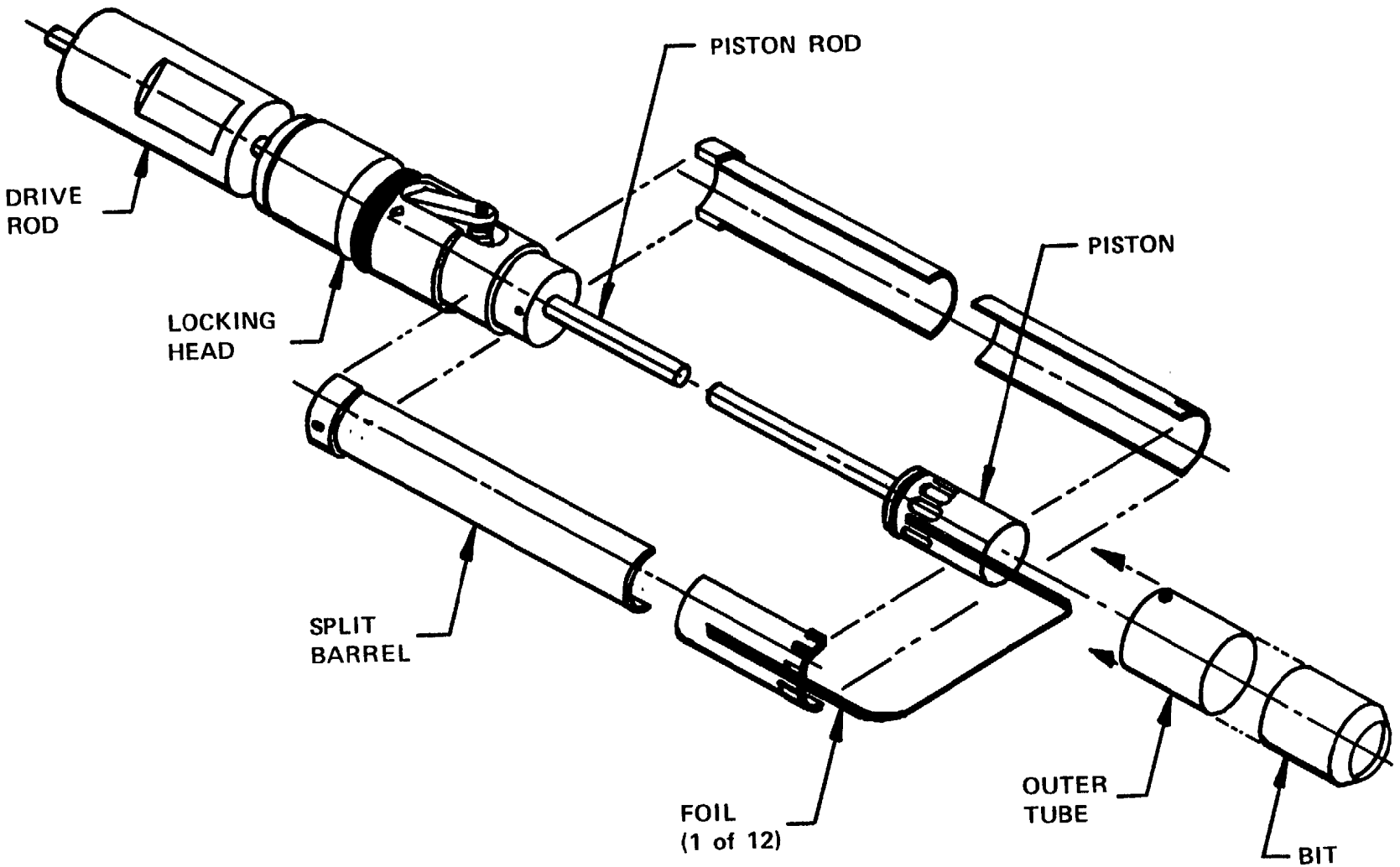

FIGURE 61
Details of Sampling Head: Foil Sampler

FIGURE 62
Sludge Sampler Shield Cask
Being Removed From Riser

Overall recovery, calculated by recovered weights from each section is graphically shown in Figure 63. The soft layer and part of the top of the hard layer were lost by leakage through the split barrel of the sampler. (It was initially thought that part of the soft layer had been recovered but based on information from a second sample, this is now thought to have been eroded hard layer.) However, samples were obtained from the first seven 25 mm hard layer segments. These samples represent ~80 percent of the hard layer. The eight samples were transported to the Babcock and Wilcox Analytical Laboratories (B&W) for analytical work.

Sample Washing

The samples were received by B&W in 10 mL "pyramid" vials. A small amount of deionized water was placed in the vials, the vials placed in an ultrasonic apparatus to enhance recovery, and the solids recovered on a 0.45 μm filter. Further washing was done on the filter. The objective was to remove all the entrainment and solubles (sodium/potassium salts). However, insufficient washing was done on six of the eight samples, and corrections had to be made for remaining supernatant salts, and in the case of Samples 1, 2, and 3*, for sodium sulfate solids.

Wash Solution Analysis

The gamma-emitting radionuclides were measured in the wash solution as well as selected cations and all detectible anions. Based on these results (See Table 14), the following conclusions were reached:

1. Solid phase sodium sulfate was present in Samples 1, 2, and 3. The calculated amounts, expressed as a percentage of supernatant-free solids are:

Sample	Wt. % Na_2SO_4
1	84.8
2	68.0
3	13.2

2. The low amounts of gamma-emitting radionuclides other than Cesium-137/134 indicate negligible solubilization of solid phase components other than the sodium sulfate.

3. Anions detected in the wash solution were Cl^-, NO_2^-, NO_3^-, $SO_4^=$, $CO_3^=$ and HCO_3^-, consistent with the major anions in the supernatant. Other than the sulfate, the concentration of these anions were reasonably consistent with removal of that amount of supernatant corresponding to the cesium analysis. A check on analytical accuracy can be made by summing the equivalents of anions and cations to see if they "balance." The balance was reasonably close on all samples except number one. Trial adjustments were made to the anions and/or the sodium cation to close the balance. The effect on the calculated amount of solid phase sodium sulfate present was negligible.

* Samples are numbered from the bottom of the tank.

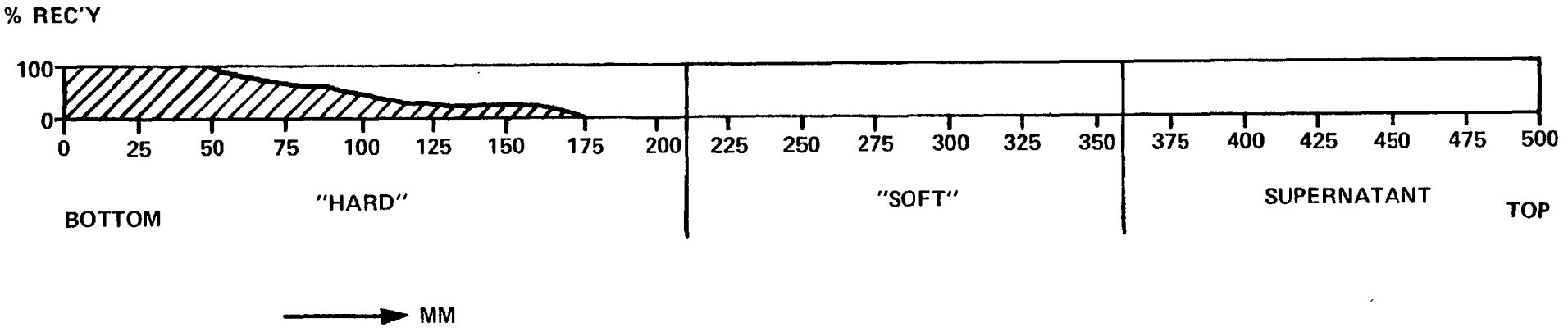

FIGURE 63
Core Sample Recovery

4. Another analytical check was to determine if the Cesium-137/Cesium-134 ratio was the same as that measured by Westinghouse Labs on the supernatant (See Section 2), after correcting for 1.6 years decay. This was found to be the case within a few percent:

Westinghouse Lab Data (mCi/gm)
(corrected to 1984)

Cs-137	Cs-134	Cs-137/Cs-134
2.73	1.37×10^{-2}	199

B&W Data

Sample	Cs-137/Cs-134
1	198
2	190
3	195
4	198
5	193
6	195
7	193
8	209

Washed Solids Analysis

A dissolved solids stock solution was prepared for each of the eight samples. The solutions were prepared by dissolving from 3 to 40 mg of accurately weighted dried solids in 2 to 3 mL of 12M HCl. The stock solutions were diluted to 25.0 mL with 6M HCl.

The scheme for the radiochemical analysis is shown in Figure 64. In addition to the radiochemical analysis, the solutions were analyzed for metals by emission spectroscopy. Based on these results, additional metals were analyzed more precisely using other analytical techniques. Most of the metals could be analyzed with the atomic absorption spectrometer using the flame or the graphite furnace, and in the case of mercury, the cold vapor technique.

Zirconium could not be measured with atomic absorption spectrometry, but was expected in concentrations greater than one percent. Therefore, the zirconium was precipitated with cupferron and determined by X-ray fluorescence.

In addition to the metals analyses just described, the washed solids were also analyzed for carbonate concentration. For the carbonate analysis, a sample aliquot from each section was accurately weighed into a 6 mL gas vial and 0.5 mL of 18M sulfuric acid were added. The evolved carbon dioxide gas was removed from the vial with a gas syringe and injected into a gas chromatograph. The concentration of carbon dioxide gas in the vial is proportional to the concentration of carbonate present in the sample.

TABLE 14: WASH SOLUTION COMPOSITION

Sec. No.[1]	mL	pH	Cl^-	NO_2^-	NO_3^-	$SO_4^=$	$CO_3^=$	HCO_3^-	Na^+	K^+	Cs^+ Al^{+++}	Sr^+ x1000	x1000	Anions	Cations	Cs-137	Cs-134	Eu-154	Co-60	Sb-125
1	50	10.4	1.9	14	24	190	<4.0	<3.0	173	0.75	0.22	14	3.8	4.9	7.6	397	2.01	1.7 E-1	1.0[3]	1.0
2	25	10.4	1.4	34	53	100	13	10	105	1.50	0.14	30	0.30	4.3	4.6	847	4.46	9.0 E-2	5.5 E-4	2.5 E-2
3	50	8	1.9	22	32	20	0.7	4	4	0.84	0.33	17	0.22	1.65	1.88	503	2.58	LD[5]	LD[5]	LD[5]
4	50	[2]	3.2[3]	98	10.5	[4]	[4]	66	1.97	0.96	41	0.34	--	--	1,222	6.17	3.7 E-2	5.8 E-3	LD[5]	
5	25	6	1.9	12.5	19	2.0	[4]	[4]	16	0.49	0.13	10.3	0.15	0.67	0.72	338	1.75	1.2 E-1	9.3 E-3	LD[5]
6	25	6	0.12	5.6	8.6	1.03	[4]	[4]	7.9	0.23	0.016	3.8	0.063	0.29	0.35	125	0.64	5.0 E-2	LD[5]	LD[5]
7	25	7.1	2.8	28	39	5.6	[4]	[4]	31	0.97	0.40	19	0.16	1.43	1.42	600	3.11	8.6 E-2	4.5 E-3	LD[5]
8	50	6	7.8	24	36	3.8	[4]	[4]	32	1.20	0.46	23	0.55	1.40	1.47	714	3.41	LDS	9.5 E-3	LD[5]

Notes: [1] Section numbers 1-7 are from the bottom of the tank up in 25 mm increments; Section 8 is the eroded upper part of the hard layer
[2] HCl inadvertently added to sample
[3] Estimated
[4] pH too low for measurement
[5] LD = below limit of detection

RLC0642:ENG-261

Metal Content

A preliminary metals survey was done by emission spectrometry which is a semiquantitative analytical method. This was followed up by atomic absorption spectrometry for selected elements. Uranium was determined by mass spectroscopy. Plutonium, americium, and curium were determined directly by alpha spectroscopy. Neptunium was determined by means of the major isotope, Np-237.

Based on a weighted average of the analytical results from the eight samples, a new reference sludge composition was published. Since this was modified slightly by analytical results from a second core sample, details are saved until later. However, the significant results from this initial analytical work were[18]:

1. Chemical and radiological composition as a function of depth were reasonably constant except for sodium sulfate.

2. Sodium sulfate solids are present in the bottom three 25 mm sections of the sludge solids. If this is assumed to be representative, there is a calculated 15,000 - 20,000 kg of sodium sulfate sludge solids in the tank. The sulfate was not expected because of its relatively high water solubility. However, subsequent experimentation has demonstrated that the supernatant is close to sulfate saturation because of the common ion effect of the high sodium content. It is theorized that the radiolytic self heating of the sludge solids may have caused concentration of the interstitial liquid causing the deposition. The fact that sodium sulfate is inversely soluble helped promote this. This deposition on the bottom was apparently "protected" from later solubilization by the overlying sludge layers. Since sodium sulfate is an unwanted component of melter feed, this discovery had a significant impact on the sludge washing process (See Section 8).

3. The supernatant salts and solid phase sodium sulfate are amenable to leaching by water washing.

4. The close agreement of the analytical fission product radioactive isotope content (Sr-90, Ru-106, Sb-125, Pm-147, Sm-151, Eu-154, Eu-155) with previous theoretical determinations is an indication that the samples obtained were representative of the sludge solids as a whole.

5. Plutonium and uranium isotopic composition in the sludge solids agreed with that previously determined in the supernatant (within data uncertainty limits). This was expected since solubility is a chemical phenomenon and would be the same for all isotopes, and thus is a confirmatory finding.

6. The total calculated quantity of plutonium in the 8D-2 tank (assuming a representative sample) agrees closely with that determined by NFS processing data (within 10 percent).

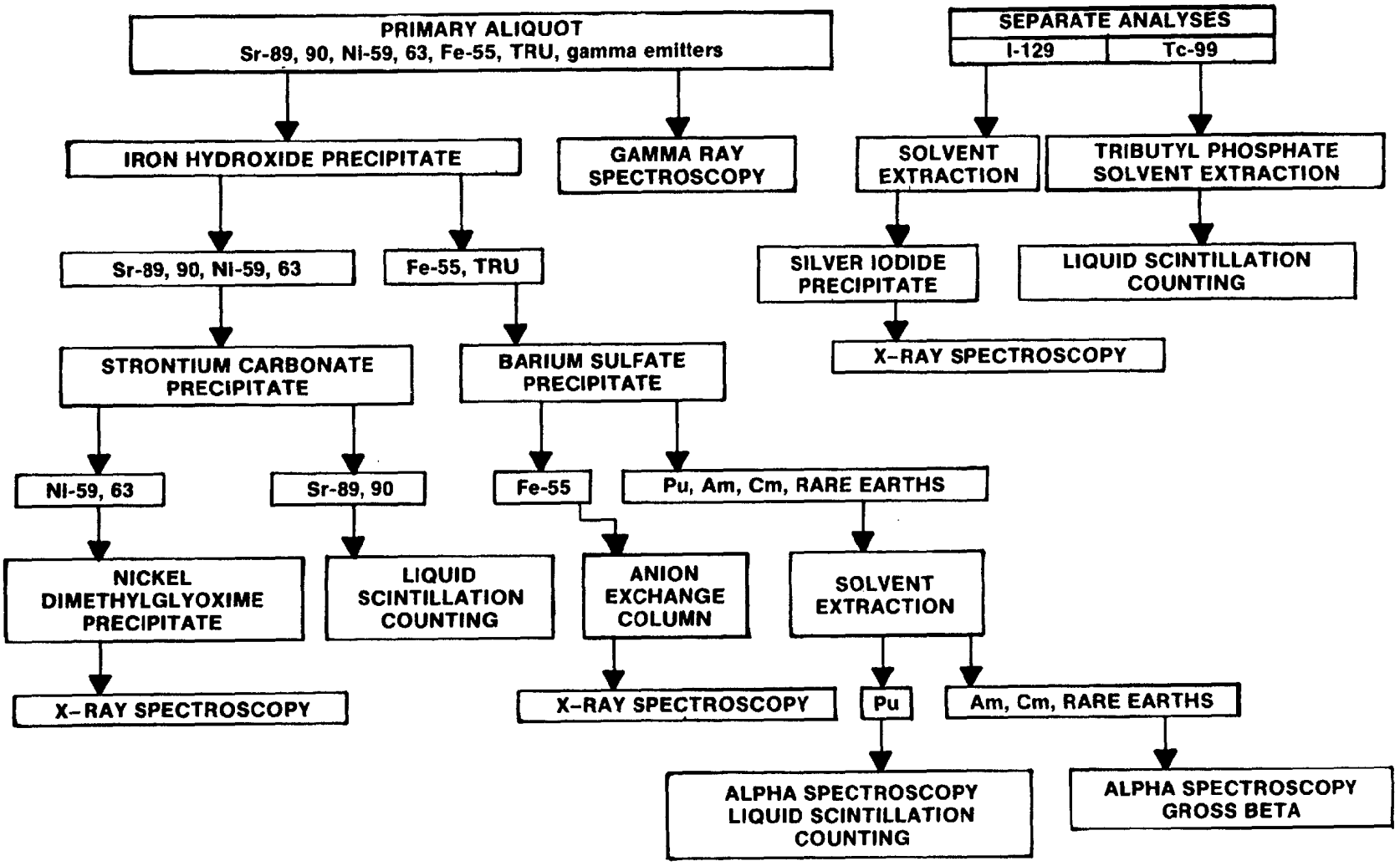

FIGURE 64
Washed Solids Radiochemical Analysis

7. Other constituents (in addition to sodium sulfate) not previously in the reference sludge were calcium carbonate ($CaCO_3$) and silicon (assumed to be as SiO_2 or sand). Since the silica is present in the reference glass in much larger quantities, its presence was deemed insignificant. The calcium carbonate (later traced to lime addition to a NFS waste stream) turned out to be an unwelcome addition due to the formation of a calcium phosphate "scum" on the glass melt surface. However, it is felt that the relatively small amount present (~0.5 percent in the glass including that from the zeolite IX exchanger) can be accommodated.

8. Other radionuclides measured (by beta scan) were Co-60, Ni-59, Ni-63, and Fe-55. These are activation products which could not be theoretically determined.

9. Scanning Electron Microscopy (SEM) pictures (See Figures 65 - 70) showed a combination of crystalline "spikes" and amorphous material. The amorphous material is very friable when dry and appears to be able to be subdivided indefinitely. Ferric hydroxide/oxide is probably the main constituent of the amorphous material. Sodium sulfate is probably a main constituent of the spikes, although uranium was identified in one of the spikes (by qualitative X-ray spectra). Significantly, in-cell work on settling characteristics indicates that the wet material acts as primary particles between 5 and 60 microns (even after being sheared). The breakup into submicron particles appears to occur only upon drying.

In addition to the analytical work, tests were run to determine particle size distributions and the washed insolubles ~9 gm were mixed with glass formers and THOREX waste to make ~30 gm of glass.

In-Cell Testing of a Second Core Sample

The experience gained from the first sample gave guidance to the sampling methods and testing to be done on a second sludge sample.

The sampler used for the second sludge sample was similar to the first, except that a less complex sample head was used. Instead of the previously described sample head with the outer barrel, split inner barrel and moving foil liner, a single, unsplit sampler head was used. The inner piston was retained to improve sample retention. The rest of the sampler and auxiliary equipment were virtually identical to the first. The purpose of these changes was to obtain greater recovery - particularly of the soft layer. Since the main interest of this second sample was bulk sample properties, the "nonsmearing" aspect of the first sampler was deemed to be of secondary importance.

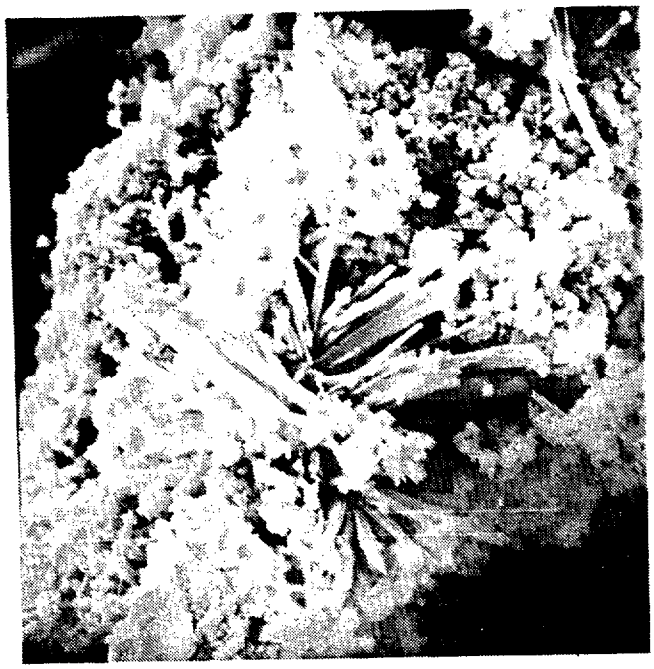

FIGURE 65
3000 X

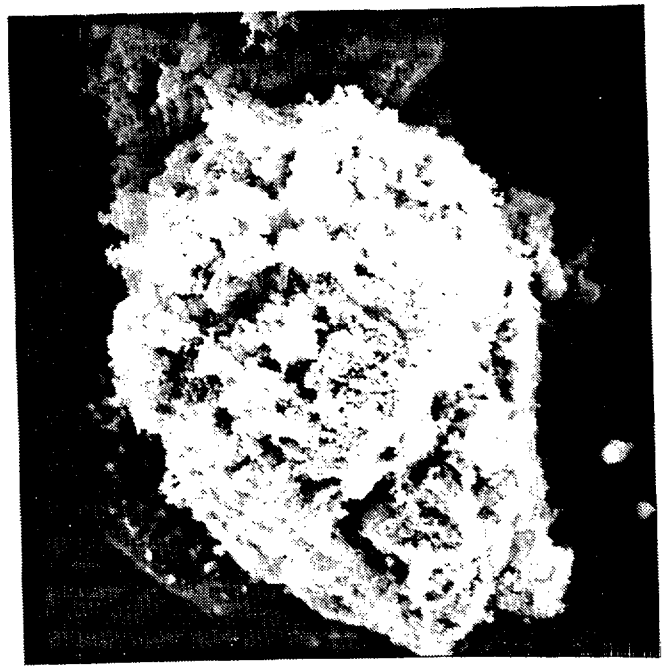

FIGURE 66
1000 X

FIGURE 67
50,000 X

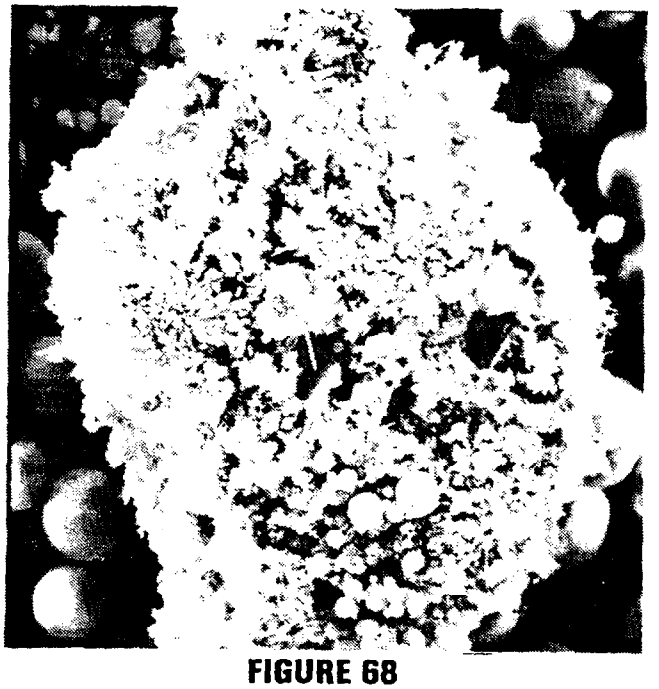

FIGURE 68
1,000 X

FIGURE 69
10,000 X

FIGURE 70
50,000 X

The sludge testing plan that was followed is shown in Figure 71. As can be seen, the tests to date have been nondestructive in nature. The final steps culminating in a sample of glass are awaiting more definitive melter feed makeup protocol.

Some highlights of the results:

1. Overall recovery of insolubles was 0.70 gm of soft layer material and 31.56 gm of hard layer material.

2. Solids/supernatant split in the "as sampled" core was calculated as:

Layer	Wt. % Solids	Wt. % Supernatant
Soft	6.5	93.5
Hard	55.3	44.7

This can be combined with B&W analytical data and tank probing results to calculate the following table:

	DEPTH FROM TANK BOTTOM			
	Hard Layer		Soft Layer	
Component	0-75 mm	75 mm-267 mm	267 mm-470 mm	Total (kg)
Supernatant	22,093	62,546	94,269	179,908
Na_2SO_4	16,264	0	0	16,264
Insolubles	13,141	83,452	6,633	103,226

3. Particle densities were determined:

Soft Layer 2.00 ±0.10 g/mL
Hard Layer 3.45 ±0.10 g/mL

4. Settling tests on the soft-layer material gave the following results:

   a. No clear settling interface which indicates a wide range of particle sizes.

   b. Limiting, i.e., smallest particle sizes = 75-100 μm (equivalent spherical diameter) as calculated from Stoke's Law.

5. Settling tests on the hard layer material gave the following results:

   a. Approximately 5 μm limiting sized particles based on initial qualitative results.

   b. The procedure called for complete washing, i.e., removal of all soluble salts in order to determine the settling rate of the insoluble solids. This resulted in peptization (electrostatic repulsion of particles) and Stoke's Law settling did not occur. Subsequent conversations with Savannah River Laboratory (SRL) personnel indicated that this occurs only at a very low salt concentration (much below WVNS projected wash solutions).

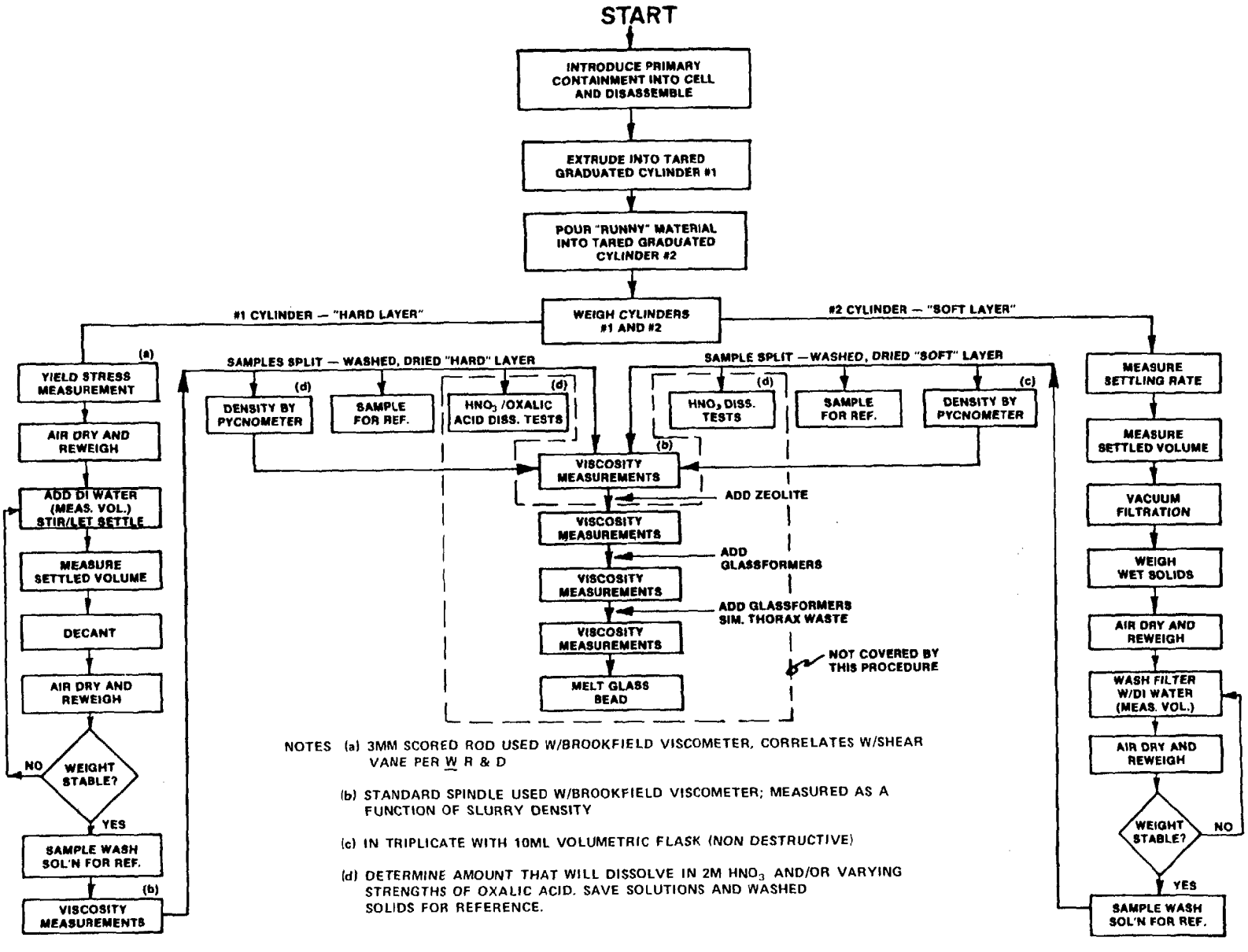

NOTES (a) 3MM SCORED ROD USED W/BROOKFIELD VISCOMETER, CORRELATES W/SHEAR VANE PER W R & D

(b) STANDARD SPINDLE USED W/BROOKFIELD VISCOMETER; MEASURED AS A FUNCTION OF SLURRY DENSITY

(c) IN TRIPLICATE WITH 10ML VOLUMETRIC FLASK (NON DESTRUCTIVE)

(d) DETERMINE AMOUNT THAT WILL DISSOLVE IN 2M HNO_3 AND/OR VARYING STRENGTHS OF OXALIC ACID. SAVE SOLUTIONS AND WASHED SOLIDS FOR REFERENCE.

FIGURE 71
8D-2 Sludge Testing Plan

6. Both hard and soft layers settle compactly (1.2 L/kg and 1.4 L/kg for hard and soft layers respectively). Indications are that in-tank thermal currents keep the soft layer suspended.

7. Prior to any washing or drying of the solids, hard-layer material was packed into a small vial. A Brookfield* LVTD Viscometer was used to measure the reaction torque when a 3 mm scored rod was inserted in the sludge and rotated at 0.3 rpm. In theory, this type of test is similar to the in situ shear vane test run on the 8D-2 tank sludge (See Section 4); however, it was found not to correlate with the shear vane test, apparently because the large decrease in scale resulted in not accurately measuring particle interactions. This test has proven useful in developing a suitable simulant (kaolin clay/water mixture) for use in scale model testing of sludge mobilization.

Analytical Work on Second Sludge Sample

Reference samples of the washed hard layer solids, the washed soft layer solids, and a composite hard layer wash solution were sent to Westinghouse AESD Laboratories for analysis.

7. REFERENCE SLUDGE SOLIDS COMPOSITION

The combined data from the B&W analyses (horizon samples from the first sludge sample) and these samples, together with other data (such as NFS data on tank input) were used to come up with the current estimate of the 8D-2 sludge solids quantity and chemical composition.

As would be expected, there were inconsistencies in the data and certain judgments had to be made. Nominal confidence intervals were developed for all components. These intervals necessarily cannot be based on rigorous statistical theory, but represent judgments based on the reliability of the various input data and the extent of corroboration from independent sources.

Metals Content

The cation composition for the two sets of analytical data are reported in Table 15. The significantly lower metal content in the soft layer tends to explain the lower density. The soft layer apparently consists of hydrated compounds, in particular of iron hydroxide. Major discrepancies exist for zirconium (Zr) and uranium (U). For the purpose of the reference, it was assumed that the amount of Zr was the calculated amount of fission product Zr plus an additional amount reported by NFS. This gives an amount approximately half way between the two analyses. Since the fission product total should be considered the lower limit, the nominal variation was considered ±100 percent for nonfission Zr.

* Brookfield Engineering Labs, Inc., Stoughton, MA

TABLE 15: 8D-2 SOLIDS CATION COMPOSITION

Weight Percent Based on Insolubles

Component	B&W (Hard Layer)	Westinghouse (Hard Layer)	Westinghouse (Soft Layer)
Fe	41.82	41.50	28.20
Mn	4.51	3.21	2.84
Al	2.82	2.45	2.00
Ca	1.99	1.41	1.44
Ni	0.97	0.77	0.60
Cu	0.36	0.27	0.26
Zn	0.26	0.09	0.09
Zr	1.28	0.14	0.29
Si	0.7	___(a)	___(a)
Sr	0.13	___(a)	___(a)
Mg	0.27	0.26	0.28
Cr	<0.2	0.035	0.047
Hg	0.020	0.023	0.037
U(b)	2.08	0.37	0.19
Pu(b)	0.035	0.039	0.023
Total	57.28(c)	51.40(d)	37.13(d)

(a) Not determined

(b) By radiometric analysis

(c) Westinghouse results used for Cr

(d) B&W results used for Si and Sr

The analytical plutonium are in close agreement, and both are in agreement with NFS accounting numbers. The B&W number for uranium is fairly close to the NFS accounting number (~15 percent low). since both Pu and U were NFS reprocessing products, it is assumed that fairly rigorous accounting procedures were employed to track these components. Therefore, NFS accounting totals were used for these elements.

For the remaining metals, the ranges represented by the two sets of analytical data represent only minor oxide variation in the final glass (<0.5 percent). For the purpose of the reference, the Westinghouse analysis was used based on the following considerations.

1. The samples are believed to be more representative. The total sample collected was washed, mixed thoroughly, and then sampled. The B&W analysis represents a weighted average from eight horizon samples.

2. B&W inadvertently did not wash all the solubles out of the samples (as requested). Corrections had to be made for entrainment which further increases the uncertainty.

A particular metal content is calculated by using the ratio of the metal with iron for both the hard and soft layer.

Anions

Referring to Table 16, based on the B&W analyses, total carbonate agrees stoichiometrically with Ca + Mg, so the carbonate was paired with these elements (this is immaterial as far as glass composition goes). The Sr and Ba were originally assumed (rather arbitrarily) to be sulfates, making a total of 238 kg SO_4. Westinghouse analyses (total S as SO_4) indicate <85 kg. Since the vast majority of the melter feed sulfate will come from entrained supernatant and soluble sodium sulfate resulting from necessarily incomplete sludge washing (See Section 8), the original assumption was not changed. Fluoride was analyzed for the first time, and is (again, rather arbitrarily) paired with some of the aluminum as AlF_3. There is no independent verification of this number so a nominal ±20 percent variation is used.

The phosphorous came from degradation products of the TBP used for processing. The original reference amount was an NFS accounting number based on emission spectroscopy (considered to be highly unreliable) of their input streams. They reported 17,809 kg as PO_4 of which 2,205 kg were found by analyzing the supernatant. The Westinghouse number is the first (and, so far, only) analytical determination that we have. Although B&W was not able to analyze for PO_4, a relatively low amount may be inferred by the high percentage of metals, which does not "leave room" for a large amount of high molecular weight anions, e.g., phosphates as opposed to hydroxides. Westinghouse did their measurement by ion-coupled plasma spectroscopy (ICPS) which measures all phosphorous (as opposed to just PO_4). They believe their method is good and report a ±3 percent (hard layer) and ±5 percent (soft layer) 95 percent confidence level in the analysis. Subsequent to these determinations, PNL did a series of tests in which they neutralized simulated PUREX wastes with varying initial PO_4 contents to a final pH of ~10 (same as

TABLE 16: 8D-2 SOLIDS ANION COMPOSITION

Component	Wt. % Based on Insolubles		
	B&W	Westinghouse (Hard Layer)	Westinghouse (Soft Layer)
CO_3	3.68	--*	--*
PO_4	--*	2.18	2.45
SO_4	--*	<0.22	0.76
F	--*	0.40	0.40

* Not Determined

8D-2 and determined the split between the solution and solid phase. Their "best fit" number was ~90 percent of the NFS number. Since P_2O_5 is a major glass component, the whole range has to be considered within the "realm of possibilities."

The current strategy is:

1. The high PO_4 content (NFS number) is being used to define the reference West Valley glass (designated WV-205).

2. If the actual waste contains less than this amount, there will be two options:

   a. Prequalify a glass encompassing the entire range.

   b. Backadd phosphorous to bring the composition up to the WV-205 reference.

Fission/Activation Product Radionuclides

The comparative data for the fission product and activation product radionuclides is given in Table 17. Agreement is reasonable, and is taken to back up the chemical fission product content of 8D-2 (based on theoretical considerations).[2] A nominal ±5 percent was used for uncertainty.

Transuranics

The comparative data for the transuranics is shown in Table 18. There is fairly close agreement between B&W and Westinghouse with the exception of Np. Agreement with theoretical (ORIGEN) calculations is reasonable, considering that a number of simplifying assumptions had to be made in order to use this program.[19] Since their contribution to the chemical composition was small, further refinements were not considered necessary, and the higher of the theoretical or Westinghouse analytical numbers were used with a nominal ±50 percent confidence.

Total Iron Content

The key to coming up with a reference solids total is fixing the amount of iron (Fe) in the tank. NFS data give a total input of 36,870 Fe. Ten kg were found in the supernatant, leaving 36,860 kg in the sludge solids. Assume that 93 percent of the total insolubles are in the hard layer and 7 percent in the soft layer (based on in-cell tests and tank probing). The Westinghouse analysis indicates that the hard layer is 41.5 percent Fe and the soft layer 28.2 percent Fe. This gives $\frac{0.415\ (0.93)}{0.415\ (0.93) + 0.282\ (0.07)} \times 36{,}860 = 35{,}066$ kg Fe in the hard layer and 36,860 - 35,066 = 1,794 kg Fe in the soft layer.

TABLE 17: RADIONUCLIDE COMPOSITION OF INSOLUBLE SLUDGE SOLIDS

		μCi/gm		Total Ci in Solids	
Component	Half-Life (years)	B&W[a]	(Hard Layer) Westinghouse	Westinghouse[c]	Theoretical[a,b]
Fe-55	2.7	16.3	--[f]	--[f]	--[d]
Ni-59	8×10^4	0.79	--[f]	--[f]	--[d]
Co-60	5.27	67.1	59.9	5,380	--[d]
Ni-63	100	53.5	--[f]	--[f]	--[d]
Sr-90	29	77,450	77,700	6.92×10^6	7.22×10^6
Sb-125	2.73	111	98.6	8,780	7,280[e]
Eu-154	8.2	1,375	1,160	104,000	157,000[e]
Eu-155	4.70	342	336	30,000	30,000[e]
Total Rare Earth β	--	535,000	[f]	[f]	902,000[e]

Notes:
(a) Decay corrected to August 26, 1985, (date of Westinghouse analysis).

(b) See Reference 19 for method and assumptions.

(c) Assumes 93 percent hard layer, 7 percent soft layer by weight and 36,870 kg Fe in solids.

(d) Activation products - not able to be determined theoretically.

(e) Due to relatively short half-life, this value is very sensitive to assumed age of fuel.

(f) Not determined.

TABLE 18: TRANSURANICS IN INSOLUBLE SOLIDS

	μCi/gm		Total Curies	
Component	B&W[a] (Hard Layer)	Westinghouse (Hard Layer)	Westinghouse[c]	Theoretical[a,b]
Am-241	760	779	69,200	69,200
Am-243	---[d]	5.28	471	500
Am-243/Cm-243	14.8	---[d]	---[d]	791
Cm-242	6.64	8.13	722	302
Cm-243	---[d]	---[d]	---[d]	291
Cm-244	---[d]	---[d]	---[d]	18,900
Cm-243/244	214	227	20,200	19,190
Cm-245	---[d]	---[d]	---[d]	2.41
Cm-246	---[d]	---[d]	---[d]	0.377
Pu-238	69.0	78.6	6,557	1,652
Pu-239	---[d]	20.3	1,691	1,710
Pu-240	---[d]	14.4	1,203	994
Pu-239/240	31.6	34.7	2,894	2,700
Pu-241	870	987	82,552	84,300
Pu-242	<0.08	0.015	1.29	1.47
Np-237	0.68	0.26	22.4	26.3

Notes: (a) Decay corrected to July 1, 1987.

(b) See Reference 19 for method and assumptions. This method was modified by use of ORIGEN2[13] (rather than original version), assumption of 3.9 years out of reactor before processing (versus one year) and 0 recovery of Np (versus 50 percent).

(c) Assumes 93 percent hard layer, 7 percent soft layer by weight and 36,870 kg Fe in solids.

(d) Not determined.

Independent corroboration of total iron is based on a "theoretical" total curie content of Sr-90[2] and the ratio of Sr-90/Fe in the Westinghouse analyses (Tables 15 and 17 show very close agreement of this ratio between Westinghouse and B&W in the hard layer). The formula used:

$$\text{Ci Sr-90} = \underbrace{\frac{\text{Ci Sr-90}}{\text{g solids}} \times \frac{\text{g solids}}{\text{g Fe}} \times \text{g Fe}}_{\text{Hard Layer}} + \underbrace{\frac{\text{Ci Sr-90}}{\text{g solids}} \times \frac{\text{g solids}}{\text{g Fe}} \times \text{g Fe}}_{\text{Soft Layer}}$$

$$= \frac{7.77 \times 10^{-2}}{0.282} \times 35{,}066{,}000 + \frac{5.65 \times 10^{-2}}{0.282} \times 1{,}794{,}000$$

$$= 6.92 \times 10^{6} \text{ (agrees within -4 percent)}$$

It should be noted that the ratio of Sr-90/Fe is very close in both the hard and soft layer, so that total curies is not a strong function of the relative amounts of soft and hard layer. The use of 36,860 kg total Fe was thus used with a nominal ±10 percent variation.

Table 19 and 20 gives the current nominal reference composition of the 8D-2 sludge solids (insolubles) and Table 21 summarizes the estimated nominal uncertainties based on the characterization work to date.

Radionuclide Composition

Table 22 gives our reference composition for the 8D-2 sludge solids. The fission product nuclides are based on theoretical considerations (see earlier discussion) which have been substantiated by the analytical work. Westinghouse and B&W are in close agreement with the isotopic breakdown of the uranium and plutonium isotopes, and agreement is close for both the supernatant and sludge solids analysis. Totals are based on NFS accounting numbers. The remaining actinides are based on Westinghouse analytical work or ORIGEN2 runs, whichever is higher. These are reasonably close to the B&W work (See Table 18).

8. SLUDGE WASH CALCULATIONS:

A critical part of the pretreatment of the HLW prior to vitrification is washing impurities out of the 8D-2 sludge solids. Based on our current knowledge, a SO_3 content of the glass less than 0.3 percent is deemed to be important to prevent the formation of a second liquid phase on top of the molten glass. This is to be accomplished by batch washing in the 8D-2 tank.

The batch washing process will take place as shown in the schematic in Figure 72. The supernatant will be decanted from the sludge to as close to the sludge layer as possible. Water will then be added and the sludge/liquid mixture homogenized with sluicing pumps (long-shafts pumps of Savannah River design which are submerged in the slurry, use the slurry as the motive liquid, and discharge through rotating nozzles in the pump head). After settling, the wash solution will be decanted as close to the settled sludge layer as possible. More water would then be added and the process repeated as many times as necessary. Assuming complete mixing and complete solubilization of the sodium sulfate solids (verified experimentally), the final melter feed, and ultimately, glass composition would be a function of:

TABLE 19: 8D-2 INSOLUBLE SOLIDS CHEMICAL COMPOSITION

Component	Reference (kg)
$Fe(OH)_3$	66,040
$FePO_4$	6,351
$Al(OH)_3$	5,852
AlF_3	536
MnO_2	4,581
$CaCO_3$	3,208
$UO_2(OH)_2$	3,087
$Ni(OH)_2$	1,088
SiO_2	1,263
$Zr(OH)_4$	159(a)
$MgCO_3$	826
$Cu(OH)_2$	376
$Zn(OH)_2$	128
$Cr(OH)_3$	65
$Hg(OH)_2$	23
Fission Products(b)	
F.P. hydroxides	1,485
R.E. hydroxides	1,484
F.P. sulfates	520
Transuranics	
NpO_2	42
PuO_2	37
AmO_2	27
CmO_2	0.3
Total	97,178

(a) Excludes fission product zirconium

(b) See Table 20 for breakdown

TABLE 20: INSOLUBLE SOLIDS FISSION PRODUCTS

	Components	kg in Solids
	$SrSO_4$	217
	$Y(OH)_3$	103
	$Zr(OH)_4$	805
	$Ru(OH)_4$	458
	$Rh(OH)_4$	79
	$Pd(OH)_2$	34
	AgOH	0.7
	$Cd(OH)_2$	1.7
	$In(OH)_3$	0.3
	$Sn(OH)_4$	2.5
	$Sb(OH)_3$	0.7
	$BaSO_4$	303
	$La(OH)_3$	185
	$Ce(OH)_3$	354
	$Pr(OH)_3$	170
Rare	$Nd(OH)_3$	621
Earths	$Pm(OH)_3$	1.5
	$Sm(OH)_3$	143
	$Eu(OH)_3$	7.5
	$Gd(OH)_3$	1.7

TABLE 21: INSOLUBLE SOLIDS CONFIDENCE INTERVALS

Component	Percentage (±)	Basis	Range (kg)
Fe	10	Tank Total	33,183 - 40,557
PO_4	NA	Tank Total	1,995 - 15,703
Al	10	Ratio to Fe	1,780 - 2,660
Mn	10	Ratio to Fe	2,345 - 3,503
Ca	10	Ratio to Fe	1,036 - 1,552
U	10	Tank Total	2,175 - 2,659
Ni	10	Ratio to Fe	558 - 834
Si	50	Ratio to Fe	295 - 886
Zr (nonfission product)	100	Tank Total	0 - 182
Mg	10	Ratio to Fe	214 - 262
Cu	10	Ratio to Fe	221 - 270
Zn	10	Ratio to Fe	87 - 107
Cr	10	Ratio to Fe	27 - 40
Hg	10	Ratio to Fe	16 - 24
Fission Product Elements	5	Tank Total	2,147 - 2,373
SO_4	100	Tank Total	0 - 476
F	20	Ratio to Fe	262 - 480
Pu	5	Tank Total	31 - 35
Np	50	Ratio to Fe	19 - 45
Am	50	Ratio to Fe	14 - 40
Cm	50	Ratio to Fe	0.15 - 0.45

TABLE 22: REFERENCE 1987 RADIONUCLIDE CONTENT (CURIES) OF WEST VALLEY SLUDGE SOLIDS

Radionuclide	Total Curies	Radionuclide	Total Curies	Radonuclide	Total Curies
3-H	7.3E+0	208-Tl	4.3E-02	232-Th	5.9E-09
14-C	9.9E-2	209-Pb	6.6E-6	234-Th	8.0E-01
55-Fe	1.0E+3	211-Pb	9.1E-4	231-Pa	2.9E-04
59-Ni	7.9E+1	212-Pb	1.2E-1	233-Pa	2.3E+01
60-Co	4.1E+0	211-Bi	9.1E-4	234m-Pa	8.0E-01
63-Ni	5.4E+3	212-Bi	1.2E-1	232-U	4.4E+0
90-Sr	6.9E+6	213-Bi	6.6E-6	233-U	6.9E+0
90-Y	6.9E+6	212-Po	7.6E-2	234-U	4.0E+0
93-Zr	2.3E+2	213-Po	6.5E-6	235-U	8.9E-2
93m-Nb	1.4E+2	215-Po	9.1E-4	236-U	2.7E-1
106-Ru	1.3E+2	216-Po	1.2E-1	238-U	7.9E-1
106-Rh	1.3E+2	217-At	6.6E-6	237-Np	2.6E+1
107-Pd	1.2E+0	219-Rn	9.1E-4	239-Np	5.0E+3
113m-Cd	2.1E+3	220-Rn	1.2E-1	236-Pu	8.2E-1
121m-Sn	1.5E-1	221-Fr	6.6E-6	238-Pu	6.5E+3
125-Sb	4.5E+3	223-Fr	1.3E-5	239-Pu	1.7E+3
125m-Te	1.0E+3	223-Ra	9.1E-4	240-Pu	1.3E+3
126-Sn	4.0E+1	224-Ra	1.2E-1	241-Pu	8.5E+4
126m-Sb	4.0E+1	225-Ra	6.6E-6	242-Pu	1.7E+0
126-Sb	5.6E+1	228-Ra	4.8E-9	241-Am	6.9E+4
144-Ce	1.4E+1	225-Ac	6.6E-6	242-Am	8.6E+2
144-Pr	1.4E+1	227-Ac	9.1E-4	242m-Am	8.6E+2
146-Pm	1.5E+1	228-Ac	4.8E-9	243-Am	5.0E+3
147-Pm	3.1E+5	227-Th	9.0E-4	242-Cm	7.2E+2
151-Sm	2.1E+5	228-Th	1.2E-1	243-Cm	3.1E+1
152-Eu	4.2E+2	229-Th	6.6E-6	244-Cm	2.0E+4
154-Eu	1.3E+5	230-Th	1.5E-2	245-Cm	2.4E+0
155-Eu	2.3E+4	231-Th	8.9E-2	246-Cm	3.8E-1
207-Tl	9.1E-4				

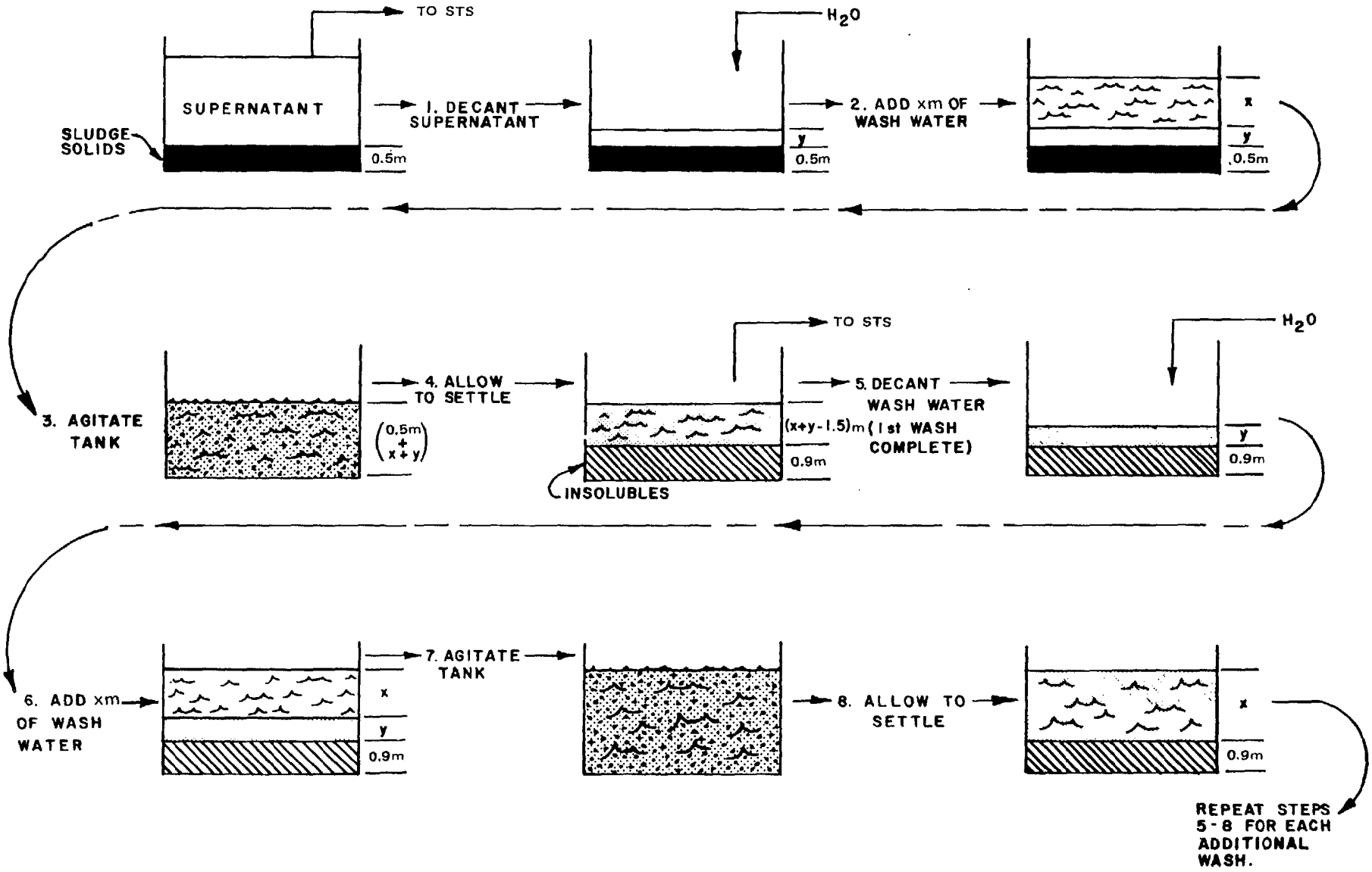

FIGURE 72
Schematic of Wash Sequence

1. Number of water washes.

2. Volume of water/wash.

3. Depth to which resuspended sludge settles.

4. Decant level (distance above sludge layer to which supernatant/wash solutions can be pumped).

In order to come up with a reference, the following assumptions were made (thought to be conservative):

1. The sludge in the bottom of the 8D-2 tank has an average depth of 0.5 metres.

2. The insolubles settle to a depth of 1.0 metres after each wash step (in-cell testing indicates this is conservative).

3. The insoluble solids total 100,000 kg and have an average specific gravity of 3.5 (subsequent in-cell testing established the average at 3.35 ± 0.1).

4. The total glass production is 450,000 kg. (current mass balance reference is 490,000 kg).

5. The glass specification is <0.3 weight percent SO_3.

It can then be shown[20] that the weight fraction of impurity remaining after n washes is:

1) $A(x) \cdot B(x)^{n-1}$ where:

2) $$A(x) = \frac{(1.0 + y) - z}{(0.5 + x + y) - z}$$

and

3) $$B(x) = \frac{(1.0 + y) - z}{(1.0 + x + y) - z}$$

where x = amount of water added per wash, expressed as a depth in the tank, metres (x >0.5)

y = decant level, metres

z = equivalent metres displaced by sludge insolubles, e.g.,

$\frac{100,000 \text{ kg}}{3.5 \text{ kg/L}}$ = 28,571 litres which is equivalent to 0.08 metres.

The 0.5 and 1.0 in equations (2) and (3) are the depth of the initial and resettled sludge depth respectively, in metres.

This type of analysis leads to a relationship between the number of washes, amount of water/wash and the weight percent SO_3 in the final glass as shown in Figures 73 and 74. Based on this analysis, a reference of three washes of 632,000 litres each was established. With a (conservative) estimate of 20,000 kg of solid phase sodium sulphate in the sludge solids, the composition of the three wash solutions to be processed can be expressed as a mixture of water, sodium sulphate solids, and supernatant as shown in Table 23.

This analysis assumed that the amount of insoluble sulfate in the sludge solids was small. This was confirmed by an analysis of the washed sludge solids from the second sludge sample. One risk in treating the wash solution compositions as a mixture of the listed three components is the possibility that the more dilute wash solutions may cause some of the sludge "insolubles" to go into solution.

Strontium and Plutonium Solubility

Of particular concern was dissolution of the strontium (due to the large amount of Sr-90 in the sludge solids) and those actinides that would contribute to the classification of the solidified LLW resulting from wash solution processing (decontamination through the IX columns).

To determine the extent of this additional dissolution, washed 8D-2 sludge solids were equilibrated with simulated number 3 wash solution (>48 hours with intermittent agitation). The simulated wash solution was prepared from actual supernatant, (decontaminated by passing it through a column of IE-96), deionized water, and reagent grade sodium sulfate. The resulting solution was filtered and analyzed for Pu-238, Pu-239/240, and Sr-90). Additional data was generated by simulating the washing steps in-cell by washing in a beaker, adding water, agitating the solids, allowing them to settle, and decanting the solution. A composite was made of the initial decants. The total salt concentration indicates that it is roughly equivalent to the weighted average of the three projected wash solutions. A gross alpha analysis was done on the filtered composite. The results of these two measurements are given in Table 24 below:

These data were converted to µgPu/g solution by assuming:

1. Isotopic composition of Pu is as determined from the analytical work (corrected for decay).

2. All alpha activity in Sample 2 is from Pu isotopes.

The results are given in Table 25, with the solubility for 8D-2 supernatant also given for comparison.

If we assume that 0.032 µgPu/g water represents the "best" case and 0.13 µgPu/g water represents the "worst" case, the implications for the Liquid Waste Treatment System (LWTS) can be calculated.

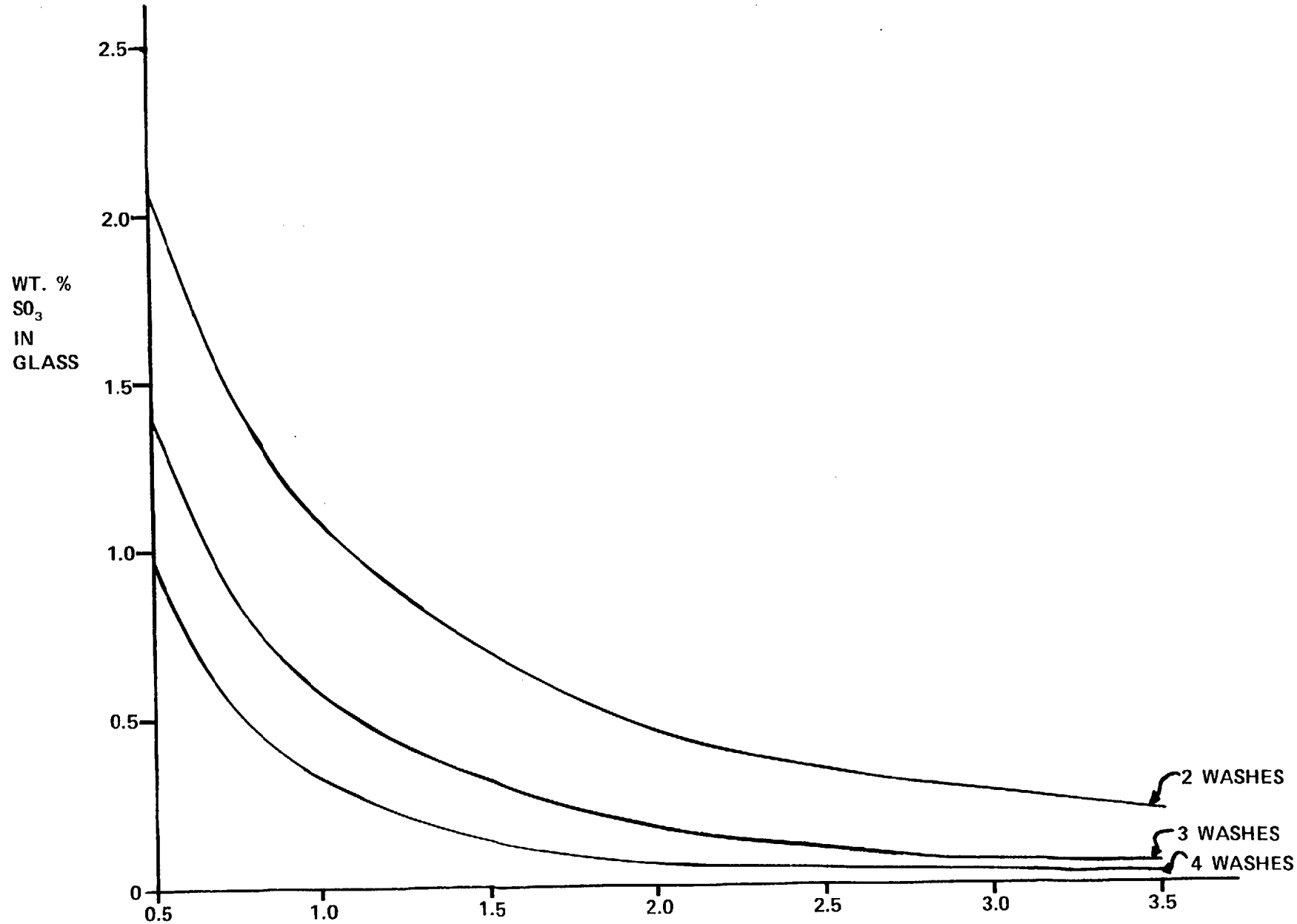

FIGURE 73
Wash Curves (0.15m Decant)

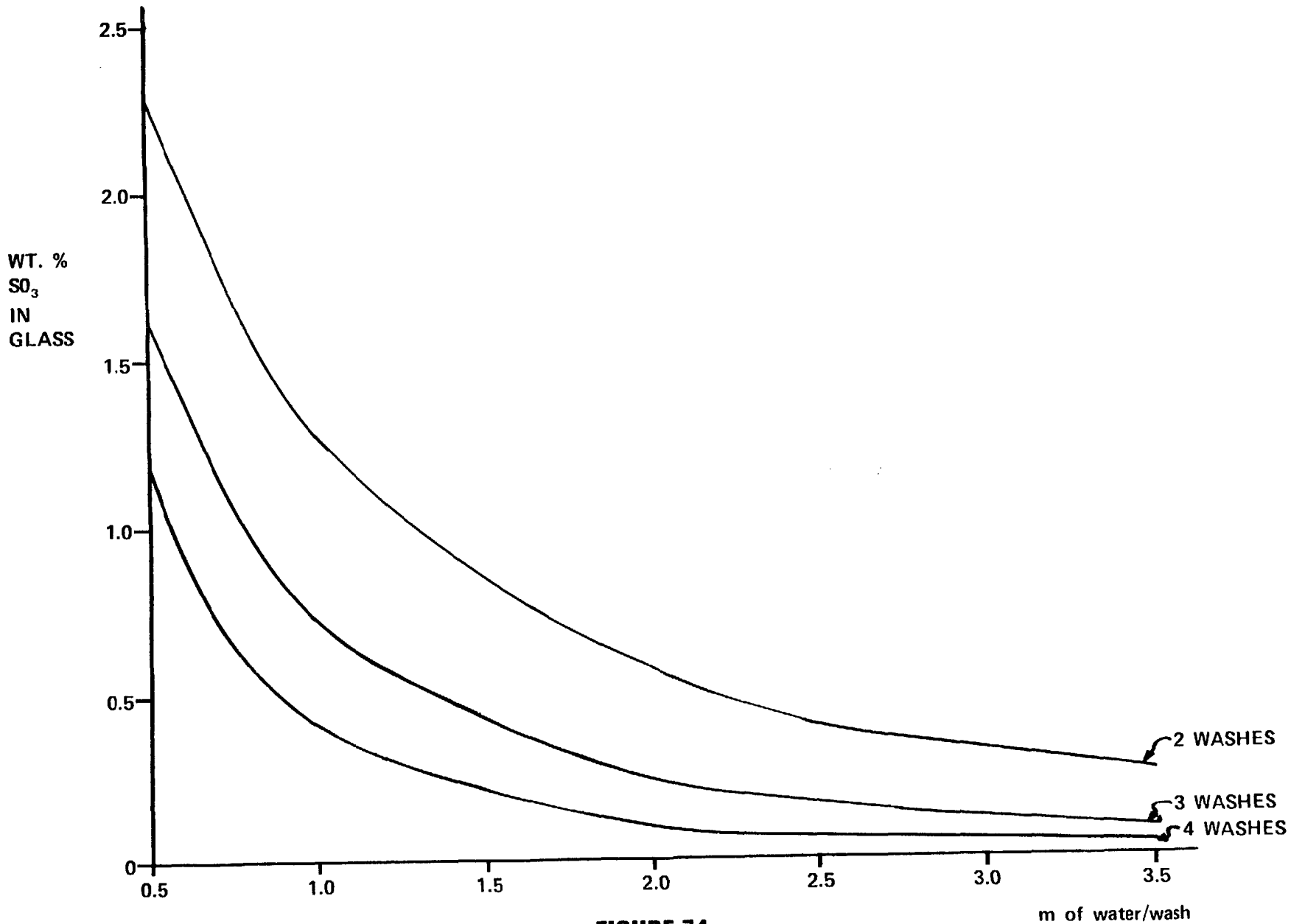

FIGURE 74
Wash Curves (0.3m Decant)

TABLE 23: REFERENCE CHEMICAL COMPOSITION OF WASH SOLUTION

Wash No.	kg			
	H_2O	Supernatant	$NaSO_4$	Total
1	337,595	171,948	10,680	520,223
2	562,571	91,082	5,657	659,310
3	604,836	35,795	2,223	642,854

TABLE 24: WASH SOLUTION DATA

		Analytical Results				
Sample	Wt. % Salt (approx.)	Sr-90	Pu-238	Pu-239/240	α Activity	Units
1	2.6	4.48×10^{-1}	2.65×10^{-2}	1.13×10^{-2}	(b)	μCi/mL
2	8.5	$<6 \times 10^{-3}$	_____b	_____b	1.0×10^{-2}(a)	μCi/g

(a) All alpha activity

(b) Not determined

TABLE 25: CALCULATED PLUTONIUM SOLUBILITY

Sample	μgPu/g Solution		μgPu/g Water
1	1.3×10^{-1}	1.3×10^{-1}	
2	3.6×10^{-2}	3.2×10^{-2}	
Supernatant		1.8×10^{-1}	6.9×10^{-2}

Assume:

1. Evaporation to 48 weight percent salts.

2. 0.7 water to cement weight ratio.

3. Density of cement solidified waste = 1.7 g/mL

4. 55-gallon drums filled to 95 percent of capacity.

For the purpose of determining whether Class "C" LLW limitations are exceeded (per 10 CFR Part 61), the critical components are Tc-99, Pu-241, and total long-lived alpha emitters.[3] The C-14 and I-129 contribute only a negligible amount, while the short-lived radionuclides are well under the limit. For these three components, the sum of fractions applies:

$$\sum_{i=1}^{3} \frac{C(i)}{T(i)} < 1$$

Where C(i) = actual concentration of nuclide i

T(i) = allowable concentration of nuclide i

Table 26 summarizes the "best" and "worst" cases for solidification of the three wash solutions. Supernatant is also included for comparison.

From Table 26, it appears that the solidified supernatant and first wash solution will qualify as Class "C" waste, the second wash will be marginal, and the third wash will not qualify. All wastes could qualify by not concentrating as much. For example, the "worst" case third wash solution could meet Class "C" by concentration to only 8.2 weight percent salts which would make 1,123 drums rather than 177.

Table 27 summarizes these calculations.

The "worst" case is the reference for the Pu concentration. The wash solutions will be sampled prior to processing to determine their actual composition.

Pickup of significant quantities of Sr-90 was also a concern. Referring back to the three solubility tests (Table 24), Sr-90 was measured on both samples. The two values were:

$4.48 \times 10^{-1} \times 1/1.01$ mL/gm = 4.44×10^{-1} and $< 6 \times 10^{-3}$ μCi/gm.

There is no ready explanation for this large difference. The first test was done in a sealed vial, while the other was done in an open beaker. Since $SrCO_3$ is highly insoluble, perhaps equilibration with the atmosphere affected the solubility. However, even assuming the higher number is correct, the amount of curies are small and would not impact the Class "C" waste limit as shown in Table 28. Again the "worst" case numbers are used for the reference wash solutions.

Reference Wash Solutions:

The chemical composition is not affected by the above solubility data and is as given in Table 23.

TABLE 26: WASTE CLASSIFICATION OF SOLIDIFIED STS SOLUTIONS

Solution	Component		Contribution to Sum of Fractions[a] "Best" Case	"Worst" Case
Wash No. 1	Tc-99	0.181	0.181	
Wash No. 1	Pu-241		0.0306	0.124
Wash No. 1	α-Emitters		0.0157	0.638
Wash No. 1	TOTAL	0.369	0.943	
Wash No. 2	Tc-99	0.182		
Wash No. 2	Pu-241	0.0807	0.328	
Wash No. 2	α-Emitters		0.423	1.775
Wash No. 2	TOTAL	0.686	2.285	
Wash No. 3	Tc-99	0.182	0.182	
Wash No. 3	Pu-241	0.208	0.845	
Wash No. 3	α-Emitters		1.036	4.346
Wash No. 3	TOTAL	1.426	5.373	
Supernatant	Tc-99		0.210	
Supernatant	Pu-241		0.092	
Supernatant	α-Emitters			0.402
Supernatant	TOTAL		0.704[b]	

Notes: (a) Plutonium isotopes decay-corrected to 1987; solubility (μg/g) assumed constant.

(b) Subject to an estimated ± ~10 percent variability due to analytical uncertainty.

TABLE 27: NUMBER OF DRUMS REQUIRED TO STAY WITHIN CLASS "C" LIMITS

Number of 55-gallon Drums (95% Capacity)

STS Solution		Base	"Best" Case	"Worst" Case
Supernatant		10,815	10,815	10,815
Wash No. 1		849	849	849
Wash No. 2		449	449	1,026
Wash No. 3		177	268	1,123
TOTAL	12,481	12,381		13,813

TABLE 28: Sr-90 CONTENT OF LOW-LEVEL WASTE (1987)

	Ci/m^3 - Sr-90*		Total Ci Sr-90		
Solution	"Best" Case	"Worst" Case	Class C Limit	"Best" Case	"Worst" Case
Supernatant	0.66	0.66	7,000	3,740	3,740
Wash No. 1	<0.015	1.09	7,000	<4	270
Wash No. 2	<0.027	2.03	7,000	<5	378
Wash No. 3	<0.100	7.44	7,000	<5	383
TOTAL			3,740	4,771	

* Assumes concentration to 48% salts in all cases.

9. 8D-2 TANK TEMPERATURE MEASUREMENTS

For the purpose of design of the 8D-1 and 8D-2 structural modification necessary for various HLW pretreatment steps, a better understanding of the heat generation and removal mechanism and the temperature properties of the 8D-2 tank and vault system were required. To accomplish this temperature measurements were taken down a 12.7 mm airline next to the inner vault wall on 8D-2, of the injection walls surrounding 8D-2, and in the 8D-2 M-1 riser.

Heat Generation:

Heat is generated by radioactive decay of radionuclides in the 8D-2 waste tank; principally the Cs-137/Ba-137m decay chain in the supernatant and the Sr-90/Y-90 decay chain in the sludge solids. The watts of heat generated are directly related to the curies of radionuclide present. Heat generation in kilowatts for the hard layer sludge, soft layer sludge, and supernatant (basis 1985) are shown in Figure 75. Approximately 62 percent of the total heat is generated in the bottom -0.5 metre sludge layer.

Sludge Temperature Measurements

Of special interest were the temperature measurements taken in the 8D-2 tank (See Figures 76 and 77). The soft layer sludge temperatures range from 89.4 - 91.1°C, indicating close thermal communication with the supernatant, primarily by convection (one of the conclusions of the in-cell sludge characterization work was that thermal convection currents keep the soft layer solids partially suspended). The hard layer sludge temperatures can be correlated by assuming, as a model, conduction through a flat plate with uniform internal heat generation. The thermal conductivity of the "hard layer" sludge can then be calculated. This was determined to be

$2.54 \frac{\text{watts}}{\text{m-}^{\circ}\text{K}}$[21].

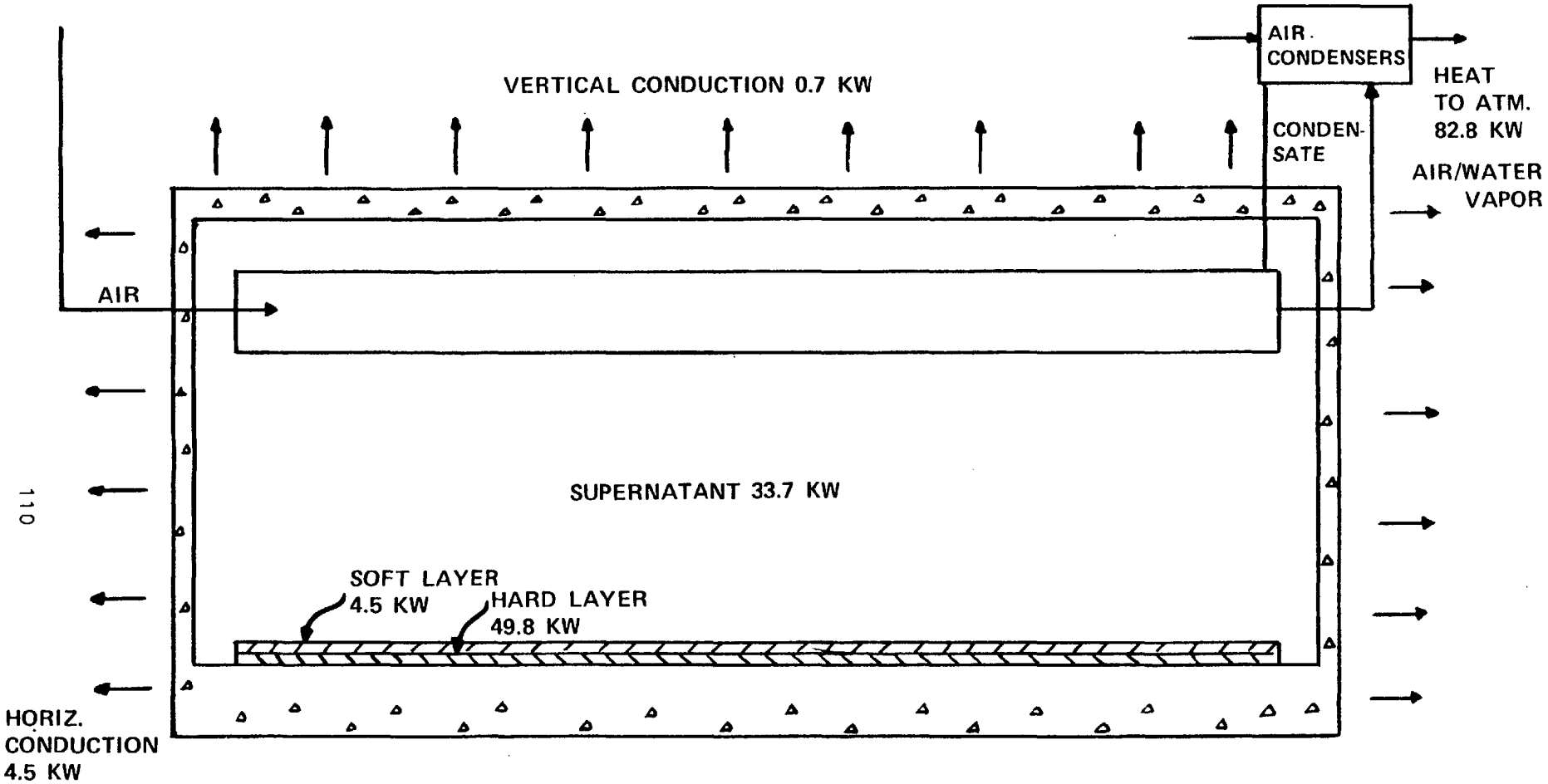

FIGURE 75
8D-2 Tank Heat Balance

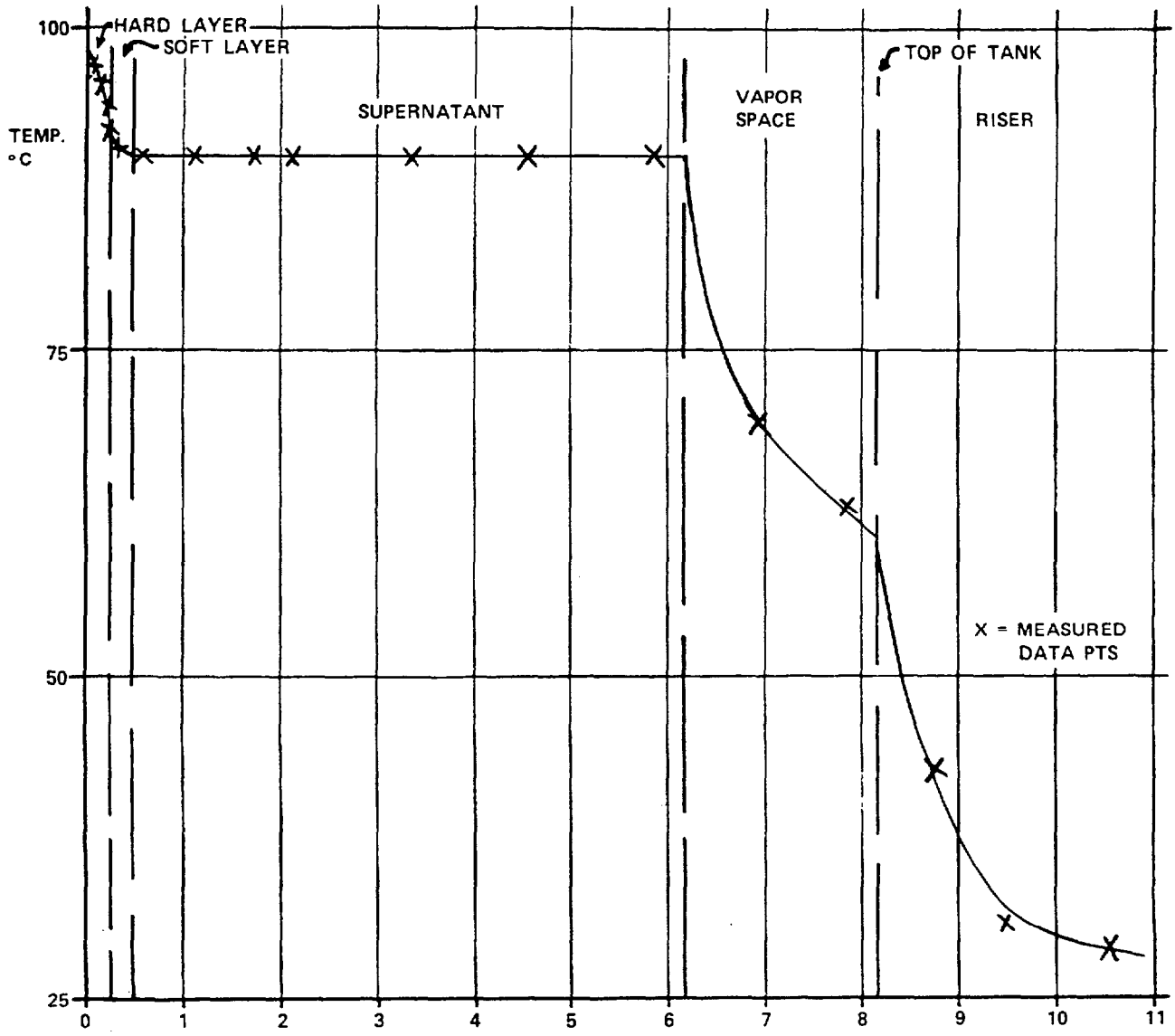

FIGURE 76
M-1 Riser Temperature Measurements

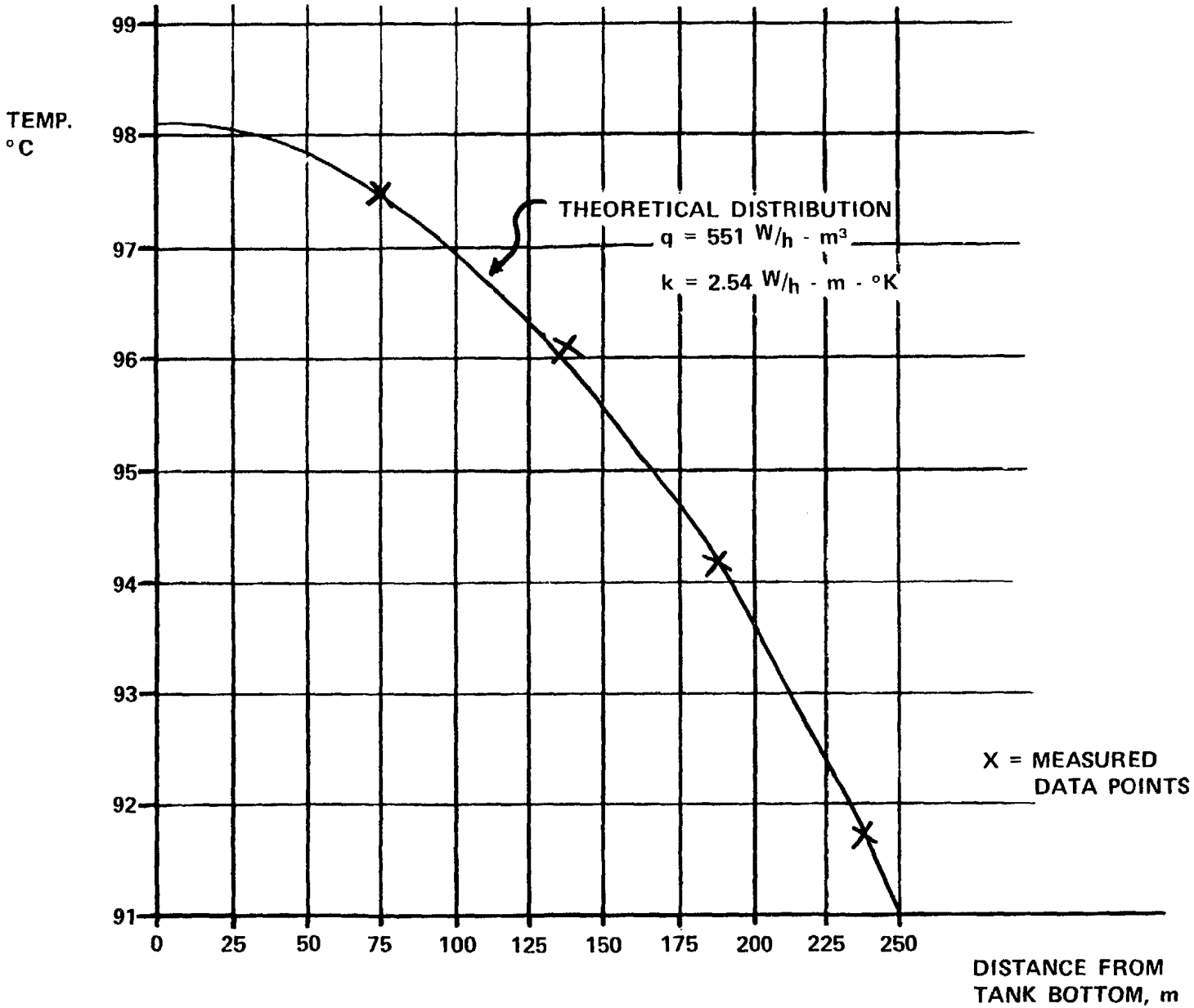

FIGURE 77
Temp. Distribution
in 8D-2 Sludge Hard Layer

10. CITED REFERENCES

[1] DOE/EIS-0081, "Final Environmental Impact Statement: Long-Term Management of Liquid High-Level Radioactive Waste Stored at the Western New York Nuclear Services Center, West Valley, U. S. Department of Energy, June 1982.

[2] ENDF292, National Nuclear Data Center, Brookhaven, 1980.

[3] "Licensing Requirements for Land Disposal of Radioactive Wastes," 10 CFR Part 61, Federal Register, Vol. 47, No. 248, December 27, 1982.

[4] L. A. Bray, et al, PNL-4969, "Experimental Data Developed to Support the Selection of a Treatment Process for West Valley Alkaline Supernatant," January 1984.

[5] L. E. Rykken, "In-Cell Supernatant Decontamination Tests," WD:83:0599, WVNS, Inc., West Valley, NY, December 13, 1983.

[6] L. E. Rykken, "Additional Ion Exchange Tests With 8D-2 Supernatant," WD:83:0721, WVNS, Inc., West Valley, NY, November 14, 1984.

[7] "Measurement of the Leachability of Solidified Low-Level Radioactive Wastes," Prepared by the American Nuclear Society Committee Working Group ANS - 16.1, Third Draft of a Standard, November 16, 1982.

[8] D. C. Grant, E. E. Smeltzer, and M. C. Skriba, "Leachability of Cement Encapsulated West Valley Low-Level Waste Streams," February 15, 1984, Westinghouse R&D Document No. 84-863-EASTV-R2.

[9] L. E. Rykken, "Leachability of Cement Encapsulated Supernatant," WD:85:0611, WVNS, Inc., West Valley, NY, September 30, 1985.

[10] "Technical Position on Waste Form," Branch Technical Position of the NRC Low-Level Waste Licensing Branch, May 1983, Rev. 0.

[11] Design Criteria, Supernatant Treatment Systems, Rev. 1, WVNS-DC-013, WVNS, Inc., NY, December 1985.

[12] John R. Ferraro, et al, "The System Thorium Nitrate - Water - Nitric Acid at 25° and the Hydrates of Thorium Nitrate," Journal of American Chemical Society, 76, 909-11 (1954).

[13] CCC-371, "ORIGEN2: Isotope Generation and Depletion Code - Matrix Exponential Method," Radiation Shielding Information Center, Oak Ridge National Laboratory, September 1983.

[14] L. A. Bray and B. M. Wise, "Chemistry Required for 8D-4 Thoria Waste Removal," WVST 86/59, Pacific Northwest Laboratories, Richland, Washington, April 30, 1986.

[15] M. S. Abdelhamid, P. C. Newsom, L. E. Rykken, "In Situ Characterization of High-Level Waste Sludge at West Valley," Advances in Ceramics, Vol. 8, Nuclear Waste Management, American Ceramic Society.

[16] M. J. Hvorslev, "Subsurface Exploration and Sampling of Soils for Civil Engineering Purposes," US Army Core of Engineers, Waterway Equipment Station, Vicksburg, Mississippi (1949).

[17] W. Kjellman, T. Kollstenius, and O. Wager, "Soil Sampler With Metal Foils," Royal Swedish Geotechnical Institute Proceedings, No. 1, Stockholm, Sweden (1950).

[18] L. E. Rykken, J. A. Wilson, and T. L. Hardt, "Analytical Characterization of West Valley High-Level Waste Sludge," American Nuclear Society International Meeting, March 24-29, 1985, Tucson Arizona.

[19] L. E. Rykken, "Updated Analytical Data on 8D-2 Supernatant," WD:84:0401, WVNS, Inc., West Valley, NY, July 12, 1984.

[20] L. E. Rykken, "Sludge Washing Calculation," WD:84:0690, WVNS, Inc., West Valley, NY, October 5, 1984.

[21] L. E. Rykken, "8D-2 Tank Temperature Control," WD:85:0645, WVNS, Inc., West Valley, NY, October 11, 1985.

11. ADDITIONAL BIBLIOGRAPHY

1) TID-28950-2, Western New York Nuclear Service Center Study, DOE.

2) L. E. Rykken, L. W. Wiedemann, Z. L. Kardos, "Characterization of High-Level Waste Supernatant at West Valley," Advances in Ceramics, Vol. 8, Nuclear Waste Management, American Ceramic Society.

3) E. R. Johnson Associates, Inc., "Alternate Waste Management Options," Final Report, Task 2 on Contract 31-109-38-4190, Nuclear Fuel Services, Inc., May 10, 1978.

4) L. E. Rykken, "8D-2 Sludge Characterization Data," WD:82:0375, December 28, 1982.

5) L. E. Rykken, L. W. Weidemann, and Z. L. Kardos, "Sampling and Analysis of High-Level Waste at West Valley," Vol. 2, Proceedings of the Symposium on Waste Management, American Nuclear Society International Meeting, February 27 - March 3, 1983, Tucson, Arizona.

6) L. E. Rykken, "Report on Analysis of 8D-4 (THOREX) Waste Tank," WD:83:0501, WVNS, Inc., West Valley, NY, October 27, 1983.

7) L. E. Rykken, "8D-2 Sludge Topographical Data," WD:83:0502, WVNS, Inc., West Valley, NY October 27, 1983.

8) L. E. Rykken, M. A. Schiffhauer, P. C. Newsom, R. R. Blickwedehl, "Characterization of High-Level Waste Sludge and Development Plan Par Removal," Vol. 2 Proceedings of the Symposium on Waste Management, American Nuclear Society International Meeting, March 15, 1984, Tucson, Arizona.

9) L. E. Rykken, "In-Cell Tests on 8D-2 Sludge," WD:84:0217, WVNS, Inc., West Valley, NY, April 12, 1984.

10) L. E. Rykken, "Thirty mL Column Test on IE-95," WD:84:0297, WVNS, Inc., West Valley, NY, July 12, 1984.

11) L. E. Rykken, "Composition of 8D-2 Sludge Wash Solutions, "WD:86:0026, WVNS, Inc., West Valley, NY, January 15, 1986.

12) L. E. Rykken, "Nominal 8D-2 Sludge Composition and Confidence Intervals," WD:86:0027, WVNS, Inc. West Valley, NY, January 15, 1986.

13) L. E. Rykken, "Video Inspection of 8D-3 and 8D-4 Tanks," WD:86:0042, WVNS, Inc. West Valley, NY, January 21, 1986.

14) L. E. Rykken, "In-Cell Testing of 8D-2 Sludge Sample," WD:85:0465, WVNS, Inc., West Valley, NY, July 25, 1986.

APPENDIX A: SUMMARY - PROPERTIES OF STS SOLUTION

TABLE OF CONTENTS

TABLES

FIGURES

APPENDIX A: SUMMARY - PROPERTIES OF STS SOLUTIONS

I. 8D-2 SUPERNATANT STANDARD:

A. Definition of Standard

The properties of the 8D-2 supernatant will vary with temperature, dilution, and time (for radiological properties). The "standard" is taken to be the supernatant that was in the 8D-2 tank on September 26, 1982, when it was sampled for extensive analysis. This can be radiologically corrected to the time of interest.

The tank volume at the time of sampling was ~600,000 gallons (~2,270,000 litres). Measured in-tank density was 1.27 at 87°C. Correcting for solids, (28,571 litres) total supernatant was taken to be 2.856×10^6 kg.*

Concentration by evaporation is continually occurring. Condensate is collected in 8D-1 and periodically returned to 8D-2. Tank volume measurements are done at the end of each month by Facilities Engineering.

B. Compositional Correction Example

Compositional corrections should be done as follows:

If tank volume is reported as 570,000 gallons, calculate the salt concentration correction factor (F).

Assume: (1) No volume change of dilution.
(2) Only water is removed of Sp.G. = 1 kg/L

Standard: 1,129,038 kg salts
1,727,164 kg water
2,856,202 kg total

$$F = \frac{2,856,202}{2,856,202 - 30,000\ (3.785)} = 1.0414$$

To get "new" salt content multiply reference weight percent (Table A-1) by 1.0414.**

---

* Corrections were not made for Na_2SO_4 (found later). Data accuracy does not justify making this minor correction.

** A temperature correction could also be made (Section IV), if the temperature is significantly different from 87°C.

II. CHEMICAL COMPOSITION OF STANDARD SUPERNATANT

A. Data

The chemical composition of the "standard" 8D-2 Supernatant (as defined in Section I) is given in Table A-1. Radioactive decay does not significantly affect this composition and thus, this composition is not time dependent. It should be noted that only elemental and anionic analyses were performed, so there is a certain amount of judgment in the compositional salts given. However, this type of format has proved useful from the standpoint of making up simulated solutions.

B. Experimental Verification

Total Dissolved Salts (TDS) were measured by PNL on decontaminated supernatant adjusted to a Sp.G. of 1.32 at 20°C. The measured value of 38.18 percent is within experimental error of the calculated value of 39.53 percent.

III. RADIONUCLIDE COMPOSITION

Unlike the chemical composition, the radionuclide composition is a function of time. For reference, decay correction to July 1, 1986, was used. If concentrations are used, e.g., μCi/mL, corrections for tank volume and/or dilution should be made similar to those for salt content. Total curie content and methods for decay correction are given in Table A-2.

IV. DENSITY

A. Experimental Data:

The sampled "standard" supernatant had a measured density of 1.32 g/mL at 20°C. An in-tank buoyancy probe measurement at about the same time gave a density of 1.27 g/mL at the tank temperature of 87°C.

B. Recommended Correlations for Temperature/Dilution Corrections:

Using the two experimental points, using a handbook tabulation for water density, and assuming that the "effective" soluble salt density varies linearly with temperature, Table A-3 can be derived:

The supernatant density is calculated from the formula:

$$(1)\quad \rho_{Super} = \frac{(\rho_{H_2O})(\rho_{Salts})}{(0.6047)\rho_{Salts} + (0.3953)\rho_{H_2O}}$$

TABLE A-1: 8D-2 SUPERNATANT CHEMICAL COMPOSITION

Compound	Wt. % Wet Basis	Wt. % Dry Basis	Total Kg in Supernatant
$NaNO_3$	21.10	53.38	602,659
$NaNO_2$	10.90	27.57	311,326
Na_2SO_4	2.67	6.76	76,261
$NaHCO_3$	1.49	3.77	42,557
KNO_3	1.27	3.21	36,274
Na_2CO_3	0.884	2.24	25,249
NaOH	0.614	1.55	17,537
K_2CrO_4	0.179	0.45	5,113
NaCl	0.164	0.42	4,684
Na_3PO_4	0.133	0.34	3,799
Na_2MoO_4	0.0242	0.06	691
Na_3BO_3	0.0209	0.05	597
$CsNO_3$	0.0187	0.05	534
NaF	0.0176	0.04	503
$Sn(NO_3)_4$	0.00859	0.02	245
$Na_2U_2O_7$	0.00808	0.02	231
$Si(NO_3)_4$	0.00806	0.02	230
$NaTcO_4$	0.00620	0.02	177
$RbNO_3$	0.00416	0.01	119
Na_2TeO_4	0.00287	0.007	82
AlF_3	0.00271	0.007	77
$Fe(NO_3)_3$	0.00152	0.004	43
Na_2SeO_4	0.00054	0.001	15
$LiNO_3$	0.00048	0.001	14
H_2CO_3	0.00032	0.0008	9
$Cu(NO_3)_2$	0.00022	0.0005	6
$Sr(NO_3)_2$	0.00013	0.0004	4
$Mg(NO_3)_2$	0.00008	0.0002	2
TOTAL	39.53	100.00	1,129,038
			1,727,164
H_2O (by difference)	60.47		

TABLE A-2: SUPERNATANT RADIONUCLIDE COMPOSITION

(as of 7/1/86)

ISOTOPE	$T_{1/2}$ (HALF LIFE)	Ci	METHOD OF DECAY CORRECTION
H-3	12.3 yr	103	x $e^{-\lambda\tau}$*
C-14	5,730 yr	137	x $e^{-\lambda\tau}$
Ni-63	100 yr	895	x $e^{-\lambda\tau}$
Se-79	6.5×10^4 yr	37	x $e^{-\lambda\tau}$
Sr-90	29 yr	2,956	x $e^{-\lambda\tau}$
Y-90	64 hr	2,956	Same as Sr-90 (short-lived daughter)
Zr-93	1.53×10^6 yr	0.23	x $e^{-\lambda\tau}$
Nb-93m	13.6 yr	0.14	From Decay chain Zr-93 →Nb-92m →Nb-93
Tc-99	2.13×10^5 yr	1,599	x $e^{-\lambda\tau}$
Ru-106	368d	2.8	x $e^{-\lambda\tau}$
Rh-106	30s	2.8	Same as Ru-106 (short-lived daughter)
Pd-107	6.5×10^6 yr	1.2×10^{-2}	x $e^{-\lambda\tau}$
Cd-113m	14.6 yr	21	x $e^{-\lambda\tau}$
Sn-121m	50.0 yr	1.5E-3	x $e^{-\lambda\tau}$
Sb-125	2.73 yr	72	x $e^{-\lambda\tau}$
Te-125m	58d	16.6	23% of Sb-125 (short-lived daughter, 23% of Sb-125 →Te 125m)
Sn-126	1.05×10^5	0.40	x $e^{-\lambda\tau}$
Sb-126m	19m	0.40	Same as Sn-126 (short-lived daughter)
Sb-126	12.5d	0.16	40% of Sb-126m based on 40% of Sb-126m→ Sb-126
I-129	1.59×10^7 yr	0.21	x $e^{-\lambda\tau}$
Cs-134	2.06 yr	1.94×10^4	x $e^{-\lambda\tau}$
Cs-135	2.3×10^6 yr	156	x $e^{-\lambda\tau}$
Cs-137	30.0 yr	7.43×10^6	x $e^{-\lambda\tau}$
Ba-137m	2.5m	6.98×10^6	94% of Cs-137 (short-lived daughter, 94% of CS-137 → Ba-137m)
Ce-144	284d	7.23×10^{-5}	x $e^{-\lambda\tau}$
Pr-144	17m	7.23×10^{-5}	Same as Ce-144 (short-lived daughter)
Pm-147	2.62 yr	217	x $e^{-\lambda\tau}$
Sm-151	93 yr	1.11	x $e^{-\lambda\tau}$
Eu-152	13.4 yr	4.47×10^{-2}	x $e^{-\lambda\tau}$
Eu-154	8.2 yr	14.9	x $e^{-\lambda\tau}$
Eu-155	4.76 yr	2.73	x $e^{-\lambda\tau}$
U-233	1.59×10^5 yr	0.5	x $e^{-\lambda\tau}$
U-234	2.44×10^5 yr	0.3	x $e^{-\lambda\tau}$
U-235	7.04×10^8 yr	6.5×10^{-3}	x $e^{-\lambda\tau}$
U-236	2.34×10^7 yr	2.0×10^{-2}	x $e^{-\lambda\tau}$
U-238	4.47×10^9 yr	5.8×10^{-2}	x $e^{-\lambda\tau}$
Pu-238	87.7 yr	130	x $e^{-\lambda\tau}$
Pu-239	2.4×10^4 yr	25	x $e^{-\lambda\tau}$
Pu-240	6,537 yr	19	x $e^{-\lambda\tau}$
Pu-241	14.4 yr	1.58×10^3	x $e^{-\lambda\tau}$
Pu-242	3.8×10^5 yr	2.50×10^{-2}	x $e^{-\lambda\tau}$

* $\lambda = \frac{\ln 2}{T_{1/2}}$

τ = Time from reference (may be negative)

$T_{1/2}$, τ in same units

TABLE A-3: SUPERNATANT DENSITY TEMPERATURE CORRELATION

Temp. (°C)	ρ_{H_2O} (g/mL)ρ	Salts (g/mL)	ρ_{Super} (g/mL)
0	0.99987	2.6542	1.327
5	0.99999	2.6416	1.326
10	0.99973	2.6291	1.323
15	0.99913	2.6165	1.322
20	0.99823	2.6040	1.320
25	0.99707	2.5915	1.317
30	0.99567	2.5789	1.315
35	0.99406	2.5664	1.312
40	0.99224	2.5538	1.309
45	0.99025	2.5413	1.305
50	0.98807	2.5287	1.302
55	0.98573	2.5162	1.298
60	0.98324	2.5036	1.294
65	0.98059	2.4911	1.290
70	0.97781	2.4785	1.292
75	0.97489	2.4660	1.281
80	0.97183	2.4535	1.277
85	0.96865	2.4409	1.272
90	0.96534	2.4284	1.267
95	0.96192	2.4158	1.262
100	0.95838	2.4033	1.257

The density of diluted supernatant should be calculated by the following formula (assumes no volume change of dilution):

(2) $\rho_{Dil\ Super} = (\Phi_{Super})\rho_{Super} + (1 - \Phi_{Super})\ \rho_{H_2O}$

where Φ_{Super} is the volume fraction of supernatant.

The density of concentrated supernatant can be calculated by using the salt concentration correction factor (F) as defined in Section I. Equation (3) should then be used:

(3) $$\rho_{Conc.\ Super} = \frac{(\rho_{H_2O})(\rho_{Salts})}{[1-0.3953(F)]\ \rho_{Salts} + 0.3953(F)\ \rho_{H_2O}}$$

C. Example:

Calculate the density of 3:1 diluted supernatant at 6°C. A 3:1 dilution is defined as two parts water to one part supernatant. Therefore $\Phi_{Super} = 0.333$; $\Phi_{H_2O} = 0.667$. From Table 2:

$$\rho_{Super} = \frac{(0.99997)(2.6392)}{0.6047(2.6392) + 0.3953(0.99997)} = 1.325\ g/mL$$

From equation (2): $\rho_{3:1\ Super} = 0.333(1.325) + 0.667(0.99997)$ = 1.108 g/mL (@6°C)

V. VISCOSITY

A. Experimental:

Viscosity was measured with a Brookfield digital LVT viscometer equipped with a UL adapter. Eight speeds ranging from 0.3 to 60 rpm are able to be used. Only those speeds that gave a reading >10.0 (on a 0 to 100 scale) were used per the vendor's recommendation. When two or more readings were obtained, the viscosity used was the average. The solutions were found to be Newtonian. Data were obtained with standard supernatant and a 3:1 diluted supernatant (two parts water to one part supernatant). Data were obtained with decontaminated supernatant, i.e., supernatant that had been run through zeolite to remove the cesium. Since some concentration had occurred, water was added until a specific gravity of 1.32 was obtained at 20°C. It was assumed that the ion exchange of Na^+ for Cs^+ did not affect its properties. The data obtained are tabulated in Table A-4:

B. Data Correlation:

On Figure 1, the data are plotted as log viscosity vs $\frac{1}{T} \times 10^3$ where T is the temperature in °K. Handbook data for water is also plotted on the same graph. "Least squares" lines for these curves were calculated:

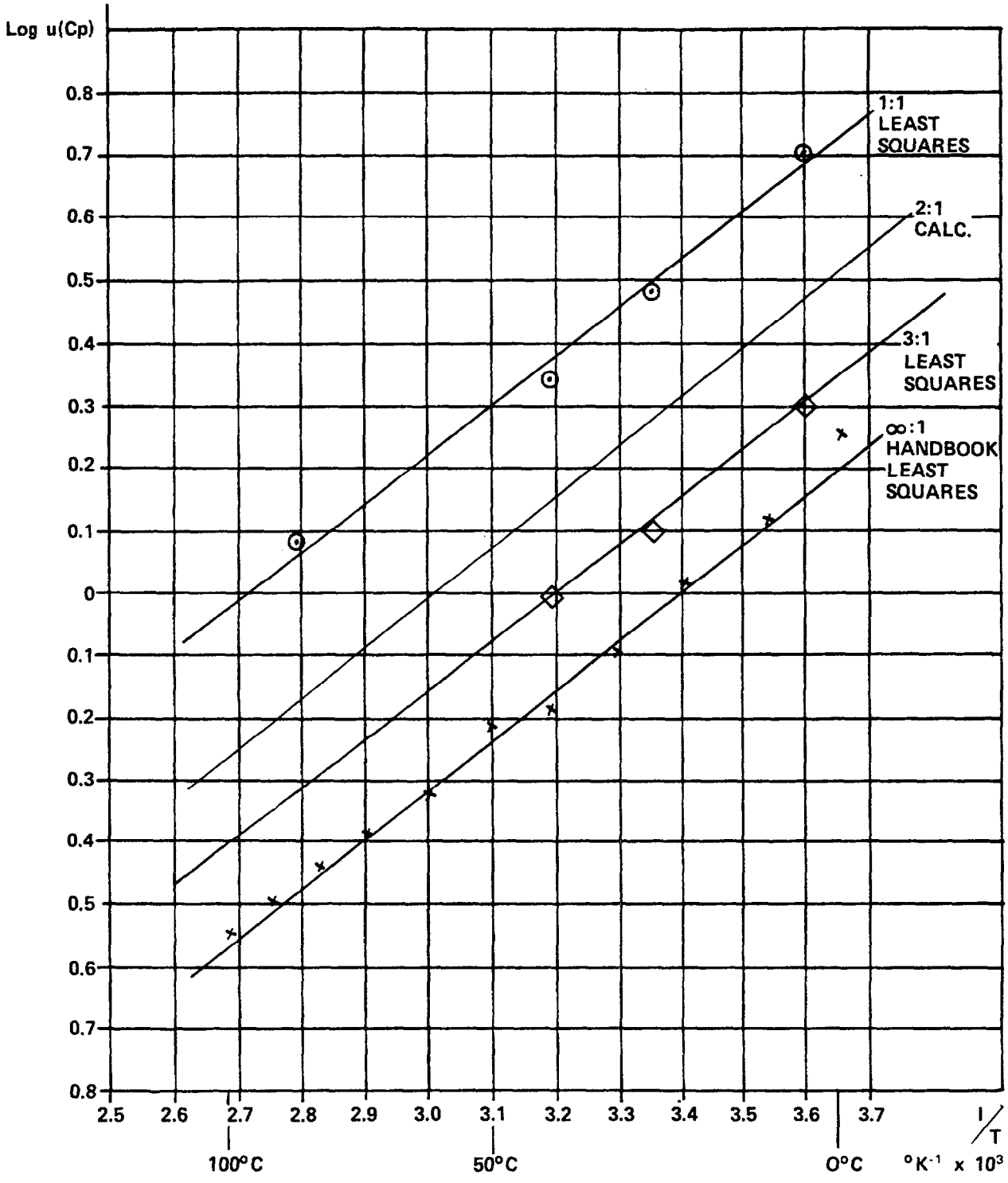

FIGURE A-1
8D-2 Supernatant Viscosity Data

TABLE A-4: SUPERNATANT VISCOSITY DATA

t(°C)	Viscosity (Cp) 1:1 DILUTION	3:1 DILUTION
5	5.12	2.02
25	3.03	1.26
40	2.22	0.99
85	1.20	---- (all readings, <10.0 on scale)

$Y = a_o + a_1X$; where $Y = \log \mu$ (μ in Cp)

$X = \frac{1}{T} \times 10^3$ (T in °K)

a_o a_1 = Constants

ITEM	a_o	a_1
1:1 Supernatant	-2.1144	0.7785
3:1 Supernatant	-2.4815	0.7732
Water	-2.7155	0.7987

The closeness of the slopes when the data are plotted this way suggest the following correlations for calculating constants for other dilutions:

Calculate a_o' from the following equation:

(4) $a_o' = \varepsilon[\Phi(-2.1144) + (1 - \Phi)(-2.7155)]$
where Φ = volume fraction supernatant*
ε = correction factor = 0.9866 (from substituting experimental data points into equation (4).
Calculate a_1' as follows:
Between 1:1 and 3:1 dilution, let $a_1' = \frac{0.7785 + 0.7732}{2} = 0.7758$

Above 3:1 dilution, ($\Phi < 0.33$) or for concentrated supernatant,
let (5) $a_1' = [\Phi(0.7758) + (1-\Phi)(0.7987)]$
where Φ = volume fraction supernatant*

C. Sample Calculation:

Calculate viscosity of 2:1 diluted supernatant at 47°C
$a_o' = 0.9866\ [0.5(-2.1144) = 0.5(-2.7155)] = -2.3577$

$\log \mu = 07758\ \left[\frac{10^3}{47 + 273}\right] - 2.3577$
$\mu = 1.10$ Cp

VI. BOILING POINT RISE (BPR)

A. Experimental:

Standard supernatant (decontaminated supernatant adjusted to a Sp.G. of 1.32 at 20°C), supernatant diluted 3:1 (two parts water to one part supernatant), supernatant with a concentration factor (CF) of 1.5 (standard supernatant evaporated to 2/3 of its original volume), and deionized water were placed in a temperature bath. The temperature was slowly raised until boiling commenced. The data obtained are summarized in Table 5:

*Concentrated supernatant can be handled by letting Φ = concentration factor (CF) where CF= $\frac{\text{original volume}}{\text{new volume}}$.

TABLE A-5: SUPERNATANT BOILING POINT DATA

Item	BPR * (°C)	Calc. Wt. % Solids
Standard Supernatant	11.0, 9.0	39.5
3:1 Supernatant	4.5	12.7
Conc. Supernatant (CF=1.5)	10.0	53.0

* Δt between start of boiling of solution and deionized water.

B. Correlation:

The experimental points are plotted in Figure A-2. It is recommended that the "least squares" line constrained to go through the origin be used. This has the formula:

(6) $y = 0.2261(x)$

where y = BPR (°C)

x = weight percent solids

The data scatter indicate that this is probably no better than ±2°C.

VII. CRYSTALLIZATION/FREEZING TEMPERATURES

A) Experimental:

Straight supernatant and 3:1 diluted supernatant were slowly cooled with visual observations being made during cooling. With the straight supernatant, extremely fine particles were visible starting at -4°C, with no significant change down to -13°C (this was the lowest achievable temperature with the equipment). With the 3:1 diluted supernatant, the solution began to get cloudy at -8°C and froze at -8.75°C.

B) Correlation:

An engineering approximation for the freezing point would be to sum the freezing point depressions for the individual salts based on handbook data. This is done for 1:1 and 3:1 supernatant in Table A-6.

The 7.2°C can be compared to the experimental 8.75°C for 3:1 diluted supernatant. The correlation would thus appear to be "conservative."

VIII. pH

The STS feed solutions are well buffered and change only slightly with dilution. All solutions that have been measured have had pH's between 9.5 and 10.0.

IX. OTHER PROPERTIES

It is expected that other physical properties that need to be determined can be estimated within Engineering accuracy by using standard correlations. For example, heat capacity is often determined by using a weighted specific heat, where the specific heat of the salt is for the crystalline state[2]. The weighted average of the specific heat of the major salts [3] and for water are:

Temp. (°C)	c_p (BTU/lb-°F or Cal/g-°C)	
	SALT	WATER
0°	0.242	1.007
50°	0.264	0.999
100°	0.287	1.007

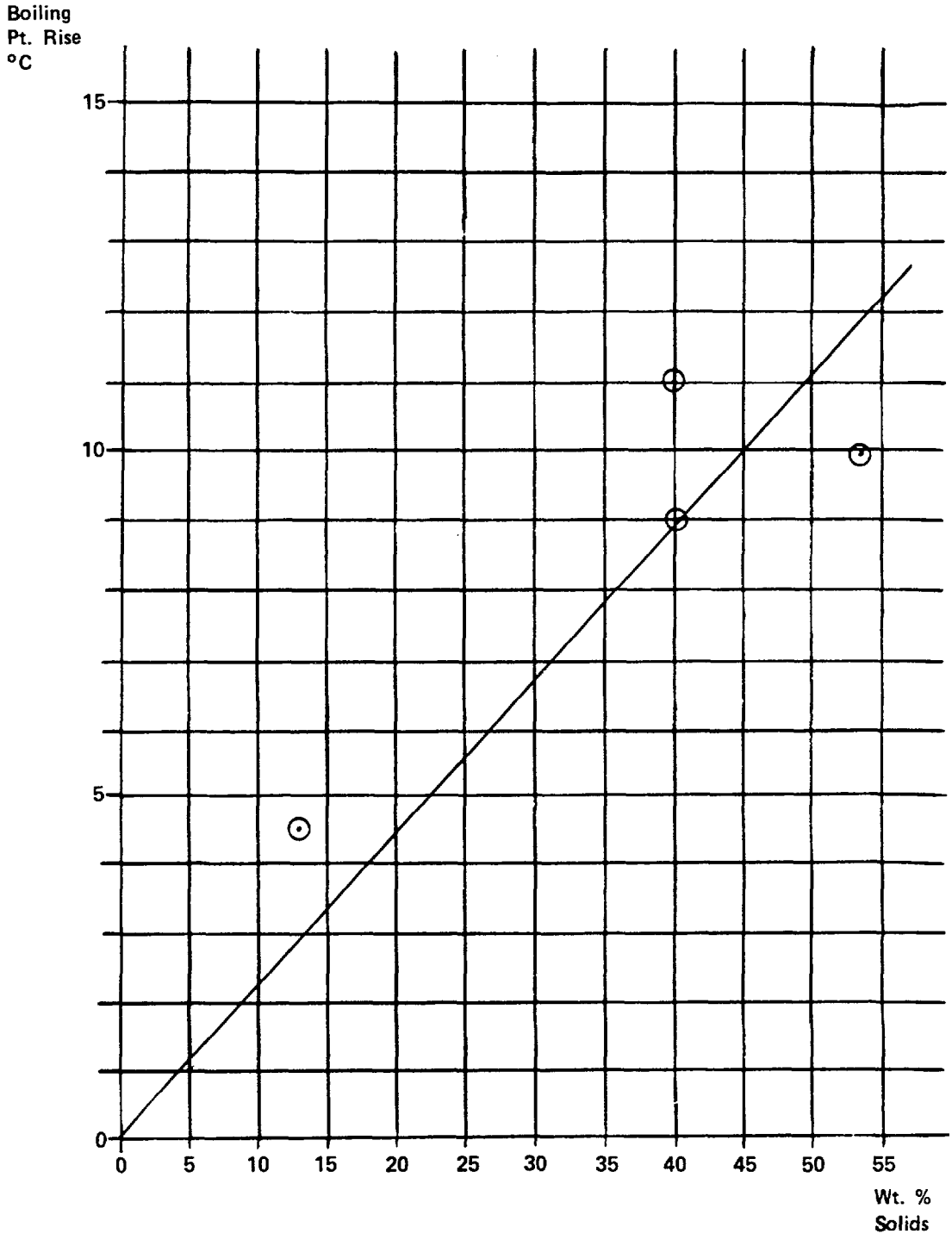

FIGURE A-2
B.P.R. of Diluted/Concentrated Supernatant

TABLE A-6: FREEZING POINT DEPRESSION DATA[1]

Component	$\bar{M}(1:1)$ (a)	$\bar{M}(3:1)$ (b)	Molal Lowering at Concentration		Contribution to Fr. Pt. Depression	
			1:1	3:1	1:1	3:1
$NaNO_3$	4.151	1.188	2.295	2.979	9.527	3.539
$NaNO_2$	2.642	0.756	2.642	3.114	6.980	2.211
Na_2SO_4	0.314	0.090	3.730	4.450	1.171	0.400
$NaHCO_3$	0.290	0.083	3.384	3.678	0.981	0.305
KNO_3	0.250	0.071	3.131	3.382	0.783	0.240
Na_2CO_3	0.140	0.040	4.332	4.808	0.606	0.192
NaOH	0.257	0.074	3.408	3.428	0.876	0.254
NaCl	0.047	0.083	3.539	3.594	0.166	0.047
TOTAL	----------				21.09	7.19

(a) Normalized to 39.53 percent total salts

(b) Normalized to 15.76 percent total salts

For example, to chill 3:1 diluted supernatant from 50°C to 6°C, an interpolated value for t (Avg) = 28°C would be:

$$0.1573(0.254) + 0.8427(0.998) = 0.881 \text{ Cal/g-°C}$$

Since the heat capacity range for most common salts is fairly narrow (~0.2 to ~0.3), this value is probably good to within ± ~1 percent.

X. CORRELATIONS FOR WASH SOLUTIONS

A. Recommended Correlation

Reference modeling of the sludge washing process assumes three wash solutions which can be represented by a combination of water, supernatant, and sodium sulfate solids as follows:

	kg			
Wash No.	H_2O	Supernatant	Na_2SO_4	Total
1	337,595	171,948	10,680	520,223
2	562,571	91,082	5,657	659,310
3	604,836	35,795	2,223	642,854

Since the properties of Na_2SO_4 solutions are well documented, the following correlations are recommended for these solutions: Rearrange the wash solution components as follows as shown in Table A-7 - the weight percent sodium sulfate chosen in each case is approximately equivalent to the weight percent total salts.

Assume that a particular property of a mixture of diluted supernatant and a Na_2SO_4 solution can be approximated by the following equation:

$$(7) \qquad \Psi_w = \phi_1 \Psi_1 + (1 - \phi_1) \Psi_2$$

Ψ_w = property of the wash solution.
Ψ_1 = property of the Na_2SO_4 solution.
Ψ_2 = property of the supernatant/water solution.
Φ_1 = volume fraction of Na_2SO_4 solution.

Ψ_2 can be estimated from previously presented correlations.
Ψ_1 is available from standard references.

B. Example

Calculate the density and viscosity of wash solution number two at 30°C:

TABLE A-7: WASH SOLUTION COMPONENTS

Wash No.	kg		
	H_2O	Supernatant	Na_2SO_4 Sol.(Wt. %)
1	277,075	171,948	71,200 (15.0)
2	481,197	91,082	87,031 (6.5)
3	518,139	35,795	88,920 (2.5)

The relative volumes are:

$H_2O = \frac{481,197}{0.99567} = 483,290$ L (Table 3)

Supernatant $= \frac{91,082}{1.315} = 69,264$ L (Table 3)

Na_2SO_4 solution $= \frac{87,031}{1.0555} = 82,455$ L (Reference 4)

$$\Phi_1 = \frac{82,455}{483,290 + 69,264 + 82,455} = 0.1298$$

$$\Phi_{Super} = \frac{69,264}{69,264 + 483,290} = 0.1254$$

From equation (2), Section IV:

$\rho_{Dil\ Super} = 0.1254(1.315) + 0.8746(0.99567) = 1.0357$

From equation (7)

$\rho_W = 0.1298(1.0555) + 0.8702(1.0357) = 1.038$ g/mL

From Section V, equations (4) and (5)

$a_1' = 0.9866[0.1254(-2.1144) + 0.8746(-2.7155)] = -2.6047$

$a_1' = [0.1254(0.7758) + 0.8746(0.7987)] = 0.7958$

For diluted supernatant:

$$\log \mu_{DS} = 0.7958 \left[\frac{10^3}{30 + 273} \right] - 2.6047$$

$\mu_{DS} = 1.0219$

From Reference 4: $\mu_S = 0.9777$ Cp

For wash solution:

$\mu_W = 0.1298(0.9777) + 0.7702(1.0219) = 0.914$ Cp

APPENDIX A

APPENDIX REFERENCES

[1] CRC Handbook of Chemistry and Physics, 41st Edition, Page 2299

[2] Perry's Chemical Engineers Handbook, Fourth Edition 3-221

[3] International Critical Tables, McGraw Hill

[4] CRC Handbook of Chemistry and Physics, 60th Edition, D-267.